

TURUN YLIOPISTON JULKAISUJA  
ANNALES UNIVERSITATIS TURKUENSIS

---

SARJA - SER. A I OSA - TOM. 461

ASTRONOMICA - CHEMICA - PHYSICA - MATHEMATICA

# LUMINESCENT LANTHANIDE REPORTERS:

## New Concepts for Use in Bioanalytical Applications

by

Johanna Vuojola

TURUN YLIOPISTO  
UNIVERSITY OF TURKU  
Turku 2013

From the Department of Biochemistry and Food Chemistry / Biotechnology  
University of Turku  
Turku, Finland

**Supervised by**

Professor Tero Soukka, Ph.D.  
Department of Biochemistry and Food Chemistry / Biotechnology  
University of Turku  
Turku, Finland

and

Professor Emeritus Timo Lövgren, Ph.D.  
Department of Biochemistry and Food Chemistry / Biotechnology  
University of Turku  
Turku, Finland

**Reviewed by**

Scientific Director Timo Piironen, Ph.D., Adjunct Prof.  
SYRINX Bioanalytics Oy  
Turku, Finland

and

PD Dr. habil. Axel Dürkop  
Institute of Analytical Chemistry, Chemo- and Biosensors  
University of Regensburg  
Regensburg, Germany

**Opponent**

Professor Niko Hildebrandt, Ph.D.  
Institute of Fundamental Electronics  
University of Paris-South  
Paris, France

The originality of this dissertation has been checked in accordance with the University of Turku quality assurance system using the Turnitin OriginalityCheck service.

ISBN 978-951-29-5392-9 (PRINT)  
ISBN 978-951-29-5393-6 (PDF)  
ISSN 0082-7002  
Painosalama Oy – Turku, Finland 2013

If we knew what it was we were doing,  
it would not be called research, would it?

- Albert Einstein

# CONTENTS

<b>CONTENTS .....</b>	<b>4</b>
<b>LIST OF ORIGINAL PUBLICATIONS .....</b>	<b>6</b>
<b>ABBREVIATIONS.....</b>	<b>7</b>
<b>ABSTRACT .....</b>	<b>8</b>
<b>1 INTRODUCTION .....</b>	<b>9</b>
<b>2 REVIEW OF THE LITERATURE.....</b>	<b>11</b>
<b>2.1 The lanthanide series.....</b>	<b>11</b>
2.2.1 Electronic structure, lanthanide ion sensitization, and quenching .....	14
2.2.2 Ligand and lanthanide ion excitation .....	16
2.2.3 Non-radiative and radiative relaxation of excited lanthanide ions .....	18
2.2.4 Lanthanide luminescence in solid crystal hosts .....	20
2.2.5 Resonance energy transfer to an acceptor fluorophore .....	22
<b>2.2 Electronic transitions of lanthanide complexes.....</b>	<b>14</b>
2.3.1 Desirable features.....	24
2.3.2 Lanthanide chelates.....	25
2.3.3 Lanthanide-dyed nanoparticles .....	28
2.3.4 Lanthanide-doped inorganic nanocrystals.....	30
2.3.5 Lanthanide-binding peptides.....	32
2.3.6 Others .....	33
<b>2.3 Luminescent lanthanide reporters .....</b>	<b>24</b>
<b>2.4 Bioanalytical applications .....</b>	<b>35</b>
2.4.1 Bioaffinity assays.....	36
2.4.2 Luminescent sensors based on lanthanide complexes.....	38
2.4.3 Microscopy and imaging.....	40
2.4.4 Future trends .....	42
<b>3 AIMS OF THE STUDY.....</b>	<b>45</b>
<b>4 SUMMARY OF MATERIALS AND METHODS .....</b>	<b>46</b>
<b>4.1 Lanthanide-based donors.....</b>	<b>46</b>
4.1.1 Lanthanide chelates.....	46
4.1.2 Lanthanide-doped upconverting nanoparticles .....	47
4.1.3 Lanthanide-binding peptides.....	47
<b>4.2 Acceptor fluorophores.....</b>	<b>47</b>
4.2.1 Fluorescent proteins .....	48

4.2.2 Alexa Fluor dyes .....	48
4.2.3 Quencher molecule .....	49
<b>4.3 Instrumentation and instrument settings .....</b>	<b>49</b>
4.3.1 Plate readers .....	49
4.3.2 Fluorescence spectrophotometer .....	50
4.3.3 Frequency-domain luminometer .....	51
<b>4.4 Reagent preparation.....</b>	<b>51</b>
4.4.1 Expression and purification of recombinant proteins .....	51
4.4.2 Preparation of donor and acceptor conjugates .....	52
<b>4.5 Assay principles .....</b>	<b>52</b>
4.5.1 Homogeneous competitive FRET assay for GTP .....	53
4.5.2 Homogeneous DNA-hybridization assay.....	54
4.5.3 Homogeneous enzyme activity assays for caspase-3 .....	55
<b>5 SUMMARY OF RESULTS AND DISCUSSION .....</b>	<b>57</b>
<b>5.1 Energy transfer mechanisms .....</b>	<b>57</b>
<b>5.2 Donor and acceptor conjugates .....</b>	<b>59</b>
<b>5.3 Homogeneous assays.....</b>	<b>62</b>
5.3.1 Homogeneous competitive FRET assay for GTP (I) .....	62
5.3.2 Homogeneous DNA-hybridization assay (II) .....	64
5.3.3 Homogeneous enzyme activity assays (III, IV) .....	67
<b>6 CONCLUSIONS.....</b>	<b>71</b>
<b>ACKNOWLEDGEMENTS .....</b>	<b>73</b>
<b>REFERENCES.....</b>	<b>76</b>
<b>ORIGINAL PUBLICATIONS .....</b>	<b>89</b>

## LIST OF ORIGINAL PUBLICATIONS

This thesis is based on the following original publications, referred to in the text by their Roman numerals (**I-IV**):

- I** Johanna Vuojola, Urpo Lamminmäki, and Tero Soukka (2009). Resonance energy transfer from lanthanide chelates to overlapping and nonoverlapping fluorescent protein acceptors. *Anal Chem* **81**:5033–5038.
- II** Johanna Vuojola, Iiko Hyppänen, Marika Nummela, Jouko Kankare, and Tero Soukka (2011). Distance and temperature dependency in nonoverlapping and conventional Förster resonance energy-transfer. *J Phys Chem B* **115**:13685–13694.
- III** Johanna Vuojola, Terhi Riuttamäki, Essi Kulta, Riikka Arppe, and Tero Soukka (2012). Fluorescence-quenching-based homogeneous caspase-3 activity assay using photon upconversion. *Anal Chim Acta* **725**:67–73.
- IV** Johanna Vuojola, Markku Syrjänpää, Urpo Lamminmäki, and Tero Soukka (2013). Genetically encoded protease substrate based on lanthanide-binding peptide for time-gated fluorescence detection. *Anal Chem* **85**:1367–1373.

The original publications have been reproduced with the permission from the copyright holders.

## ABBREVIATIONS

AF	Alexa Fluor fluorophore
BHQ-3	Black Hole Quencher 3
BSA	bovine serum albumin
CB	conduction band
CCD	charge-coupled device
DELFIA®	dissociation-enhanced lanthanide fluoroimmunoassay
DTA	4,6-dichloro-1,3,5-triazin-2-yl group
DTPA	diethylenetriamine pentaacetic acid
ED	electric dipole
EDTA	ethylenediaminetetraacetic acid
ELISA	enzyme-linked immunosorbent assay
FD	frequency-domain
FQA	fluorescence quenching assay
FRET	Förster resonance energy transfer
GFP	green fluorescent protein
GTP	guanosine triphosphate
HPLC	high-performance liquid chromatography
HTS	high-throughput screening
IC <sub>50</sub>	analyte concentration inhibiting 50% of the maximum signal
ILCT	intraligand charge-transfer
ITC	isothiocyanate
LBP	lanthanide-binding peptide
LF	lateral flow
LMCT	ligand-to-metal charge-transfer
Ln	lanthanide
MD	magnetic dipole
MLCT	metal-to-ligand charge-transfer
MRI	magnetic resonance imaging
nFRET	non-overlapping Förster resonance energy transfer
NHS	N-hydroxysuccinimide
NIR	near-infrared
NMR	nuclear magnetic resonance
OLED	organic light-emitting diode
PCR	polymerase chain reaction
POC	point-of-care
QD	quantum dot
R <sub>0</sub>	Förster radius (the distance at which energy transfer efficiency is 50%)
RET	resonance energy transfer
TD	time-domain
TEOS	tetraethyl orthosilicate
TR	time-resolved
TRF	time-resolved fluorescence
TRFM	time-resolved fluorescence microscopy
TTHA	triethylene tetraamine hexaacetic acid
UC-FRET	upconversion Förster resonance energy transfer
UCP	upconverting phosphor
UV	ultraviolet
VB	valence band
YFP	yellow fluorescent protein

## ABSTRACT

Lanthanides represent the chemical elements from lanthanum to lutetium. They intrinsically exhibit some very exciting photophysical properties, which can be further enhanced by incorporating the lanthanide ion into organic or inorganic sensitizing structures. A very popular approach is to conjugate the lanthanide ion to an organic chromophore structure forming lanthanide chelates. Another approach, which has quickly gained interest, is to incorporate the lanthanide ions into nanoparticle structures, thus attaining improved specific activity and binding capacity. The lanthanide-based reporters usually express strong luminescence emission, multiple narrow emission lines covering a wide wavelength range, and exceptionally long excited state lifetimes enabling time-resolved detection. Because of these properties, the lanthanide-based reporters have found widespread applications in various fields of life. This study focuses on the field of bioanalytical applications.

The aim of the study was to demonstrate the utility of different lanthanide-based reporters in homogeneous Förster resonance energy transfer (FRET)-based bioaffinity assays. Several different model assays were constructed. One was a competitive bioaffinity assay that utilized energy transfer from lanthanide chelate donors to fluorescent protein acceptors. In addition to the conventional FRET phenomenon, a recently discovered non-overlapping FRET (nFRET) phenomenon was demonstrated for the first time for fluorescent proteins. The lack of spectral overlap in the nFRET mechanism provides sensitivity and versatility to energy transfer-based assays. The distance and temperature dependence of these phenomena were further studied in a DNA-hybridization assay. The distance dependence of nFRET deviated from that of FRET, and unlike FRET, nFRET demonstrated clear temperature dependence. Based on these results, a possible excitation mechanism operating in nFRET was proposed. In the study, two enzyme activity assays for caspase-3 were also constructed. One of these was a fluorescence quenching-based enzyme activity assay that utilized novel inorganic particulate reporters called upconverting phosphors (UCPs) as donors. The use of UCPs enabled the construction of a simple, rather inexpensive, and easily automated assay format that had a high throughput rate. The other enzyme activity assay took advantage of another novel reporter class, the lanthanide-binding peptides (LBPs). In this assay, energy was transferred from a LBP to a green fluorescent protein (GFP). Using the LBPs it was possible to avoid the rather laborious, often poorly repeatable, and randomly positioned chemical labeling. In most of the constructed assays, time-resolved detection was used to eliminate the interfering background signal caused by autofluorescence. The improved signal-to-background ratios resulted in increased assay sensitivity, often unobtainable in homogeneous assay formats using conventional organic fluorophores. The anti-Stokes luminescence of the UCPs, however, enabled the elimination of autofluorescence even without time-gating, thus simplifying the instrument setup. Together, the studied reporters and assay formats pave the way for increasingly sensitive, simple, and easily automated bioanalytical applications.

## 1 INTRODUCTION

The complexity of biological systems has for long challenged and perplexed researchers and scientists. Bioanalytical applications aim at elucidating the intricate interactions occurring in these systems. A key element in bioanalytical applications is the sensitive and specific detection of the analytes of interest (Kricka, 1994). Historically, several different labels have been used for this purpose. These include isotopic labels, enzyme labels, chemiluminescent labels, and photoluminescent labels (Soini and Hemmilä, 1979; Hemmilä, 1985; Ekins, 1998). The analytes may be present in very small concentrations in a complex aqueous matrix. This creates a need for a detection system that is able to exclude the background signal caused by the extraneous components. Lanthanide-based photoluminescent reporters are increasingly gaining interest in bioanalytical applications because of their unique photophysical properties. The most prominent advantages of luminescent lanthanide ions compared to conventional short-lifetime organic fluorophores are the large Stokes shifts, the multiple narrow emission lines, and the long emission lifetimes (Selvin, 2002; Bünzli and Piguet, 2005). Thus, lanthanides provide sensitivity by enabling the elimination of interfering background fluorescence through the use of time-resolved (TR, also called time-gated) detection (Hemmilä and Laitala, 2005; Allen and Imperiali, 2010).

The history of lanthanides dates back to the 18<sup>th</sup> century. A Swedish mineralogist Cronstedt first discovered a new heavy mineral from a mine in Sweden in 1752, but it was mistakenly thought to be calcium iron silicate, although it contained lanthanides. Then, in 1794, a Finnish mineralogist Gadolin discovered a heavy mineral in Sweden and isolated an oxide from it that he named “ytterbia” (from the name of the village, Ytterby). This oxide was later separated into fractions named “yttria”, “erbia”, and “terbia”, but these were yet again found to be complex mixtures. The first spectroscopic studies on aqueous lanthanide solutions were carried out during the 1930s and 1940s (Werts, 2005). During that time, it was discovered that some organic ligands (such as salicylaldehyde or benzoylacetonate) can photosensitize the luminescence of europium ions when excited in the ultraviolet (UV) region, where europium does not absorb (Weissman, 1942). In 1962, cells were first stained with europium, and in the 1970s, a Finnish company, Wallac Oy (currently part of PerkinElmer), began the studies with lanthanides as luminescent reporters for time-resolved immunoassays (Soini and Hemmilä, 1979). The technology developed by Wallac Oy spurred a rapid increase in the number of studies and applications in the field.

To be able to fully benefit from the exceptional properties of lanthanides in bioanalytical applications, they should be conjugated to a structure that i) shields the intrinsically weakly fluorescent ion from the quenching effects of the surrounding aqueous matrix, ii) sensitizes the lanthanide emission by absorbing excitation energy and transferring it to the lanthanide ion, and iii) enables chemical coupling to biomolecules. This can be achieved in various ways. One of the most widespread approaches is to use small organic multidentate structures, lanthanide chelates, to produce the needed functions. If improved specific activity and binding capacity are needed, the lanthanide ions can be incorporated into either organic or inorganic nanoparticles. One of the more novel approaches in the bioanalysis field is to genetically encode a short peptide sequence that is able to bind a lanthanide ion and sensitize its luminescence (Lim and Franklin, 2004).

## *Introduction*

---

The different lanthanide-based reporters have their own special features thus providing for a multitude of applications. They can be used to study, for example, protein structure and function, protein–protein interactions, and protein–ligand interactions. Lanthanides are increasingly used as a tool in fields such as medical diagnostics, sensing, and imaging. The recent trends in bioanalytical assays have been towards multiplexing, point-of-care (POC) assays (Junker *et al.*, 2010), and high-throughput screening (HTS) of vast compound libraries. For fast, simple, and affordable solutions, homogeneous (i.e., separation-free) assay formats are usually preferred (Ullman, 2001). Homogeneous assays utilizing lanthanide-based labels create high potential for novel and exciting advances in bioanalytics.

## 2 REVIEW OF THE LITERATURE

The unique properties of lanthanide-based reporters (also called lanthanide labels or lanthanide probes) have enabled their increasing use in a wide variety of applications (Hemmilä and Laitala, 2005). The scope of this literature review is limited to luminescent lanthanide labels applicable to be used in aqueous solutions. The practical examples have been limited to bioanalytical applications with emphasis on novel reporters and methods. Certain lanthanides (for example, europium and terbium) are emphasized over others because of their wider applicability and usage. This review deals only with the luminescence of the trivalent lanthanide ions, which are the most abundant form of lanthanide ions in nature (Werts, 2005). The review begins by introducing the properties of lanthanides, including their complex electronic transitions. Subsequently, the different lanthanide reporter classes are introduced, and the bioanalytical applications using these reporters are described.

### 2.1 The lanthanide series

The word lanthanide originates from the Greek word *lanthanein* translating into “lying hidden” (Bünzli and Piguet, 2005). The lanthanide series comprises the 15 elements from lanthanum (atomic number 57) to lutetium (atomic number 71). Lanthanides, in conjunction with the chemically similar elements scandium and yttrium, are sometimes called rare earth elements. However, lanthanides are relatively abundant in Earth's crust, more common in fact than gold, silver, or platinum (Leonard *et al.*, 2007). They do lie somewhat hidden, since they are mostly dispersed in the soil, and are rarely found in larger amounts in rare earth ore deposits (Tyler, 2004). The radioactive promethium does not actually occur in nature, and it was first prepared in the 1940s (Marinsky *et al.*, 1947).

The lanthanides are exceptional elements in that they very closely resemble each other in view of their chemical properties. This is due to the electronic configuration of the lanthanide atoms and their corresponding ions. All lanthanides, except lanthanum, are f-block elements, meaning that they have valence electrons in f orbitals. When progressing from cerium to lutetium, the 4f orbitals are gradually filled. These f orbitals have low radial expansion, and they are shielded from the chemical environment by the filled, energetically lower 5s and 5p sub-shells. Although lower in energy, these sub-shells are spatially located outside the 4f orbitals, causing the 4f electrons to have very little interaction with the chemical environment, and leading to the difficult separation of the lanthanides (Cotton, 2006; Werts, 2005).

The general electronic configuration of lanthanide atoms is usually denoted as  $[Xe]4f^n5d^16s^2$ , where  $[Xe]$  represents the electronic configuration of the noble gas xenon, and  $n$  represents the number of electrons from 0 to 14 (0 with La to 14 with Lu). However, depending on the relative energy levels, there are actually two types of electronic configurations for the lanthanide atoms:  $[Xe]4f^n6s^2$  and  $[Xe]4f^{n-1}5d^16s^2$  ( $n = 1-14$ ). Lanthanum, cerium, gadolinium, and lutetium belong to the latter type, and the rest of the lanthanides to the former (for terbium both configurations are energetically close to each other, so either one may be adopted). The most common oxidation state of lanthanide ions in aqueous solvents is  $\text{Ln}^{3+}$  ( $\text{Ln}$  referring to any lanthanide), as this state is usually energetically most stable. The electronic configuration of all the trivalent lanthanide ions is

$[\text{Xe}]4f^n$ , indicating that the two 6s electrons, as well as the possible 5d electron, have been lost (Huang and Bian, 2010). A summary of the electronic configurations of lanthanide atoms and trivalent lanthanide ions is presented in Table 1. Some lanthanides, such as europium, may also be present as  $\text{Ln}^{2+}$  ions. The existence of the  $\text{Eu}^{2+}$  state is possible since the 4f shell of the divalent ion is half filled, being, therefore, energetically rather stable (Hemmilä and Laitala, 2005). Even though some lanthanides, for example cerium, can exist as  $\text{Ln}^{4+}$  ions, the oxidation of lanthanides never exceeds the tetravalent stage (Melcher *et al.*, 2005).

**Table 1.** The electronic configurations of rare earth elements (adapted from Huang and Bian, 2010). The lanthanides (from La to Lu) have filled inner orbitals with 46 electrons. Scandium and yttrium have 18 electrons in the inner orbitals.

Z	Element	Configurations of neutral atoms					Configurations of trivalent ions	Atomic weight
		4f	5s	5p	5d	6s		
57	La	0	2	6	1	2	$[\text{Xe}]4f^0$	138.9
58	Ce	1	2	6	1	2	$[\text{Xe}]4f^1$	140.12
59	Pr	3	2	6		2	$[\text{Xe}]4f^2$	140.91
60	Nd	4	2	6		2	$[\text{Xe}]4f^3$	144.24
61	Pm	5	2	6		2	$[\text{Xe}]4f^4$	(147)
62	Sm	6	2	6		2	$[\text{Xe}]4f^5$	150.36
63	Eu	7	2	6		2	$[\text{Xe}]4f^6$	151.96
64	Gd	7	2	6	1	2	$[\text{Xe}]4f^7$	157.25
65	Tb	9	2	6		2	$[\text{Xe}]4f^8$	158.93
66	Dy	10	2	6		2	$[\text{Xe}]4f^9$	162.50
67	Ho	11	2	6		2	$[\text{Xe}]4f^{10}$	164.93
68	Er	12	2	6		2	$[\text{Xe}]4f^{11}$	167.26
69	Tm	13	2	6		2	$[\text{Xe}]4f^{12}$	168.93
70	Yb	14	2	6		2	$[\text{Xe}]4f^{13}$	173.04
71	Lu	14	2	6	1	2	$[\text{Xe}]4f^{14}$	174.97
		3d	4s	4p	4d	5s		
21	Sc	1	2				[Ar]	44.96
39	Y	10	2	6	1	2	[Kr]	88.91

The emission colors of the lanthanides cover the entire spectrum from UV to visible and near-infrared (NIR) ranges. Although most lanthanide ions are luminescent (with the exception of  $\text{La}^{3+}$  and  $\text{Lu}^{3+}$ ), they are not luminescent to an equal degree, and thus not equally useful or commonly applied. The luminescence intensity of the lanthanide ion is dependent on the quantum yield, which is related to the ratio of radiative and non-radiative relaxation (deactivation) processes of the excited energy levels. The quantum yield is also related to the extent of the energy gap between the lowest excited energy level of the ion (called the emissive or radiative energy level) and the highest sublevel of its ground state multiplet (Bünzli and Piguet, 2005). The partial energy level diagram for aqueous lanthanide ions, illustrating also the energy gaps, is presented in Figure 1 (Carnall *et al.*, 1968a; Carnall *et al.*, 1968b; Carnall *et al.*, 1968c; Carnall *et al.*, 1968d, Moore *et al.*, 2009). Judged by the energy gap criterion,  $\text{Eu}^{3+}$ ,  $\text{Tb}^{3+}$ , and  $\text{Gd}^{3+}$  ions have the strongest

luminescence. The most commonly used lanthanide ions in bioanalytical applications are Eu<sup>3+</sup> and Tb<sup>3+</sup>. In addition to their intense emission in the visible wavelength, this is due to their particularly long lifetime (Allen and Imperiali, 2010). The usefulness of gadolinium as a luminescent reporter is, however, limited, as it emits in the UV instead of the visible wavelength region (Werts, 2005). Dy<sup>3+</sup> and Sm<sup>3+</sup> have also found many applications, but their use has been limited because of their inferior luminescence quantum yields and shorter lifetimes (Xu *et al.*, 1992b). The applicability of the NIR emitting lanthanides (Nd<sup>3+</sup>, Er<sup>3+</sup>, and Yb<sup>3+</sup>) has long been restricted, but recently their utility has increased because of the technical advances in the detection of the weak NIR emission, and because of the development of novel sensitizing structures (Bünzli and Piguet, 2005). The photon upconversion phenomenon (i.e., a process where the energy of two or more sequentially absorbed photons combine to produce a higher energy photon) is demonstrated by several lanthanide ions, such as Tm<sup>3+</sup>, Dy<sup>3+</sup>, Er<sup>3+</sup>, and Ho<sup>3+</sup> (Güdel and Pollnau, 2000).

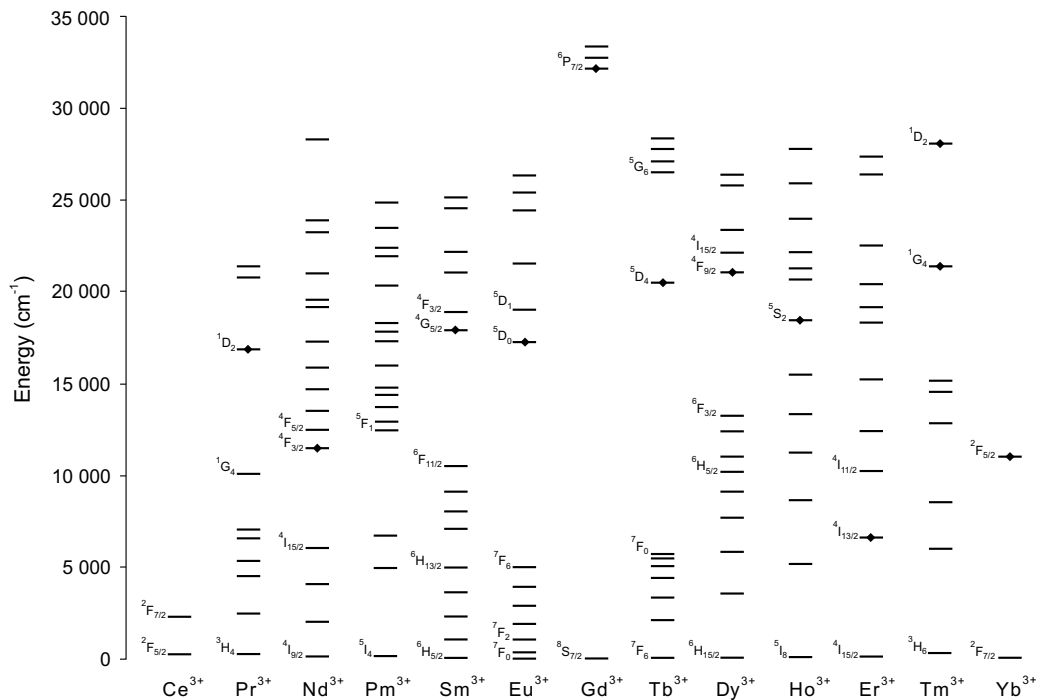


**Figure 1.** A diagram depicting the approximate energy levels for aqueous lanthanide ions (Carnall *et al.*, 1968a; Carnall *et al.*, 1968b; Carnall *et al.*, 1968c; Carnall *et al.*, 1968d, Moore *et al.*, 2009). The commonly observed emissive levels are marked with closed tilted squares.

Lanthanides with their exceptional photoluminescent properties have created a wide range of applications in fields as broad as nuclear magnetic resonance (NMR) spectroscopy and magnetic resonance imaging (MRI), X-ray crystallography, lighting, optics, metallurgy, bio-organic chemistry, medical diagnostics, and imaging (Bünzli, 2006). The bioanalytical applications of lanthanide reporters are discussed in chapter 2.4. In these applications, the lanthanide-based reporters offer several advantages over conventional organic fluorophores. Firstly, the emission bands of lanthanide complexes are very narrow (line-like or atom-like emissions) with broad Stokes shifts sometimes ranging over 250 nm (Stokes shift here refers to the difference between the excitation and emission maxima; it

was first used in the context of fluorescent compounds where, unlike in lanthanides, the emission arises from the singlet states (Charbonniere, 2011)). In addition to enabling easy spectral discrimination of the emitted light, another advantage from this is that a multitude of lanthanide complexes can be packed in close vicinity without concentration quenching (Soini and Lövgren, 1987). Secondly, the excited state lifetimes of lanthanide-based reporters can extend up to several milliseconds. This is approximately six orders of magnitude as long as the lifetimes of organic fluorophores (Werts, 2005). The long lifetime allows the use of time-resolved detection in bioassays (Yuan and Wang, 2006) and in luminescence microscopy (Connally and Piper, 2008). Thirdly, lanthanide ions display substantially reduced photobleaching, and most lanthanide ions have multiple narrow emission bands. The latter property can be exploited in multiplexing (Kokko *et al.*, 2009; Geissler *et al.*, 2012), a trend increasingly used in modern bioassays. All in all, the lanthanide-based reporters provide a flexible, robust, and sensitive detection system to be used in various kinds of bioanalytical applications (Hemmilä and Laitala, 2005).

## 2.2 Electronic transitions of lanthanide complexes

### 2.2.1 Electronic structure, lanthanide ion sensitization, and quenching

Understanding of the lanthanide luminescence requires knowledge of the intricate excitation, energy transfer, and emission mechanisms involved in the process, and also of the vast number of energy levels related to the 4f orbitals (for example the number of electronic levels created by the [Xe]4f<sup>n</sup> electronic configurations in Eu<sup>3+</sup> and Tb<sup>3+</sup> is 3003 (Bünzli and Eliseeva, 2011)). Depending on how many electrons there are in the 4f orbitals, there are several ways to distribute these electrons, although some of the distributions are energetically favored over others. Figure 2 depicts the different interactions leading to the various energy levels (using Eu<sup>3+</sup> as an example). The electronic configuration is first divided into terms because of the repulsion between the electrons within the orbitals. This interaction is termed Coulombic interaction. The terms are then split into J-levels (see also Figure 1) because of spin-orbit coupling. These represent the free ion levels and are described by the term symbols S, L, and J with the formula  $^{2S+1}L_J$ , where 2S+1 is the spin multiplicity, L is the total orbital angular momentum, and J the total angular momentum of the f electrons. Because of the shielding of the 4f orbitals by the filled 5s and 5p sub-shells, the energies of the J-levels are well-defined, and the transitions between these levels are sharp, resulting in narrow, lanthanide-specific emission bands (Frey and Horrocks, 1995). If the lanthanide ion is in a coordinating environment (for example in an organic ligand or in an inorganic crystal structure), the J levels can be further split into sublevels because of the electric field of the matrix. These splittings may be seen as the fine structure of the main emission bands of the lanthanide ion (Bünzli, 2010).

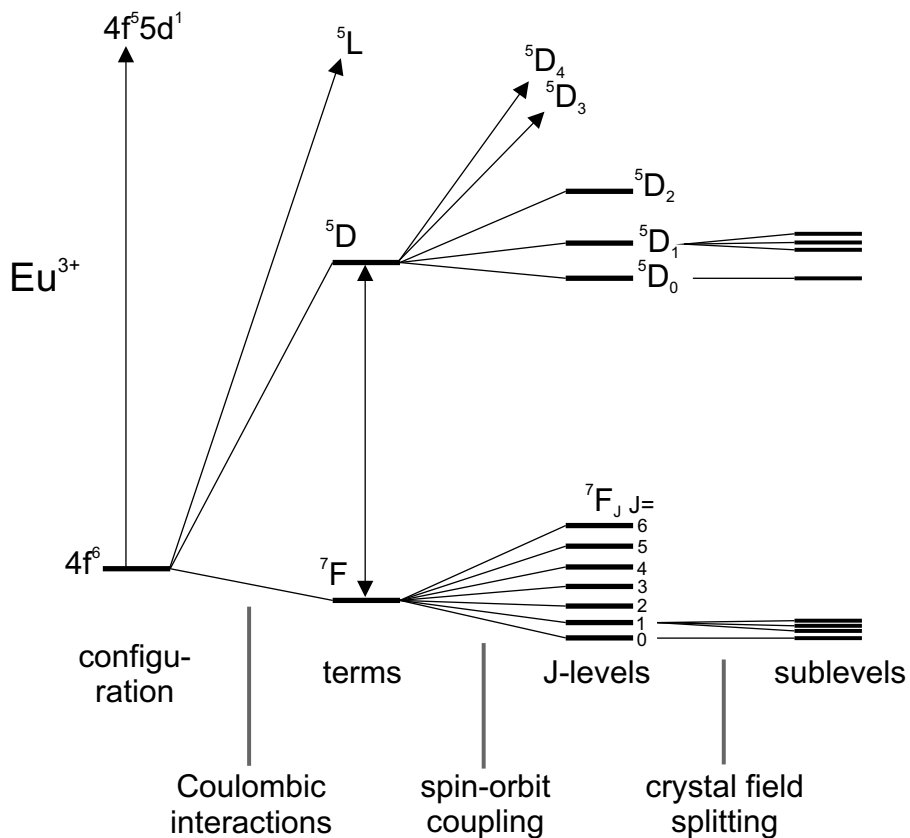


**Figure 2.** Diagram representing the interactions leading to the splitting of the electronic energy levels of a  $\text{Eu}^{3+}$  ion. In the diagram, energy increases when going up (adapted from Werts, 2005).

As with absorption, the emission of light is the result of two main types of transitions: the parity-allowed magnetic dipole (MD) transitions and the parity-forbidden electric dipole (ED) transitions. The so called Laporte selection rule forbids the ED transitions. Most of the transitions of the  $\text{Ln}^{3+}$  ions involve redistribution of electrons within the 4f sub-shell (intraconfigurational f-f transitions) being, therefore, formally forbidden. One consequence of this is that direct excitation of the lanthanide ions will only produce low levels of luminescence (the weak f-f transitions have absorption cross sections in the order of only  $1 \text{ M}^{-1} \text{ cm}^{-1}$ ). For this reason, lanthanide ions usually require indirect excitation, also called “sensitization of the metal-centered luminescence” or the “antenna effect” (Bünzli and Choppin, 1989; Selvin, 2002; Bünzli, 2006; Bünzli, 2010; Charbonniere, 2011). This means that the ion needs to be conjugated to a sensitizing structure. Usually this is a lanthanide chelate, an organic ligand containing a light absorbing chromophore structure (the sensitization in inorganic crystals is discussed in section 2.2.4) (Sabbatini and Guardigli, 1993). When a lanthanide ion is conjugated to a chemical complex (the ion is in a coordinating environment), the forbidden transitions become partly allowed. These transitions are called induced (or forced) ED transitions (Bünzli, 2010). Most of the absorption and emission bands of lanthanide complexes are the result of such induced ED transitions. Some f-f transitions are also allowed as MD transitions (such as the europium  $^5D_0 \rightarrow ^7F_1$  transition), while some transitions, e.g., most of the emission bands of  $\text{Tb}^{3+}$ , acquire strength by both ED and MD mechanisms (Bünzli and Choppin, 1989). Because

the ED transitions in lanthanide ions are induced by the ligand field, their intensities are rather sensitive to it. There are also some “hypersensitive” transitions, like the europium  $^5D_0 \rightarrow ^7F_2$ , whose strength is very sensitive to the nature of the ligand field (Richardson, 1982; Werts, 2005). Although the relative intensities, and also the fine structure of the major emission bands arising from the f-f transitions may vary, their spectral positions are not affected by the environment of the lanthanide ion. All in all, both the MD and the induced ED transitions of lanthanide ions are weak compared to the “fully allowed” transitions of organic chromophores. This gives rise to the long lifetimes of the lanthanide complexes (Bünzli and Choppin, 1989; Werts, 2005).

In addition to sensitization, another reason for conjugating of the lanthanide ion to a ligand structure is the protection of the ion from the quenching effects of the aqueous matrix. This is important, since lanthanide luminescence is efficiently quenched through non-radiative relaxation processes, especially through vibrational quenching caused by O–H vibrations. Water should thus be expelled both from the inner and the outer coordination sphere of the lanthanide ion. One should be especially careful with NIR luminescent ions, which are intrinsically very sensitive to vibrational quenching, as they have smaller energy gaps between their emissive and ground states (Eliseeva and Bünzli, 2010). Because of the large energy gap, terbium is not as susceptible to the quenching by O–H vibrations as most of the other lanthanides (Hemmilä and Laitala, 2005). However, terbium complexes may possess an energy back-transfer route from the emissive  $^5D_4$  level to an energetically close-lying ligand triplet state, which causes quenching of the luminescence and enhanced sensitivity to environmental conditions (Sabbatini and Guardigli, 1993; Hemmilä *et al.*, 1997; Alpha *et al.*, 1990). An energy difference of approximately 2500–3500 cm<sup>-1</sup> is needed to prevent this kind of back-transfer (Bünzli, 2010).

In addition to O–H vibrations, N–H and C–H vibrations can also cause quenching (Beeby *et al.*, 1999; Lis, 2002). Furthermore, interactions between matrix components in bioassays may also cause luminescence quenching. This may occur, for example, through Förster or Dexter type energy transfer (Dexter, 1953), ionic interaction (Mathis, 1993), d-block ions (Sabbatini *et al.*, 1988), metallic surfaces (Pérez-Luna *et al.*, 2002), or free radicals (Matko *et al.*, 1995). The long excited state lifetime of lanthanides causes them to have high probability for diffusion-related matrix quenching, as there is prolonged exposure to the quenching effects (Hemmilä and Laitala, 2005). A good way to reduce vibration-induced relaxation is to construct a rigid ligand field, free of any high-energy vibrations (Bünzli and Piguet, 2005). Interferences can also be circumvented by using a ratiometric measurement, by recording changes in lifetimes in addition to the changes in luminescence intensities, and by following the attenuation of the excitation light (Hemmilä and Laitala, 2005; Hemmilä, 1999). The efficiency of the sensitization process and shielding towards quenching effects can be studied by examining the luminescence from the ligand moiety, and by examining the sensitivity of the lanthanide ion luminescence to the presence of quenchers (such as oxygen) in the solution (Werts, 2005).

## 2.2.2 Ligand and lanthanide ion excitation

The ligand enhanced lanthanide luminescence is a complicated mechanism, but basically it occurs in three steps. First, the ligand absorbs the excitation light. Then the absorbed energy is transferred to the lanthanide ion (also called the central ion) and, finally, the ion

emits light (Bünzli and Piguet, 2005). In addition to the previously introduced central ion energy levels, there are also several ligand energy levels involved in the processes (de Sá *et al.*, 2000). Many of these processes are still not fully understood. Although this makes the designing of lanthanide-based reporters challenging, the complexity also creates opportunities for the development of these reporters (Hemmilä and Laitala, 2005). A simplified representation, e.g., a Jablonski diagram, can be used to illustrate the processes related to lanthanide luminescence. The energy levels in a Jablonski diagram are arranged vertically by energy and grouped horizontally by spin multiplicity. An example of a modified Jablonski diagram is depicted in Figure 3.

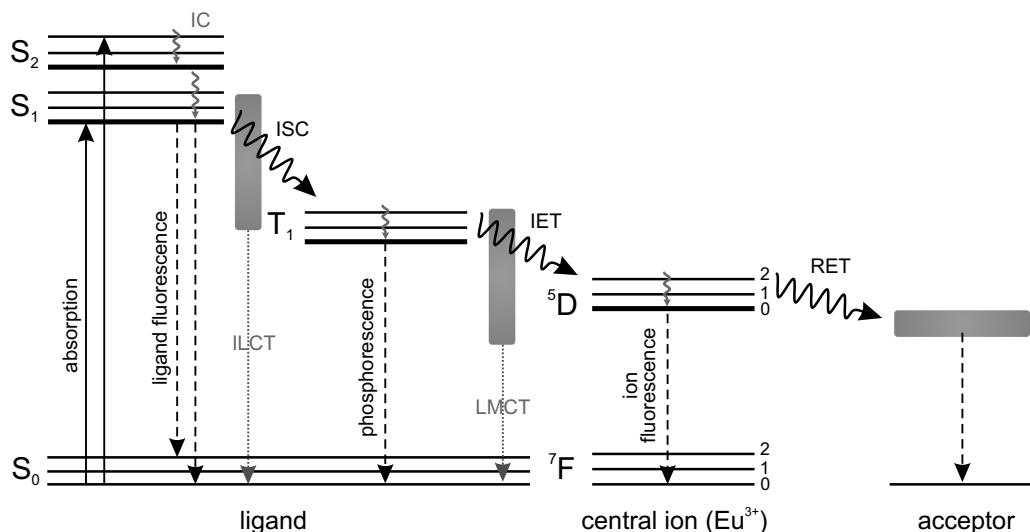


**Figure 3.** A simplified diagram depicting the energy flow in a ligand–europium complex. In the ligand, the bold horizontal lines represent electronic energy levels, and the thin lines vibrational energy levels. The solid arrows represent absorption of a photon, the wavy arrows non-radiative transition to excited energy levels, and the dashed arrows radiative emission. The gray dotted arrows represent charge-transfer transitions. The excitation and relaxation may end up to several different energy levels, but for simplicity most of these transitions have been omitted. In the vicinity of a suitable acceptor, the lanthanide ion may transfer its energy further to an acceptor fluorophore (see section 2.2.5). IC = internal conversion, ILCT = intra-ligand charge-transfer, ISC = intersystem crossing, LMCT = ligand-to-metal charge-transfer, IET = intramolecular energy transfer, RET = resonance energy transfer to an acceptor fluorophore.

The absorption of a photon is a very fast process (in the range of  $10^{-15}$  seconds). In the ligand–lanthanide complex the absorption usually occurs from the energetically lowest ground state, since in a non-excited molecule electrons tend to occupy these energetically lowest lying levels. Most lanthanide complexes are excited at near-UV range, the wavelengths rarely exceeding 350 nm. From the original excited singlet energy level of the ligand, the electrons may decrease non-radiatively via internal conversion (speed in the range of  $10^{-12}$  seconds) to some excited vibrational level, or to the lowest excited electronic level. The sensitization process may involve several ligand singlet and triplet states, and also intraligand charge-transfer (ILCT) states. Traditionally the energy flow is considered to go from the ligand singlet state to the ligand triplet state by intersystem crossing, and from the (lowest) ligand triplet state through intramolecular energy transfer to the excited energy levels of the central ion (Weissman, 1942; Crosby *et al.*, 1961; Werts *et al.*, 1999). In some cases, the singlet state may directly transfer energy to the central ion. This is,

however, not common, since the singlet state is short lived, and thus the process is not efficient (Bünzli and Piguet, 2005; Yang *et al.*, 2004).

There are two main mechanisms for the intramolecular energy transfer from the triplet state of the ligand to the central ion: the Dexter (electron exchange) mechanism and the Förster (dipole-dipole) mechanism (de Sá *et al.*, 2000). The Dexter mechanism involves a mutual electronic exchange between the ligand and the central ion (Dexter, 1953), requiring physical contact between the two components. On the other hand, in the Förster mechanism, the triplet state transition dipole moment associates with the dipole moment of the 4f orbitals. For this reason, the Förster mechanism does not require physical contact between the components, and therefore functions at longer distances compared to the Dexter mechanism (Förster, 1948; Leonard *et al.*, 2007). In addition to these main mechanisms, there are also other mechanisms for exciting the central ion, e.g., the metal-to-ligand charge-transfer (MLCT) from chromophores containing d-transition metal ions (Faulkner *et al.*, 2009) and the ligand-to-metal charge-transfer (LMCT) (Blasse, 1976). The charge-transfer transitions are allowed, but they require high energies (Bünzli, 2006) being most prominent with Sm<sup>3+</sup>, Eu<sup>3+</sup>, and Yb<sup>3+</sup>, as these are the most easily reduced ions. When utilizing the LMCT states to transfer energy to the excited 4f-states of the lanthanide ion, it has to be noted that the energy of the LMCT state should be high enough compared to the emitting energy level of the ion to minimize quenching of the luminescence (Sabbatini, 1987; Petoud *et al.*, 1999).

In addition to the f-f transitions and charge-transfer transitions, lanthanide ions also display a third type of electronic transitions: the f-d transitions, meaning the promotion of a 4f electron into the 5d sub-shell (Zolin *et al.*, 2004). The f-d transitions are allowed, broader than f-f transitions, and (contradictory to f-f transitions) their spectral position largely depends on the ligand field. However, these transitions require high energies (only those of the easily oxidized ions Ce<sup>3+</sup>, Pr<sup>3+</sup>, and Tb<sup>3+</sup> are commonly observed), being usually irrelevant for bioapplications (Bünzli, 2006).

### **2.2.3 Non-radiative and radiative relaxation of excited lanthanide ions**

The lanthanide ion can usually accept energy through several of its excited J-levels, if they lie energetically below the energy donating level. For example, Eu<sup>3+</sup> primarily accepts energy through its <sup>5</sup>D<sub>1</sub> and <sup>5</sup>D<sub>2</sub> levels above the emissive <sup>5</sup>D<sub>0</sub> level (Latva *et al.*, 1997; Hemmilä *et al.*, 1997; Gutierrez *et al.*, 2004). Tb<sup>3+</sup>, however, accepts energy directly by its emissive level, <sup>5</sup>D<sub>4</sub>. From the higher excited energy levels the excitation energy quickly relaxes non-radiatively through vibrations of the surrounding matrix. In glasses and crystals this process is known as multiphonon relaxation (Weber, 1973). The similar relaxation process in lanthanides complexed with organic ligands is even more pronounced, as in organic media such high-energy vibrations are more ubiquitous (Horrocks and Sudnick, 1981; Beeby *et al.*, 1999). The efficiency of this non-radiative relaxation is inversely proportional to the number of vibrational quanta (phonons) needed to bridge the gap between two participating energy levels (radiative emission will efficiently compete with the non-radiative relaxation processes if the energy gap equals a minimum of approximately six quanta of the highest energy vibration present in the molecule (Bünzli, 2006)). The efficient non-radiative relaxation between close-lying excited energy levels causes the luminescence of a lanthanide ion to almost exclusively occur from the lowest excited energy level having the largest gap to the next lower ground state level (Werts, 2005).

From this emissive J-level, the energy can then radiatively relax to the ground state multiplet giving rise to the emission bands. The transition may occur to several of the ground state sublevels, but usually some are favored over others. From the higher ground state sublevels, the energy may finally dissipate non-radiatively to the lowest sublevel. The non-radiative relaxation in the excited and ground state multiplets radically limits the number of lanthanide ion emission bands. Radiative emission can also occur from the upper excited energy levels above the emissive level, but the intensities are very low, and these transitions can be detected only from strongly luminescent complexes. The radiative relaxation from the central ion is called ion fluorescence (although formally fluorescence refers to transitions occurring without change in spin, and phosphorescence to transitions involving a change in spin (Melhuish, 1984)), and it has an ion-specific profile (Hemmilä and Laitala, 2005).

There are two essential spectroscopic parameters that characterize the luminescence emission from a lanthanide ion: the luminescence quantum yield ( $Q$ ) and the lifetime of the excited state ( $\tau$ ) (Bünzli, 2010). The quantum yield can be simply defined as:

$$Q = \frac{\text{number of emitted photons}}{\text{number of absorbed photons}} \quad (1)$$

However, it has to be noted that sensitized lanthanide luminescence is a two-step process. First, the ligand absorbs a photon and transfers the energy to the central ion. This step has its finite probability ( $Q_{\text{transfer}}$ ). Second, the excited lanthanide ion emits with some probability, which can be called the intrinsic or lanthanide centered quantum yield,  $Q_{Ln}$  (referring to the luminescence efficiency upon direct excitation into the 4f-levels). The overall probability of this two-step process ( $Q_{\text{total}}$ ) is the product of the probabilities of the two steps (Selvin, 2002):

$$Q_{\text{total}} = Q_{\text{transfer}} \times Q_{Ln} \quad (2)$$

As indicated in section 2.1, the intrinsic quantum yield depends on the energy gap between the emissive energy level of the lanthanide ion and the highest sublevel of its ground state multiplet. The smaller the gap is, the easier it is to bridge by non-radiative relaxation processes.

Lanthanide complexes generally have very long excited state lifetimes. From the excited state, the lanthanide ion returns to the ground state either radiatively (through the emission of photons) or non-radiatively. The former is characterized with a rate constant  $k_{\text{rad}}$ , and the latter with a rate constant  $k_{\text{nr}}$ . The intrinsic quantum yield and lifetime of the excited state are related by the following equation,

$$Q_{Ln} = \frac{k_{\text{rad}}}{k_{\text{rad}} + k_{\text{nr}}} = \frac{\tau}{\tau_{\text{rad}}} \quad (3)$$

where  $\tau_{\text{rad}}$  refers to the lifetime in the absence of non-radiative transitions.  $\tau_{\text{rad}}$  is characteristic of one emitting state, so if several excited states emit light, then each of these have their own characteristic  $\tau_{\text{rad}}$ . Based on equation 3, knowing  $\tau_{\text{rad}}$  can give access to  $Q_{Ln}$ . However, it is advisable not to use the  $\tau_{\text{rad}}$  values found in literature to estimate  $Q_{Ln}$ , as

these values are not constant for a given lanthanide ion and a given electronic level, but are dependent on the refractive index (Bünzli, 2010; Charbonniere, 2011). The  $\tau$  of a lanthanide complex in water can be used to calculate its hydration number (number of water molecules in the first coordination sphere) by comparing the  $\tau$  values in H<sub>2</sub>O and D<sub>2</sub>O (Horrocks and Sudnick, 1979).

## 2.2.4 Lanthanide luminescence in solid crystal hosts

Lanthanide-containing inorganic solid phosphorescent materials (also called inorganic phosphors) are composed of lanthanide guest ions held in place by a crystalline host lattice. The lattice matrix is normally based on oxides, fluorides, sulfides, or phosphates. There are usually two types of lanthanide ions present in the matrix: sensitizer and activator ions. The sensitizer ions absorb the excitation energy and transfer it to the activator ions, which produce the emission. Sometimes, however, the sensitizer ions are not needed, as the host lattice or the activator ions absorb the excitation energy (Blasse and Grabmaier, 1994). The lanthanide-doped inorganic materials may be categorized as downconverting or upconverting. Those that absorb a single high-energy photon and emit a lower energy photon are downconverting. Upconverting materials, on the other hand, sequentially absorb two or more low energy photons and emit one higher energy photon (Dosev *et al.*, 2008; Zijlmans *et al.*, 1999). The principles of down- and upconversion are illustrated in Figure 4.

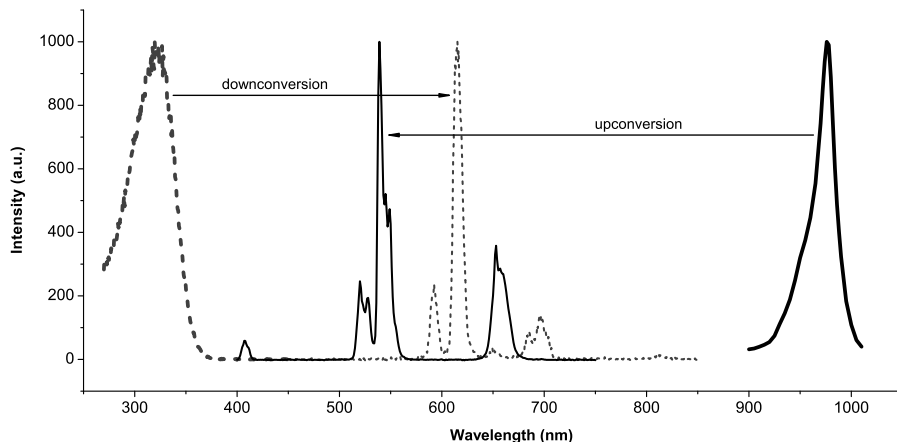


**Figure 4.** Basic principle of downconversion and upconversion photoluminescence exemplified with the excitation spectra (thick) and emission spectra (thin) of a Eu<sup>3+</sup>-chelate (dotted) and a NaYF<sub>4</sub>:Yb<sup>3+</sup>,Er<sup>3+</sup> upconverting nanocrystal (solid) (adapted from Soukka *et al.*, 2005).

The luminescence spectra of lanthanide ions differ greatly in gaseous, liquid, and solid states. The solid state spectra are, in a way, an intermediate between the two extremes of gaseous and liquid state spectra. In gaseous state spectra, the emission bands extend to very high energies, and there is no crystal field splitting because of the absence of vibronic structures. In the solution spectra, on the other hand, there are broader bandwidths (~10 nm) and much fewer multiplet states than in the gaseous spectra because of the presence of high-energy vibrations. Compared to the gaseous state, the solid state spectra also have broad bandwidths, and compared to the liquid state, in a host lattice the interionic non-radiative relaxation rate is smaller because of the minimized energy transfer between the isolated lanthanide ions. The intra-ionic non-radiative multiphonon relaxation

is also less pronounced, since there are fewer high-energy vibrations in the crystal lattice. When a lanthanide ion resides in a solid crystal host, the spherical symmetry of the ion is destroyed, and the  $^{2S+1}L_J$  multiplet level can be split up to  $2J+1$  crystal field levels (for non-Kramers ions, i.e., ions that have an even number of electrons and an integral total angular momentum  $J$  (Harris and Furniss, 1991)) (Tanner, 2011).

Just as in organic ligand structures, the lanthanide luminescence in solids can occur via different types of electronic transitions, which all greatly differ in spectral intensity and bandwidth. The main types of transitions in solids are intraconfigurational f-f transitions, band-to-band transitions, interconfigurational f-d transitions, charge-transfer transitions, and transitions resulting from defect sites and impurities. The band-to-band transition refers to the transition from a valence band (VB) to a conduction band (CB). In low band-gap hosts (like oxides or chlorides), the band-to-band transition of the host crystal overlaps with the f-f transitions, and the luminescence does not occur from the overlapping and higher 4f-levels. However, strong luminescence may occur from lower 4f-levels, because of the efficient energy transfer between the host and the lanthanide ion. The use of the intense band-to-band transitions has been eagerly studied with semiconductors to be able to sensitize lanthanide ions, but there have been complications especially with materials such as TiO<sub>2</sub> and ZnO. In f-d transitions, the emission bands are typically broad as a result of the overlapping electronic transitions and the unresolved vibrational progressions. A useful feature is that if the energy of the lowest  $4f^{n-1}5d$  level of a lanthanide ion in one host is known, the lowest  $4f^{n-1}5d$  energy level can be estimated for another lanthanide ion in the same host (Dorenbos, 2000). In the charge-transfer transitions of a crystal, the trivalent lanthanide ion receives an electron from the VB leaving a hole behind, and the resulting divalent ion becomes highly vibrationally excited. The position of the charge-transfer emission band shifts to higher wavelengths with increasing covalency of the host lattice and with increasing size of the cation site (van Pieterson *et al.*, 2000). Lastly, in a crystal host, transitions resulting from defect sites and impurities exist. The imperfections always present in crystals result in defect sites where the lanthanide ions can reside. Alternatively, the ions may have different phases, or they may be coordinated to ions like OH<sup>-</sup> on the crystal surface. The defect sites and different phases give rise to the broadening of the emission bands. The coordination to surface ions, on the other hand, results in luminescence quenching. A good way to study the purity of the material is to excite it with light of different wavelengths, each strongly exciting only a single phase. The material should also be free from impurities of unwanted lanthanide ions. These impurities can usually be easily detected, as all lanthanide ions have a characteristic emission spectrum (Tanner, 2011).

The upconverting crystal materials (also called upconverting phosphors, UCPs) are a special type of solid luminescent materials (see Figure 4), and they have increasingly aroused interest in recent years. In UCPs, the sensitizer ion is frequently Yb<sup>3+</sup>, and the activator ions are mostly either Er<sup>3+</sup>, Tm<sup>3+</sup>, or Ho<sup>3+</sup>. The host lattice composition of UCPs should be carefully considered, as it is important in minimizing unwanted radiative processes (Tanner, 2011). One of the most efficient materials for upconversion known to date is hexagonal NaYF<sub>4</sub> doped with Yb<sup>3+</sup> and Er<sup>3+</sup> (Suyver *et al.*, 2005). This material gives emission in the blue, green, and red wavelength regions. The relative intensities of the emission bands of upconversion materials depend on several factors, including temperature and dopant ion concentration (Vetrone *et al.*, 2004; Tanner, 2011). The upconversion mechanism in UCPs clearly differs from, and is considerably more efficient

than simultaneous two-photon excitation (Lakowicz, 1997; Soukka *et al.*, 2005). In UCPs, the absorption of the photons is non-coincident, made possible by the long-lifetime excited states of lanthanides, which can operate as metastable energy levels. Thus, UCPs can be efficiently excited even at relatively low excitation power densities (Haase and Schäfer, 2011), and instead of the common UV excitation sources used with lanthanide chelates, compact, efficient, and inexpensive NIR laser diodes can be used (Soukka *et al.*, 2005). However, with even the most efficient upconversion materials, the luminescence efficiency is limited if moderate light intensities are used. This is due to the weak and narrowband NIR absorption. Recently, Zou and coworkers have demonstrated that the upconversion luminescence efficiency can be dramatically enhanced by using organic NIR-dyes as sensitizers to increase the absorption of infrared light by the upconversion material (Zou *et al.*, 2012). The upconversion process itself may proceed through several different mechanisms, including second harmonic generation, two-photon absorption, ground state absorption/excited state absorption, photon avalanche, and energy transfer upconversion. These mechanisms are not discussed in more detail in this review. Thorough reports in this area exist (Auzel, 2004; Güdel and Pollnau, 2000; Gamelin and Güdel, 2000; Tanner, 2011). The advantages of the down- and upconverting nanomaterials, as well as their synthesis and surface modification methods, are discussed in more detail in chapter 2.3.4, and the bioanalytical applications of these materials are reviewed in chapter 2.4.

## 2.2.5 Resonance energy transfer to an acceptor fluorophore

An excited lanthanide ion, instead of returning to its ground state by non-radiative relaxation or ion fluorescence, may also transfer its energy non-radiatively to a suitable acceptor fluorophore. This process is known as fluorescence resonance energy transfer or Förster resonance energy transfer, FRET (after the German scientist Theodor Förster) (Förster, 1948). As lanthanide emission is formally not fluorescence (result of a singlet-to-singlet transition), and as this energy transfer process is always non-radiative, it is sometimes called luminescence resonance energy transfer or lanthanide-based resonance energy transfer, LRET. Sometimes it is also simply called RET for resonance energy transfer. In this review, however, the term FRET is used. In this process, the excited donor produces an oscillating electric dipole field, and a nearby acceptor with suitable energy levels corresponding to the frequencies of the donor electric field receives the energy becoming excited (Selvin, 2002).

The electric field produced by both lanthanides and organic fluorophores has the same distance dependence,  $R^{-3}$  (at distances shorter than the wavelength of light, the electric field fades away at this rate). The FRET phenomenon thus leads to the overall distance dependence of  $R^{-6}$  (Selvin, 2002) making FRET the prevailing energy transfer mechanism in a distance range of approximately 1–10 nm (Förster, 1948; Stryer, 1978), and making FRET a useful spectroscopic ruler (Stryer and Haugland, 1967). This is a relevant distance range in many *in vitro* and *in vivo* studies in physiological conditions, making FRET a very widely used tool in these applications (Clegg, 1995; Fairclough and Cantor, 1978; Selvin, 1995; Selvin, 2000; Hemmilä, 1999). In addition to the requirement of close proximity between the donor and acceptor fluorophores, there are also other requirements that need to be fulfilled for FRET to occur. One requirement is an appropriate alignment between the donor emission dipole moment and the acceptor absorption dipole moment (represented by the orientation factor value,  $\kappa^2$ ). This is necessary because the electric field of the donor may be polarized (Selvin, 2002).

According to the traditional definition of FRET, yet another requirement is a substantial spectral overlap between the donor emission and acceptor excitation spectra. However, according to recent studies, this is not an absolute requirement for non-radiative energy transfer, since a phenomenon termed non-overlapping FRET (nFRET; also called anti-Stokes shift FRET) has been described (Laitala and Hemmilä, 2005a; Laitala and Hemmilä, 2005b). The nFRET phenomenon is based on non-radiative energy transfer between a lanthanide donor and a spectrally non-overlapping acceptor. This means that the acceptor is excited at a higher energy level than where the donor has its main emissive transitions. The phenomenon has been reported with europium and samarium, but not thus far with terbium. Laitala and Hemmilä have proposed the energy transfer to arise from the upper excited energy levels of europium ( $^5D_1$  and  $^5D_2$ ) above the emissive  $^5D_0$  energy level, but a decisive mechanism has not yet been presented. Although nFRET and conventional FRET share some common characteristics, such as the requirement for close proximity between the donor and acceptor fluorophores, the nFRET mechanism has been shown to differ from FRET in several aspects. These include the duration and number of lifetimes observed for the sensitized acceptor emission, the dependence of energy transfer efficiency on the donor quantum yield, the distance dependence between the donor and acceptor, and the temperature dependence (Laitala and Hemmilä, 2005a; Laitala and Hemmilä, 2005b; Vuojola *et al.*, 2011). These features have implications also for bioassays. The most profound benefit of nFRET is the anti-Stokes energy transfer that eliminates the background originating from direct donor emission and from the reabsorption of donor emission by the acceptor, thereby enabling low detection limits. Furthermore, in nFRET the reduced dependence of energy transfer efficiency on the spectral overlap and donor quantum yield increases the choice of suitable fluorophores to be used in the assays. A disadvantage of the strong distance dependence in nFRET is that the effective range and thus the distances that can be studied are reduced compared to FRET. The nFRET phenomenon is discussed in more detail in chapter 5.1.

The lanthanide-based FRET (and nFRET) has several advantages over techniques that use conventional organic fluorophores. The most prominent advantage is the long donor lifetime that causes the lifetime of the sensitized (induced) acceptor emission to become substantially elongated (energy transfer also reduces both the emission intensity and the excited state lifetime of the lanthanide donor, which may be useful to be monitored in some applications). By utilizing spectral discrimination and time-resolved detection, the sensitized emission arising from the donor-acceptor energy transfer can be discriminated from all interfering sources of light: matrix autofluorescence, stray light, donor cross-talk, and directly excited acceptor fluorophores. This efficient background discrimination results in high sensitivity enabling the detection of very small analyte concentrations. It also enables the minimization of reagent usage. Other advantages of lanthanide-based FRET include strong emission signals and the accurate determination of distances due to reduced uncertainty in the  $\kappa^2$  value (Selvin, 2002). This reduced uncertainty results from the depolarization of the acceptor emission, which is a result of the long emission lifetime (Stryer, 1978). A minor disadvantage of the time-resolved detection is that it requires a slightly more complicated instrumentation compared to conventional steady-state fluorometers (Selvin, 2002).

FRET can also be used in conjunction with nonfluorescent acceptors. In this case the assays are usually called fluorescence quenching assays (FQA). Applications can be found among others in enzyme activity assays (Ylikoski *et al.*, 2004; Karvinen *et al.*, 2002).

Another variation from the conventional FRET is the use of co-fluorescence enhancement (Xu *et al.*, 1992a; Xu *et al.*, 1992b). It takes advantage of chelate-to-chelate energy transfer from “inert” metallic ions (for example gadolinium or yttrium provided in excess) to lanthanide ions complexed with chelating ligands. Together these components form small aggregates where efficient chelate-to-chelate energy transfer occurs from the inert metal ion to the luminescent lanthanide, which can result in considerably increased excitation efficiencies (Hemmilä and Laitala, 2005).

## 2.3 Luminescent lanthanide reporters

### 2.3.1 Desirable features

Research in the area of lanthanide reporters has been very extensive during the last two decades, and has produced a vast amount of information on the synthesis methods and applications of lanthanide-based reporters. The synthesis procedures are already relatively well managed, and the photophysical and biochemical properties can be sufficiently controlled (Bünzli, 2006), although many challenges still remain.

The main aim in designing luminescent lanthanide reporters is to find a structure that retains the incorporated lanthanide ion (or ions) brightly luminescent while keeping the material intact and, when necessary, introduces functions for bioconjugation. More specifically, the complex should preferably be water soluble, non-toxic, kinetically inert, photostable (resistant to photoinduced destruction), and thermodynamically stable, especially if it is used for *in vivo* experiments. Photostability of the lanthanide reporter is important, although lanthanide reporters should generally have considerably better photostability compared to organic fluorophores, as the excitation energy very quickly passes from the organic ligand to the lanthanide ion. The reporter complex should also have a suitable protective structure for the lanthanide ion (to minimize non-radiative relaxation), strong absorption of excitation energy, efficient sensitization of the lanthanide luminescence, high quantum yield, and long excited state lifetime (Werts, 2005; Bünzli, 2010). From the application point of view, the spectral properties should be suitable, and from the industrial point of view, the synthesis and final analytical characteristics of the compound should be reproducible. Lastly, the compound should be stable in storage and handling (Mathis and Bazin, 2011).

The requirement for strong absorption of excitation energy can be achieved, for example, by incorporating into a ligand structure an organic chromophore with a high molar absorption cross section (in a suitable spectral region). As discussed in section 2.2.1, free lanthanide ions, unlike most organic dyes, have intrinsically very low molar absorption cross sections, and thus require sensitizing structures. The lower limit for the excitation is approximately 300 nm, as at shorter wavelengths there is strong absorption by the aromatic amino acids in proteins. In addition, the optical materials above this wavelength area (non-quartz optics) are less expensive. In *in vivo* assays, the longer wavelengths also minimize damage to biomaterials. The upper limit for the excitation is determined by the lanthanide ion itself. To obtain efficient sensitization, the energies of the singlet and triplet excited states of the ligand should be optimized for the chosen lanthanide (Charbonniere, 2011). For europium and terbium, this means that only ligands absorbing in the UV or at slightly longer wavelengths can normally be used, although longer wavelengths would be preferred. Some reports of lanthanide complexes with high excitation maxima have been

published (Werts *et al.*, 1999). Recently Valta *et al.* have shown a ligand structure enabling the efficient excitation of europium at wavelengths up to 450 nm in micellar solutions (Valta *et al.*, 2012).

The strive towards improved lanthanide complexes has led to a great number of different scaffolds and approaches. There is a multitude of molecular multidentate lanthanide complexes reported. More recently, the interest in luminescent nanoparticles has also increased. These particles may be composed of various different substances, such as polystyrene, silica-based compounds, or inorganic crystal materials. Lanthanides are very well suited for nanoparticles, as they display minimal concentration quenching (Soukka and Härmä, 2011). The different lanthanide reporter classes will be discussed in the following sections.

### 2.3.2 Lanthanide chelates

To obtain reporters with the desirable features discussed in the previous section, a vast amount of different multidentate lanthanide complexes have been synthesized. These complexes are also collectively called lanthanide chelates, referring to the multiple coordination bonds forming between the organic structure and the central ion. As mentioned in section 2.2.1, these complexes contain a sensitizing conjugated chromophore moiety (antenna ligand) and a moiety that coordinates the central ion (lanthanide ion carrier chelate) (Hemmilä and Mukkala, 2001; Tsukube and Shinoda, 2002; Tsukube *et al.*, 2002). The development of these reporters and the instrumentation required for the time-resolved detection of their emission began already in the early 1980s (Ekins and Dakubu, 1985; Siitari *et al.*, 1983; Soini and Lövgren, 1987). Soon after, a commercial application known as the dissociation-enhanced lanthanide fluoroimmunoassay (DELFIA<sup>®</sup>) was developed (Hemmilä *et al.*, 1984). It entailed the use of a nonfluorescent lanthanide complex from which the lanthanide ion was dissociated with the help of a low pH “enhancement solution”. This solution also contained chelating structures that were able to bind the dissociated lanthanide ions and form highly fluorescent complexes in the presence of non-ionic detergents. After this approach, also intrinsically fluorescent lanthanide chelates suitable for bioconjugation were developed (Alpha *et al.*, 1987; Takalo *et al.*, 1994; Takalo *et al.*, 1997).

The most commonly used antenna ligands in lanthanide chelates are based on pyridine, bipyridine, terpyridine, salicylate, and phenanthroline, or on the derivatives of coumarin, pyrazole, triphenylene, and quinoline. A large number of the lanthanide ion carrier chelate structures, on the other hand, are composed of polyacid and macrocycle structures (Hemmilä and Laitala, 2005; Bünzli and Piguet, 2005; Selvin and Hearst, 1994). There are various ways to subdivide lanthanide chelates into groups. One is related to the way the antenna ligand is connected to the lanthanide ion carrier chelate. Based on this, the structures can be divided into those with the antenna ligand directly involved in coordination, and those where it does not participate in coordination (antenna ligand and lanthanide ion carrier chelate form distinct entities). Examples of these are given in Figure 5.

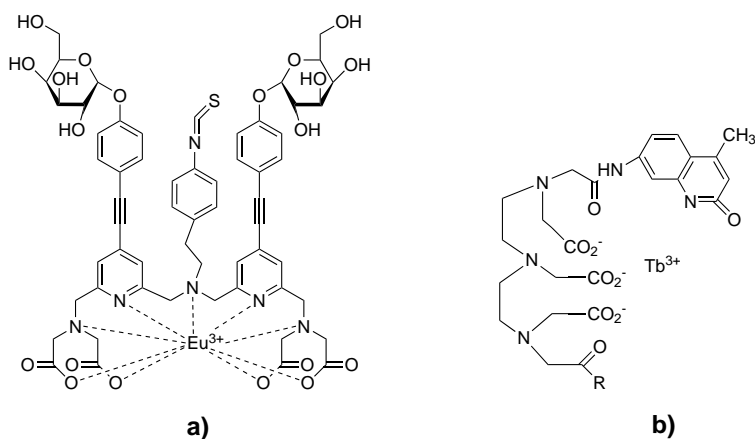


**Figure 5.** Examples of structures where the antenna ligand either (a) participates or (b) does not participate to coordination of the central ion (von Lode *et al.*, 2003; Selvin and Hearst, 1994).

Another division can be made into linear polydentate structures, macrocyclic structures, self-assembling structures, and podand structures (Bünzli and Piguet, 2005). Examples of these structures are given in Figure 6. The first group comprises of structures based on scaffolds, e.g., ethylene diamine tetraacetic acid (EDTA), diethylene triamine pentaacetic acid (DTPA), and triethylene tetraamine hexaacetic acid (TTHA) (Mathis and Bazin, 2011). The basic idea in the second group, macrocyclic structures, is to build a pre-organized cavity with several donor atoms for coordinating the lanthanide ion. The cavity diameter of the macrocycle should be tuned to match the size of the used ion. The macrocyclic structures can be based on, for example, phthalocyanines, porphyrins, coronands, and cryptands (Bünzli and Piguet, 2005; Izatt *et al.*, 1985). The third group takes advantage of both the high electric field generated by the lanthanide ions and the weak intermolecular interactions to self-assemble small coordinating units around the lanthanide ion. With this approach novel one-, two-, and three-dimensional functional edifices can be created (Stang and Olenyuk, 1997; Bünzli and Piguet, 2002; Piguet *et al.*, 2005; Bünzli and Piguet, 2005). The fourth group, called podands, consists mostly of acyclic structures with functionalized pendant arms which coordinate to the lanthanide ion. There are, for example, tripodal and tetrapodal structures (Bünzli and Piguet, 2005; Weibel *et al.*, 2004; Charbonniere *et al.*, 2006; Petoud *et al.*, 2003; Samuel *et al.*, 2008).

When constructing a lanthanide chelate reporter, the organic ligand is usually synthesized first, and the lanthanide ion is introduced afterwards. The complex formation is normally driven by the positive entropy change with the decreasing hydration level (some cage-like constructs, however, may need activation energy to bring the ion into place). This is why it is useful to utilize polydentate ligands occupying as many lanthanide ion coordination sites as possible (in solutions coordination numbers usually range from 8 to 9 (Werts, 2005)), to form a saturated inner coordination sphere. The donor atoms in these polydentate structures participate in forming the coordination bond instead of water molecules, which would cause quenching of the luminescence. These donor atoms are preferably oxygen or nitrogen in coordinating groups such as carboxylic acids, amides, or pyridines. It should also be noted that to maximize the energy transfer from the ligand to the central ion, their distance should be minimal, with the chromophore preferably directly bound to the ion (Bünzli, 2006; Werts, 2005).

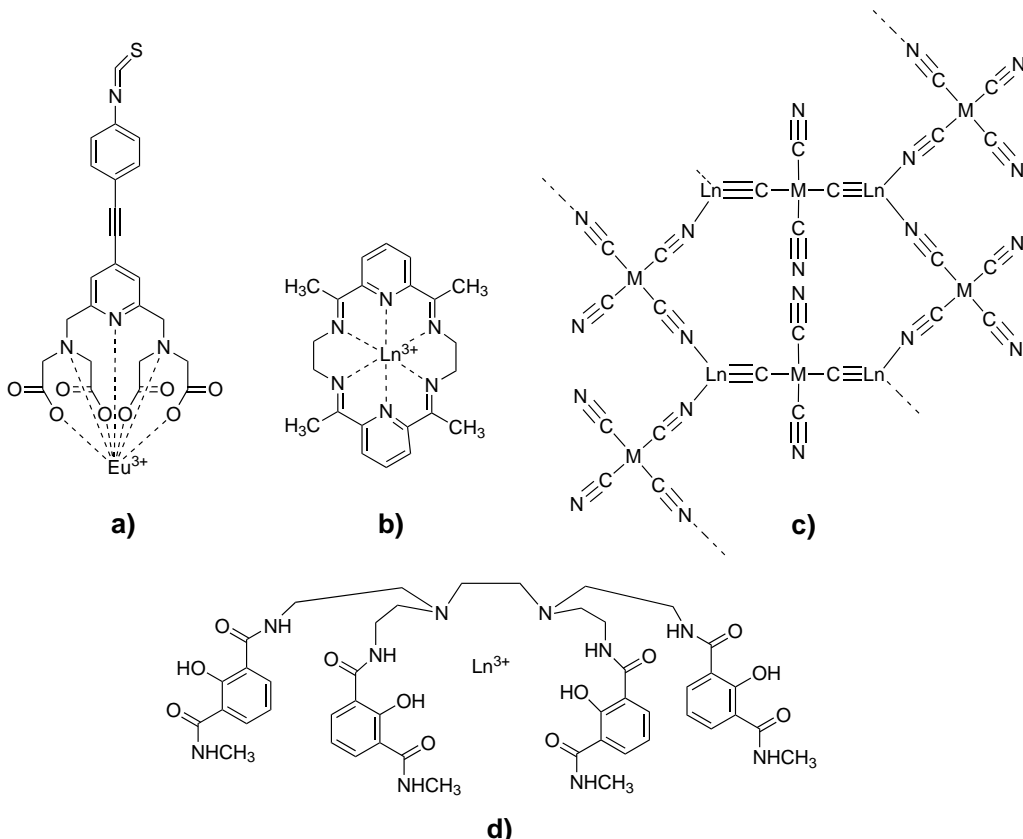


**Figure 6.** Examples of multidentate lanthanide chelates in the categories of (a) linear polydentate structures, (b) macrocyclic structures, (c) self-assembling structures, and (d) podand structures (Takalo *et al.*, 1994; De Cola *et al.*, 1986; Bünzli and Piguet, 2002; Petoud *et al.*, 2003).

The use of lanthanide chelates in bioanalytical applications commonly requires the introduction of a reactive group that can be used to conjugate the reporter to the biomaterial of interest. Several different functions can be used to achieve this: i) chlorosylfonyl (when activated, reacts with amines to form sulfonamines), ii) isothiocyanate (when activated, reacts with amines to form thiourea derivatives), iii) (4,6-dichloro-1,3,5-triazin-2-yl)amino (when activated, reacts with amines to form covalent bonds), iv) N-hydroxysuccinimide (NHS) ester (when activated, reacts with amines to form stable amide bonds), v) phosphoramidite (when activated, reacts with hydroxyl groups, for example, at the 5'-end of an oligonucleotide to form phosphite bonds), and vi) thiol (when activated, reacts with another thiol to form a disulfide bond). In addition to these, there are also some other less common coupling reactions, such as the cycloaddition reactions referred to as “click chemistry”. One such addition is the reaction between an alkyne and an azido group to form a 1,2,3-triazole. When using this reaction, it should be noted, however, that the often used copper catalyst may compete with the lanthanide ion for the coordination (Charbonniere, 2011).

The different lanthanide chelates have their own advantages and disadvantages. Generally, the chelates filling as many lanthanide ion coordination sites as possible lead to more thermodynamically stable and strongly luminescent compounds. Unlike with europium,

which forms strongly luminescent complexes with chromophores based on six-membered pyridine rings, with terbium more strongly luminescent complexes can be obtained by using five-membered rings, e.g., pyrazole, imidazole, or triazole. The selected ion also influences the lifetime of the complex, which can range from upper nanosecond scale with ytterbium, neodymium, and erbium chelates up to a few milliseconds with europium and terbium chelates (Hemmilä and Mukkala, 2001). Sugar moieties in the structure can be used to aid in water solubility (von Lode *et al.*, 2003), and high chemical stability is provided, for example, by the cage-like chelates called cryptates (Bazin *et al.*, 2002). If high sensitivity is needed, a novel approach based on a phenomenon called chelate complementation can be used, which utilizes switchable lanthanide luminescence. There the antenna ligand and the lanthanide ion carrier chelate are two completely separate moieties that, when free in solution, are nonluminescent. After controlled binding (to, for example, an analyte of interest) they form a strongly luminescent complex (Karhunen *et al.*, 2011; Lehmusvuori *et al.*, 2012). The ever increasing number and wide applicability of the lanthanide chelates ensure that this class of lanthanide reporters will continue to be very important also in the future.

### **2.3.3 Lanthanide-dyed nanoparticles**

In this section, both organic and inorganic nanoparticles are described which may either have a shell with a hollow interior, or may contain a solid matrix. Also biological nanoparticles are briefly mentioned. The next section will continue with particulate reporters, but will deal with inorganic up- and downconverting nanoparticles having a crystal structure.

The first report of particulate labels dyed with lanthanide chelates was introduced in 1978 (Frank and Sundberg, 1978). However, it took several decades before these reporters were recognized as being advantageous in bioassays (Härmä *et al.*, 2001). Since then, lanthanide-based nanoparticle reporters have been extensively used in various fields of bioanalytics fuelled by their useful chemical and photophysical properties compared to molecular reporters. Particulate reporters in general have high specific activity, which is useful when high sensitivity is needed, or miniaturized assay concepts are used. They also feature enhanced binding capacity, high stability, and usually also relatively low overall cost of the label material and detection instrumentation. Lanthanide-based nanoparticle labels in particular have some additional advantages relating to the properties of the lanthanides. They have several sharp and well-separated emission bands (band-widths as small as 10 nm) and large Stokes shifts. They are also highly stable against photobleaching and photochemical degradation, their toxicity is low, and they do not exhibit blinking. Lanthanide chelates exhibit minimal concentration quenching, which is also an important prerequisite for the formation of highly luminescent nanoparticles. Because of their large size, particulate reporters are susceptible to steric and kinetic hindrances and, therefore, may not be suitable for all types of applications. Nonetheless, they provide features that are not attainable with molecular reporters (Soukka and Härmä, 2011).

One very commonly utilized approach to obtain lanthanide-dyed nanoparticles is to pack lanthanide chelates inside a small polystyrene shell. Such reporters are commercially available for example from Seradyn Inc. (currently part of Thermo Scientific) and, for example, the 107-nm particles can have over 30 000 europium  $\beta$ -diketone chelate molecules packed inside a single shell (Härmä *et al.*, 2001). The shell of a polystyrene

particle produces a hydrophobic environment around the chelates protecting them from the quenching effects of the aqueous environment and from other detrimental effects. Kokko and coworkers studied the effect of pH and the presence of metal ions on the fluorescence of both europium chelate-dyed nanoparticles and free lanthanide chelates (Kokko *et al.*, 2007). They concluded that nanoparticles are preferred labels over individual chelates in homogeneous bioaffinity assays, when interfering compounds are known to be present. In addition to dyeing the shells with lanthanide chelates after the polymerization is complete, the chelates can also be embedded during the polymerization (Chen *et al.*, 1999; Tamaki and Shimomura, 2002). This approach has been used to prepare polystyrene nanoparticles dyed with terbium, samarium, and dysprosium chelates (Huhtinen *et al.*, 2005). These chelates were dispersed in the solid polystyrene matrix that was formed through copolymerization using styrene and acrylic acid monomers. The cross-linked matrix helps to reduce the leaking of the chelates, and it also minimizes, e.g., oxygen diffusion, which might cause photobleaching. In addition to dye leaking, polystyrene particles may sometimes suffer from swelling and agglomeration (Santra *et al.*, 2001). The diameter of the polystyrene particles can be tuned by changing the synthesis conditions and the stoichiometry of the starting materials, and also very small particles can be obtained (Wen *et al.*, 2008; Shim *et al.*, 1999; André and Henry, 1998).

In addition to polystyrene, compounds such as latex and polyethylene glycol can be used in nanoparticle preparation (Guo *et al.*, 1992; Tamaki and Shimomura, 2002). Silica is also commonly used in the preparation of lanthanide-dyed nanoparticles. The so called Stöber method for the preparation of silica nanoparticles was introduced in 1968 (Stöber *et al.*, 1968). Many techniques have since been introduced, but this well-established method uses the hydrolysis of tetraethyl orthosilicate (TEOS) to form the particles (Xu and Li, 2007; Zhang *et al.*, 2007). The lanthanide chelates can either be incorporated in the condensation reaction (Chen *et al.*, 2007), or the chelates can be covalently attached to the silane monomer prior to polymerization (Hai *et al.*, 2004). As with polystyrene particles, the size of the silica nanoparticles can be controlled by changing the synthesis conditions or the reagent stoichiometry. Advantages of silica nanoparticles include inertness as well as optical transparency, which reduces the possibility of spectral interferences (Soukka and Härmä, 2011). Some silica nanoparticles may, however, suffer from dissolution, which can be further accelerated in biological media (Mahon *et al.*, 2012).

For the nanoparticles to be functional in bioanalytical applications, particularly bioaffinity assays, biomolecules need to be coupled to their surface. A suitable functionalization scheme depends on the particle surface characteristics and on the biomolecules to be attached. With polystyrene particles, the copolymers in the polymerization reaction can be chosen to contain desirable structures that will introduce reactive groups on the particle surface. These groups can also be used to affect the hydrophobicity and charge of the particle (Lück *et al.*, 1998). Similarly, with silica nanoparticles, the silane derivatives can be chosen to encompass desirable functional groups. For example, carboxylic acid groups on the surface enable simple and convenient conjugation to virtually any biomolecule (Härmä *et al.*, 2001). The high surface-to-volume ratio of particulate reporters with respect to most other solid supports gives them much enhanced binding capacity, but at the same time creates demands. The surface properties of the nanoparticles are essential, since they have a major impact on the function and thus the applicability of the reporters. High colloidal stability and low unspecific binding are some of the key features that should be carefully addressed, especially in homogeneous bioaffinity assays.

Biological nanoparticles, such as liposomes and proteins, can also serve as hosts for lanthanide complexes, and they can be easily produced in large quantities with a controllable diameter. Several model assays have been designed using such biological nanoparticles (Laukkonen *et al.*, 1995; Orellana *et al.*, 1996; Okabayashi and Ikeuchi, 1998; Pihlasalo *et al.*, 2009; Jääskeläinen *et al.*, 2007; Roy *et al.*, 2003). However, in several of these assays, the particle was not directly luminescent, but signal generation required an additional step to extract the lanthanide ion and to enhance its luminescence (Soukka and Härmä, 2011).

### **2.3.4 Lanthanide-doped inorganic nanocrystals**

The structure and electronic transitions of the lanthanide-doped inorganic materials were already introduced in section 2.2.4. The advantages of these lanthanide-doped inorganic nano-sized crystals with respect to most other nanoparticles and molecular fluorescent reporters are their practically infinite shelf life, non-toxicity (which is sometimes an issue with quantum dots, QDs, another class of inorganic nanoparticles), essentially non-existent photobleaching, and superior stability regarding environmental conditions such as pH and temperature. The lanthanide-doped inorganic nanocrystals also possess fewer non-radiative relaxation channels for excited lanthanide ions compared to molecular reporters, and thus more easily exhibit NIR luminescence and photon upconversion (Werts, 2005). However, the smaller the nanoparticle, the bigger the surface-to-volume ratio and, therefore, the more pronounced the non-radiative relaxations due to surface defects and solvent quenching. This can be reduced by passivating the nanoparticle surface (Huignard *et al.*, 2000; Fang *et al.*, 2005). Additionally, lattice impurities may increase multiphonon relaxation rates and reduce the emission intensity (Schäfer *et al.*, 2007). The major drawbacks of inorganic nanocrystals are related to the challenges of nanoparticles in general: their susceptibility to steric and kinetic hindrances, and their tendency to aggregate or exhibit unspecific binding in non-optimal conditions. Compared to the lanthanide-dyed nanoparticles, the lanthanide-doped inorganic nanocrystals also exhibit weaker luminescence per lanthanide ion because of the weaker absorption of individual ions. This can, however, be compensated to some extent by increasing the dopant ion concentrations. Inorganic nanoparticles, in general, can be prepared readily in large quantities using fairly simple methods, and their size and shape can be controlled with careful optimization of the reaction conditions (Soukka and Härmä, 2011).

Inorganic nanocrystals have been prepared through several different techniques such as ball-milling of bulk materials, gas phase condensation, combustion methods, and wet chemistry methods (Beverloo *et al.*, 1992; Riwozki *et al.*, 2000; Hebbink *et al.*, 2002; Körnpe *et al.*, 2003; Buissette *et al.*, 2004; Stouwdam and van Veggel, 2004; Wang *et al.*, 2010). Ball-milling of larger particles is not a preferred method, since it produces a large size distribution and limits the obtainable particle size to approximately 100 nm, which is not sufficiently small for many bioaffinity assays (Soukka and Härmä, 2011; Dosev *et al.*, 2008). The wet chemistry methods are currently very actively studied for the preparation of lanthanide doped nanocrystals, because they usually have relatively low cost, and are rather easy to scale up (Werts, 2005). The aim in the nanocrystal synthesis, especially regarding bioaffinity assays, is to obtain small particles with narrow size distribution and high colloidal stability in aqueous solutions. Irrespective of the vast amount of research in the field, these requirements may sometimes be challenging to satisfy.

After the synthesis, the lanthanide-doped inorganic nanocrystals usually do not have suitable reactive groups on their surface for bioconjugation purposes, and thus require a surface modification step. In addition to bioconjugation, this step is also required to provide colloidal stability in aqueous solutions, and to retain the functionality of the used biomolecules. The surface functionalization protocols have largely been derived from the methods used with other nanoparticles, such as silica nanoparticles and QDs (Medintz *et al.*, 2005; Yao *et al.*, 2006). Two popular methods are physical adsorption of biomolecules and silica coating followed by the conjugation of biomolecules to the introduced functional groups. The former is a simple and gentle method, but often suffers from the detachment of the coating. The latter provides covalent attachment, and the surface chemistry of silica is also well documented. Other surface functionalization schemes include polymer encapsulation with polyacrylic acids, utilization of electrostatic interactions between nanoparticles and oppositely charged polymers, and the use of layer-by-layer method based on the sequential deposition of oppositely charged materials on the particle surface (Dosev *et al.*, 2008).

The UCPs represent a novel lanthanide-based reporter class introduced in the late 1990s (Wright *et al.*, 1997; Zijlmans *et al.*, 1999). As discussed in section 2.2.4, the upconverting materials have sensitizer and activator ions embedded within the crystal lattice. The sensitizer ion absorbs two or more photons and transfers the energy to the activator ion that emits one higher energy photon. The upconversion phenomenon (anti-Stokes photoluminescence) is so exceptional that it does not occur in nature. It enables total elimination of autofluorescence and scattered excitation light, as emission is measured at shorter wavelengths than where the excitation occurs (Wright *et al.*, 1997; Soukka *et al.*, 2005). The NIR excitation also makes UCPs useful in biological applications, as it minimizes the loss of excitation light intensity due to protein absorption. Furthermore, the UCPs usually have emission bands in the optical window where there is no longer any interfering absorption from blood (hemoglobin in particular) and not yet any interfering absorption from water (Bünzli and Piguet, 2005). This rare advantage makes the UCPs applicable as reporters in whole blood (Kuningas *et al.*, 2007; Rantanen *et al.*, 2008). Multiplexing is also possible by using several UCPs co-doped with different activator ions. All in all, low detection limits in bioaffinity assays can be achieved using an uncomplicated detection system that does not require instrumentation for time-resolved detection (Niedbala *et al.*, 2001; Soukka *et al.*, 2005; Zijlmans *et al.*, 1999). In addition to bioaffinity assays, the applications of UCPs have been extended to luminescence imaging because of the NIR excitation enabling deep tissue penetration (Bünzli, 2010; Wang *et al.*, 2009; Mi *et al.*, 2011).

The field of nanoparticle reporters is very dynamic and intensively studied. In addition to the lanthanide-based nanoparticles, noble metal nanoparticles, magnetic nanoparticles and QDs, for example, have found many applications in bioanalytical assays. Sometimes, additional advantages can be achieved by constructing multifunctional nanoparticles combining the properties of the above-mentioned materials. As an example, lanthanide-based materials can be combined with magnetic materials or noble metal materials (Son *et al.*, 2007; Son *et al.*, 2008; Massue *et al.*, 2008; Wang *et al.*, 2008; Sun *et al.*, 2005; Sun *et al.*, 2006). These novel nanoparticles hold promise for new and exciting applications.

### 2.3.5 Lanthanide-binding peptides

The lanthanide chelates and lanthanide-containing nanoparticles provide several advantages as reporters in bioanalytical applications but, unfortunately, they cannot be genetically encoded. To be able to study biological systems, the reporter must usually be attached to biomolecules, most often proteins. For example, to attach lanthanide chelates to antibodies, a chemical labeling step is required, which may often be laborious, nonspecific, and thus also poorly repeatable. This problem can be circumvented by using lanthanide-binding peptides (LBPs, also called lanthanide-binding proteins or lanthanide-binding tags) (MacManus *et al.*, 1990; Lim and Franklin, 2004), small peptide sequences of approximately 20 amino acids that selectively bind lanthanide ions with high affinity. LBPs can be encoded at the DNA level, and incorporated into proteins using standard molecular biology techniques (Allen and Imperiali, 2010).

When a LBP structure is excited, the energy is absorbed by a tryptophan residue and subsequently transferred to the lanthanide ion (most often  $\text{Tb}^{3+}$ ). The ion can then transfer the energy further to an acceptor fluorophore in close proximity (Vazquez-Ibar *et al.*, 2002). When designing the LBP sequences, naturally occurring protein sequences based on structures such as the  $\text{Ca}^{2+}$ -binding EF-hand motifs (helix-loop-helix topology) have been used as the starting point (Allen and Imperiali, 2010; Clark *et al.*, 1993). Since their discovery, the LBPs have been extensively studied, and with careful optimization of the peptide sequence, highly fluorescent and strongly coordinating LBPs with affinities in the low nM range have been obtained (Sculimbrene and Imperiali, 2006). These complexes can show very long excited state lifetimes of the lanthanide ion demonstrating that there are no water molecules in the inner coordination sphere (Nitz *et al.*, 2004). In addition to the long lifetime and ease of incorporation into recombinant proteins, the advantages of LBPs over conventional fluorophores include their resistance to photobleaching, the site-specificity of the labeling, and the minimization of adverse effects to protein function.

As, chemically, the trivalent lanthanide ions closely resemble  $\text{Ca}^{2+}$  ions, LBPs can be used as calcium analogs in studying Ca-protein structure and function (Lim and Franklin, 2004). LBPs have also been used in NMR spectroscopy and MRI utilizing the paramagnetic properties of lanthanides (Barbieri *et al.*, 2002; Martin *et al.*, 2007), and in X-ray-crystallography (Silvaggi *et al.*, 2007; Barthelmes *et al.*, 2011) because of the excellent X-ray scattering power of lanthanides. Furthermore, LBPs can be used as reporters in studying protein expression and characterization, and as designed artificial endonucleases (lanthanides are efficient catalysts of hydrolysis because of their strong Lewis acidity) (Lim and Franklin, 2004; Snyder *et al.*, 1990). However, even though LBPs have been studied for several decades, only few reports exist on their use in energy transfer applications. These include a study of the intra- and intermolecular distances in macromolecules (Vazquez-Ibar *et al.*, 2002), and a study on protein-peptide interactions (Sculimbrene and Imperiali, 2006). More recently, Arslanbaeva *et al.* have used LBPs and fluorescent proteins as FRET pairs, and proposed their use in time-resolved fluorescence (TRF) applications (Arslanbaeva *et al.*, 2010; Arslanbaeva *et al.*, 2011). Using this approach, there is considerable potential for the LBPs in bioaffinity assays and medical diagnostics.

### 2.3.6 Others

The reporter classes discussed in the previous sections provide countless options for constructing lanthanide-based reporters, but they are far from being the only useful lanthanide-based reporter classes. There is a great deal of research being carried out on other types of reporter complexes. Furthermore, the distinction between these classes is not well-defined. There are extensive reviews in this area (Binnemans, 2009; Carlos *et al.*, 2011), and in this section, only some examples have been chosen, namely multimetallic assemblies, metallomesogens, and organic–inorganic hybrid materials (Figure 7).

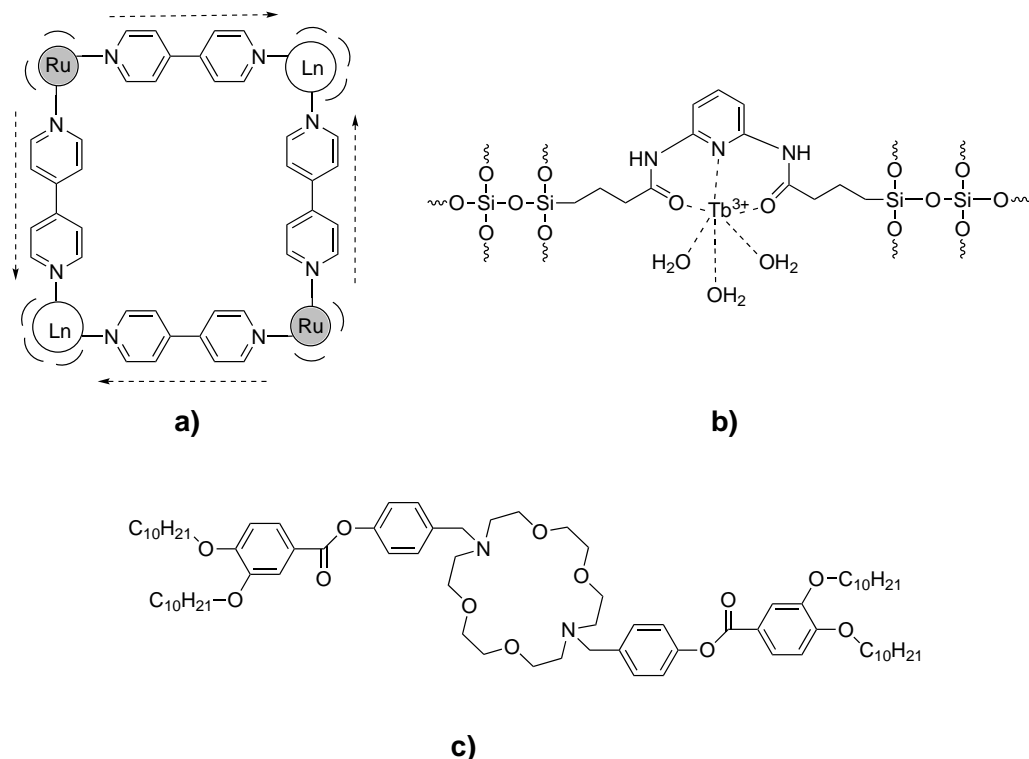


**Figure 7.** (a) A tetrametallic complex exhibiting  $\text{Ru}^{2+}$ -to- $\text{Ln}^{3+}$  directional energy transfer;  $\text{Ln}^{3+}$  ions are in  $[\text{Ln}(2\text{-thenoyl trifluoroacetonate})_3]$  complexes and  $\text{Ru}^{2+}$  ions are bound to bipyridyl units (Bünzli and Piguet, 2005); (b)  $\text{Tb}^{3+}$ -containing organic–inorganic hybrid material derived from 2,6-bis(propyltriethoxysilylureylene)-pyridine (Binnemans, 2009); (c) A ligand capable of forming metallomesogenic complexes with  $\text{Ln}^{3+}$  nitrates (Bünzli and Piguet, 2005).

Multimetallic assemblies have two or more metal ions inserted into complexes, where there is intermetallic communication between the ions. The lanthanide ions used in this kind of multimetallic assemblies are usually  $\text{Nd}^{3+}$ ,  $\text{Er}^{3+}$ , or  $\text{Yb}^{3+}$ , the NIR emitting lanthanide ions. In addition to lanthanide ions, these multimetallic assemblies usually contain d-block transition metal ions, such as  $\text{Ru}^{2+}$ ,  $\text{Os}^{2+}$ ,  $\text{Re}^{1+}$ ,  $\text{Pt}^{2+}$ , or  $\text{Cr}^{3+}$  (Shavaleev *et al.*, 2005; Torelli *et al.*, 2005). NIR emitting lanthanides are used because of their low-energy excited levels that are more easily fed from a d-block donor compared to the excited levels of the other lanthanides. The energy transfer between the ions occurs mainly by through-bond or through-space directional energy transfer mechanism (Bünzli and Piguet, 2005). The history of this kind of multimetallic assemblies containing lanthanide ions and transition

metal ions dates back a century to 1916, when a series of lanthanide hexacyanocobaltates,  $\text{Ln}[\text{Co}(\text{CN})_6] \cdot n(\text{H}_2\text{O})$ , were synthesized (James and Willand, 1916). Since then, several synthetic strategies have been used utilizing the advances made in coordination chemistry and crystal engineering (Huang *et al.*, 2009). The multimetallic assemblies continue to raise interest today because of their potential as luminescent reporters, catalysts, adsorption materials, and magnetic materials (Zhao *et al.*, 2006; Aspinall, 2002; Luo *et al.*, 2007).

Metallomesogens are metal complexes of organic ligands which exhibit liquid crystalline character (also referred to as mesomorphic character). They combine the properties of metal-based coordination compounds with the exceptional physical properties of liquid crystals. When synthesizing metallomesogens, many different metals from the s-, p-, d-, and f-block can be incorporated into the structure. Various monodentate, bidentate, and polydentate ligand structures can also be used, e.g.,  $\beta$ -diketonates, carboxylates, phthalocyanines, and porphyrins (Giroud-Godquin and Maitilis, 1991). The currently known lanthanide-containing metallomesogens belong to four classes: i) lanthanide alkanoates, ii) Schiff base derivatives, iii) macrocyclic complexes (which were among the first reported lanthanide-containing metallomesogens), and iv) complexes with tridentate aromatic receptors derived from substituted 2,6-bis(benzimidazolylpyridine) (Bünzli and Piguet, 2005). In metallomesogens, the molecular shape and intermolecular forces play an important role in determining the mesophase character. The molecular polarizability (regarding the metal atoms electron density) is a key factor in determining whether a molecule will form liquid crystals. An important prerequisite for a metallomesogen is a rigid core that is usually unsaturated, has a rod- or disk-like shape, and bears several long hydrocarbon tails. The metal atom is normally situated at or near the center of gravity of the molecule. The use of several different metals in the structures further widens the range of properties and the applicability of these compounds in fields such as bio-analysis and materials science (Giroud-Godquin and Maitilis, 1991).

In the last decade, the research of lanthanide-based compounds has expanded from purely inorganic crystals or molecular lanthanide compounds to organic–inorganic hybrid materials. There are many different classes of these, for example, sol–gel materials, mesoporous materials, ionogels, and polymers, and the distinction between these classes is again not well-defined. In sol–gel materials, for example, molecular lanthanide complexes are embedded in an inorganic host matrix. Alternatively, the porous network of silica can be used to confine liquids containing dissolved luminescent lanthanide ions or lanthanide complexes. The organic–inorganic hybrid materials can have superior mechanical properties and better processability compared to the molecular lanthanide complexes. The hybrid matrix also improves the thermal stability and luminescence output of the complex (Binnemans, 2009). For example, the useful properties of sol–gel derived organic–inorganic hybrid materials include highly controlled purity, versatile shaping and patterning, thermal and chemical stability, biocompatibility, and control of the hydrophobic–hydrophilic balance (Carlos *et al.*, 2011). The research in the field of organic–inorganic hybrid materials is very active, and the number of publications in the field is increasing. There is also a clear shift towards the study of more complex systems with exciting new properties. In recent years, the research has focused on the development of eco-friendly, versatile and multifunctional systems with applications ranging from optics (optical amplifiers, optical waveguides, and organic light-emitting diodes or OLEDs) to energy and biomedicine (Carlos *et al.*, 2011; Binnemans, 2009).

As is evident from the review above, there is a wide selection of luminescent lanthanide reporters available. The choice is dependent on both the intrinsic properties of the reporter, and on the specific application. Each reporter has its own strengths and weaknesses, and these should be carefully considered when setting up an experiment. Table 2 summarizes the advantages and disadvantages of the main lanthanide-based reporter classes.

**Table 2.** Advantages and disadvantages of lanthanide-based reporter classes. Because of the variability within the classes, some generalizations have been made. A minus sign indicates a disadvantage. Increase in plus signs indicates enhancement in the desirable property.

	Ln chelates	Ln-dyed nanoparticles	Ln-doped nanocrystals	Ln-binding peptides
Luminescence intensity	–	++	+	–
Water solubility	+ <sup>a)</sup>	+	– <sup>b)</sup>	++
Biocompatibility	+	+\sup{c)}	–\sup{d)}	++
Photostability	–	+\sup{e)}	++	–
Thermodynamic stability	–	+\sup{e)}	++	–
Non-radiative relaxation	–	+	++	–
Binding capacity	–	++	++	–
Ease of synthesis	+	+	–	++
Shelf-life	+	+	++	–
Cost <sup>f)</sup>	–	–	+	+
Upconversion capability	n/a	n/a	++	n/a
Steric issues / unspecific binding	++	–	–	++
Genetical encoding capability	n/a	n/a	n/a	++
Tunability <sup>g)</sup>	+	+	+	–

Abbreviations: n/a, not applicable

<sup>a)</sup> Water solubility can be enhanced, for example, by incorporating sugar moieties

<sup>b)</sup> Non-water soluble particles can be rendered soluble by surface functionalization

<sup>c)</sup> Silica nanoparticles and biological nanoparticles have increased biocompatibility

<sup>d)</sup> No severe toxicity has yet been reported during *in vivo* applications

<sup>e)</sup> Cross-linking of the matrix improves stability

<sup>f)</sup> Cost of production and detection instrumentation

<sup>g)</sup> Tunability in physicochemical and biological behavior

## 2.4 Bioanalytical applications

Because of their versatility and exceptional photophysical properties, luminescent lanthanide reporters have been utilized in application areas ranging from lighting industry (e.g., lamp phosphors and OLEDs) to telecommunication (e.g., optical fibers) (Kido and Okamoto, 2002; Bünzli and Piguet, 2005). However, this review focuses on the use of lanthanide reporters in biological and medical applications. Still, this field is quite extensive, and only a small portion of the reported applications are covered here. Various reviews in this area can be found (Selvin, 2002; Hemmilä and Laitala, 2005; Handl and Gillies, 2005; Bünzli and Piguet, 2005; Bünzli, 2010; Stenman, 2011; Moore *et al.*, 2009).

The full potential of the lanthanide reporters in bioapplications is revealed when using time-resolved detection (Soini and Lövgren, 1987; Hagan and Zuchner, 2011; Dickson *et al.*, 1995; Bazin *et al.*, 2002; Morrison, 1988). In TRF measurements, a pulsed excitation

light is used, and there is a certain time delay before the long-lived emission of the lanthanide reporter is recorded. This cycle of excitation, delay, and measurement can then be repeated several thousand times. With time-resolved spectroscopy, it is possible to eliminate the short-lived autofluorescence originating from biological materials, and scattered excitation light. Furthermore, when using lanthanide-based donors in time-resolved energy transfer-based assays (TR-FRET), the prolonged lifetime of the sensitized acceptor emission can be detected using time-resolution and, therefore, also the short-lifetime emission from directly excited acceptor molecules can be eliminated. Because of the background reduction, the use of time-resolution considerably increases assay sensitivity (Soini and Lövgren, 1987).

#### **2.4.1 Bioaffinity assays**

The operation of bioaffinity assays relies on reversible binding events between biomolecules. These recognition reactions may be, for example, between two proteins, between a protein and a small ligand molecule, or between nucleic acids. Often the aim is to determine the concentration of an analyte of interest. There are different ways to categorize the bioaffinity assays. One division can be made into heterogeneous and homogeneous bioaffinity assays based on how the signal from the specific binding reaction is generated. In the former type, the formed complex is physically separated from other interfering assay components with the help of one or more washing steps before measuring the signal. This requires that one of the biomolecules in the complex is bound to a solid surface. In the latter type, no washing steps are required, as the binding reaction itself causes a modulation in the signal level (Ullman, 2001; Morrison, 1988). Another categorization can be made to competitive and non-competitive assays based on the source of the signal. In non-competitive assays, the signal arises from the labeled recognition biomolecule that is bound to the analyte of interest. In the competitive format, on the other hand, the signal typically arises from a labeled analyte analogue. This principal difference causes the dose-response curves to appear essentially opposite, so that in a non-competitive assay the signal increases, and in a competitive assay the signal decreases with increasing analyte concentration (Wild, 2001). The non-competitive format is generally considered to be the more sensitive of the two formats (Ekins and Chu, 1991; Kricka, 1994; Davies, 2001). Sensitivity issues in the homogeneous assays are caused by their susceptibility to sample matrix interference, but the lack of separation steps considerably improves both assay simplicity and speed, which are necessary for automation and HTS.

One of the most applied bioaffinity assays using lanthanide-based reporters are immunoassays, where the high specificity of an antibody towards its antigen is utilized (Wild, 2001). The first reporters used in immunoassays were radioactive labels (Yalow and Berson, 1960; Ekins, 1960). The early radioimmunoassays were succeeded by two-site “sandwich” immunoradiometric assays that provided better sensitivity and an improved dynamic range (Wild, 2001; Wide *et al.*, 1967). However, the issues in storage and waste disposal together with the safety concerns have led to the replacement of radioactive reporters with enzymatic-, chemiluminescent- and photoluminescent reporters (Gosling, 1990; Self and Cook, 1996). In a traditional enzyme-linked immunosorbent assay (ELISA) the presence of the analyte of interest is indicated by a color change brought about by an enzymatic reaction (van Weemen and Schuurs, 1971; Engvall and Perlmann, 1971). The most pronounced advantages of lanthanide reporter-based immunoassays compared to conventional ELISA are their greater sensitivity and wider dynamic range. For example, an

immunoassay using europium chelate reporters can be 10–100 times more sensitive compared to ELISA (Bünzli and Piguet, 2005; Yuan *et al.*, 1997; Smith *et al.*, 2001).

Of the different lanthanide-based reporter classes, the lanthanide chelates have received the most attention in immunoassay applications. The advantages of combining these reporters with time-resolved detection have produced several commercial assay technologies developed by different companies. Examples of these are presented on Table 3. These technologies have been widely used in medical industry, especially in HTS applications (Hemmilä and Laitala, 2005). Other uses of lanthanide chelates in TR-FRET applications include enzyme activity assays (Mizukami *et al.*, 2008), DNA-hybridization assays (Laitala *et al.*, 2007), and real-time polymerase chain reaction (PCR) applications (Hagren *et al.*, 2008) (Bünzli, 2010).

**Table 3.** Examples of commercial technologies based on multidentate lanthanide chelates and time-resolved fluorescence detection.

System	Provider	Reporter	Format	Reference
TRACE® <sup>a)</sup>	CisBio International	Eu-cryptate	TR-FRET	(Bazin <i>et al.</i> , 2002)
HTRF® <sup>b)</sup>	CisBio International	Eu-cryptate	TR-FRET	(Mathis, 1999; Bazin <i>et al.</i> , 2002)
LANCE® <sup>c)</sup>	PerkinElmer	Eu-chelate	TR-FRET	(Hemmilä, 1999; Karvinen <i>et al.</i> , 2002)
TruPoint®	PerkinElmer	Ln-chelate	TR-FQA	(Karvinen <i>et al.</i> , 2002)
DELFIA® <sup>d)</sup>	PerkinElmer	Ln-chelate	TRF	(Hemmilä <i>et al.</i> , 1984)
Lanthascreen®	Invitrogen	Ln-chelate	TR-FRET	(Robers <i>et al.</i> , 2008)

<sup>a)</sup> Time-Resolved Amplified Cryptate Emission

<sup>b)</sup> Homogeneous Time-Resolved Fluorescence

<sup>c)</sup> Lanthanide chelate excite

<sup>d)</sup> Dissociation-enhanced lanthanide fluoroimmunoassay

Lanthanide-based nanoparticles can mostly be utilized in similar bioaffinity applications, where also the molecular lanthanide chelates are used. Lanthanide chelate-dyed polystyrene nanoparticles have successfully been used as reporters in numerous immunoassays (in a heterogeneous non-competitive format, and in homogeneous competitive and non-competitive formats) (Pelkkikangas *et al.*, 2004; Soukka *et al.*, 2003; Soukka *et al.*, 2001; Valanne *et al.*, 2005a; Valanne *et al.*, 2005b; Jaakohuhta *et al.*, 2007; Kokko *et al.*, 2004; Järvenpää *et al.*, 2012; Kokko *et al.*, 2005; Kokko *et al.*, 2006). Silica nanoparticles conjugated to lanthanide chelates have also been used in immunoassays (Zhou *et al.*, 2012; Xu and Li, 2007). These studies have shown that the added benefit, compared to the molecular lanthanide complexes, is improvement in sensitivity, dynamic range, and kinetic properties (Soukka *et al.*, 2001; Soukka *et al.*, 2003; Huhtinen *et al.*, 2005). The inorganic lanthanide crystals have also proven to be useful in bioaffinity assays. In addition to immunoassays, UCPs have been used, for example, in enzyme activity assays and DNA-hybridization assays taking advantage of the upconversion phenomenon (Rantanen *et al.*, 2008; Rantanen *et al.*, 2009).

In addition to photoluminescent applications, lanthanide nanoparticles have also been used in a chemiluminescent application called AlphaLISA™. This homogeneous technology has been developed from the PerkinElmer Amplified Luminescent Proximity Homogenous Assay Screen (AlphaScreen®) technology, and it is based on the Luminescent Oxygen Channeling Assay (LOCI™) chemistry. In the AlphaLISA technology, a sandwich

immunocomplex is formed when the binding of an analyte of interest brings two antibody-coated polystyrene particles, the donor and the acceptor particle, into close proximity. The donor particle contains a photosensitizer that, upon excitation at 680 nm, produces singlet oxygen molecules (up to 60 000 molecules per second can be generated by a single donor particle) that migrate to the bound acceptor particle. As a result, the europium containing acceptor particle emits at 615 nm. The generated singlet oxygen molecules can travel approximately 200 nm in aqueous solution before they decay. The AlphaLISA technology provides a good alternative to conventional ELISA assays that require washing steps and suffer from relatively narrow dynamic range. The high sensitivities of AlphaLISA assays (resulting from the amplified signal and the low background levels) together with the capability for miniaturization make these assays well suited for automation and HTS. However, the most profound advantage of the technology is its suitability for the detection of analytes with highly varying sizes from small molecules to protein–protein complexes and up to whole cells. In FRET, and especially in nFRET assays, the energy transfer efficiency rapidly declines after a few nanometers, and thus analytes are mostly restricted to small molecules and peptides. On the contrary, the donor–acceptor pair in AlphaLISA assays can be separated by as much as 200 nm allowing great flexibility in analyte selection and assay design (e.g., large immunocomplexes can be accommodated). AlphaLISA assays are also applicable to be used in crude biological fluids such as cell lysates, serum, and plasma, whereas some FRET and nFRET assays may be more sensitive to matrix interferences. The main disadvantages of the AlphaLISA technology include sensitivity to intense or prolonged exposure to ambient light, sensitivity to matrix compounds that sequester singlet oxygen, and photobleaching of the donor particles limiting the measurement to a single read (Bielefeld-Sevigny, 2009; Eglen *et al.*, 2008; Ullman *et al.*, 1996).

#### **2.4.2 Luminescent sensors based on lanthanide complexes**

Chemical sensors are small instruments that respond to the presence of certain analytes by producing a measurable signal. Sensors have been designed mainly for pH, temperature, oxygen, carbon dioxide, hydrogen peroxide, glucose, proteins, nucleic acids, anions, metal ions, cofactors, and coenzymes. Chemical sensors usually consist of two connected units: a chemical receptor for analyte recognition, and a physicochemical transducer for producing a signal proportional to the analyte concentration. There are many requirements for a functional sensor in bioanalytical applications. To begin with, the sensor response should be highly specific and also reversible. Additionally, the sensors should work in physiological conditions, that is, in aqueous solutions that may contain a complex mixture of compounds, and a pH of approximately 6–9. Furthermore, the sensor should preferably have a fast response and a possibility for continuous on-line measurement, so that alterations in analyte concentration can be measured over time (Spangler and Schäferling, 2011).

Traditionally, chemical sensors have contained organic dye molecules, such as rhodamine, as luminescent compounds. A large number of such sensors are commercially available. However, these probes have several disadvantages, such as their small Stokes shifts, strong photobleaching, and short excited state lifetimes causing susceptibility to interference from sample autofluorescence (Leonard and Gunnlaugsson, 2005; Bünzli *et al.*, 2007). The photophysical properties of lanthanide-based compounds (their long lifetimes, narrow emission bands, large Stokes shifts, and high photostability) make them very promising candidates to be used in the receptor units of sensor devices. As discussed in section 2.2.1,

some of the lanthanide transitions are hypersensitive, and thus lanthanides create a good basis for sensors that follow changes in signal intensity as a result of alterations in the chemical or physical environment (in addition to fluorescence intensity, also changes in emission wavelength or, for example, in lifetime can be monitored) (dos Santos *et al.*, 2008). For example, a europium–tetracycline complex has been used for the fast and simple detection of hydrogen peroxide (Dürkop and Wolfbeis, 2005). It has to be noted, however, that not all lanthanide complexes are necessarily suitable to be used in luminescent sensors.

There are three main approaches for modulating the luminescence of a lanthanide ion in a sensor application. One option is to enhance luminescence through the direct binding of the analyte to the lanthanide complex (thus replacing water molecules from the inner coordination sphere of the ion). Another possibility to bring about a change in signal levels is to affect the efficiency of the ligand structure to sensitize the lanthanide luminescence. This can be achieved in several ways, but the idea is to affect the transitions between the different energy levels of the ligand and the central ion. Yet another option is to use an analyte that is itself capable of sensitizing (or alternatively quenching) the lanthanide luminescence. This can be achieved also without direct binding of the analyte to the central ion (Bünzli and Piguet, 2005). These three approaches are shown in Figure 8.

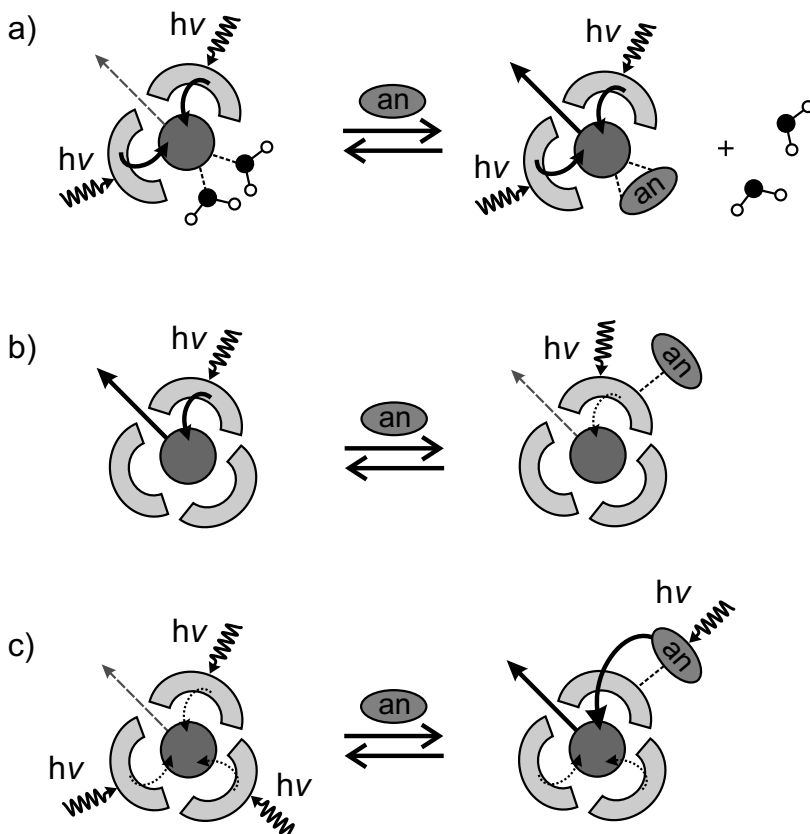


**Figure 8.** Different approaches for modulating lanthanide emission through the binding of an analyte (an): (a) analyte addition displaces water molecules, (b) analyte addition affects the efficiency of the ligand to sensitize lanthanide luminescence, and (c) analyte itself modulates the sensitization of lanthanide luminescence (adapted from Bünzli and Piguet, 2005).

To integrate the luminescent complexes into the sensor devices, it is necessary to bind them to a solid support. Common approaches have been to embed the complexes into polymer matrices (such as polyacrylonitrile or polystyrene), or to attach them to nano- or microparticles. The matrix should be carefully selected, so that it is selectively permeable to the analytes of interest. Subsequently, the formed sensor layers can be used to coat various surfaces, such as microtiter plate wells, glass or plastic surfaces, and fiber-optic devices. The luminescent sensors can then be applied to a multitude of applications: industrial process control, environmental monitoring, biomedical research, and diagnostics, to name a few (Spangler and Schäferling, 2011). Currently, there is extensive research carried out in the field of luminescent sensors, and different lanthanide reporter classes have been harnessed for this purpose. For example, lanthanide chelates have been used in sensors for pH and temperature, and for analytes such as glucose and catalase (Lobnik *et al.*, 2001; Schäferling *et al.*, 2004; Wu *et al.*, 2003; Khalil *et al.*, 2004). In addition to the commonly used lanthanides emitting in the visible wavelengths, there has been increasing interest in using NIR emitting lanthanide ions and UCPs for better tissue penetration. UCPs have been applied in sensor systems to detect pH, temperature, NH<sub>3</sub>, and O<sub>2</sub>, to name just a few (Sun *et al.*, 2009; Sedlmeier *et al.*, 2012; Mader and Wolfbeis, 2010; Achatz *et al.*, 2011).

#### **2.4.3 Microscopy and imaging**

As the advantages of lanthanide luminescence were proven in bioaffinity assays, there was an obvious interest to extend the use of lanthanide-based reporters into imaging applications. The early experiments were made without time-resolution using a standard epifluorescence microscope, and recording the emission of the used europium chelates on a photographic film (Soini *et al.*, 1988). Beverloo and coworkers replaced the visual detection with the newly-introduced charge-coupled device (CCD) cameras when using inorganic europium-doped Y<sub>2</sub>O<sub>3</sub>S particles as cytochemical markers in time-resolved fluorescence microscopy (TRFM) (Beverloo *et al.*, 1990). Despite the clear advantages of TRFM (namely the possibility to eliminate scattered light and autofluorescence originating from biological samples and optical components (Faulkner *et al.*, 2005)), it was not readily translated into commercial instruments, and is still not as frequently used as conventional wide-field or confocal fluorescence microscopy. This is partly due to the weaknesses of the initially introduced lanthanide complexes, and partly due to other methods and spectrally more suitable fluorophores developed to reduce the interfering autofluorescence of biological material (Mujumdar *et al.*, 1989; Mansfield *et al.*, 2008). Recently, however, the use of TRFM has become more widespread, and several different lanthanide-based reporters with high quantum efficiencies and low photobleaching have been utilized in these applications (Connally and Piper, 2008; Tanke, 2011).

Eu<sup>3+</sup>- and Tb<sup>3+</sup>-chelate complexes are the most widely used reporters in TRFM promoted by their favorable chemistry and relative brightness (Tanke, 2011). For example, Eu<sup>3+</sup> and Tb<sup>3+</sup> chelate-labeled antibodies have been used for the immunohistochemical detection of human kallikrein 2 and prostate-specific antigen (Siivola *et al.*, 2000). The visible emitting lanthanides, however, have some inherent drawbacks, e.g., the usual requirement of excitation with UV light, which is absorbed by biological material, and may be detrimental to biological activity. Furthermore, visible emission generated inside the sample can be absorbed by the sample material. This can be eliminated by using lanthanide chelates that emit in the NIR region, but they usually have relatively short excited state lifetimes (Bünzli

and Piguet, 2005). Another option is to use particulate lanthanide reporters, and they are quickly gaining a foothold in the field. Both lanthanide-dyed particles and inorganic lanthanide-doped crystals have been applied to microscopy and imaging. The advantages of nanoparticle labels in imaging are their high specific activities leading to signal amplification, and their resistance to photobleaching and environmental interferences. It has to be noted, however, that when using *in vivo* imaging, the biocompatibility of the nanoparticle reporters needs to be carefully studied, although the lanthanide-based nanoparticles are generally considered to be non-toxic (Dosev *et al.*, 2008). Surface coated UCPs, for example, have been proven to be non-toxic in several studies (Mader *et al.*, 2010; Hilderbrand *et al.*, 2009; Abdul Jalil and Zhang, 2008; Chatterjee *et al.*, 2008). The UCPs also exhibit other useful traits that make them very promising for imaging applications. The NIR excitation minimizes photodamage and allows deep tissue penetration (Chatterjee *et al.*, 2008). The elimination of autofluorescence resulting from the upconversion phenomenon further increases the detection sensitivity compared to imaging applications using more traditional reporters. Additionally, UCPs are readily internalized by many cell types (Mader *et al.*, 2010), and UCPs have been used, for example, in the *in vivo* imaging of the digestive system of *Caenorhabditis elegans* (Lim *et al.*, 2006) and in the imaging of blood vessels (Hilderbrand *et al.*, 2009). There is currently an increasing interest towards multifunctional (dual-mode) reporters also in imaging. For example, the particulate reporters can be made electron dense, which enables their use in electron microscopy, or elements applicable for MRI (such as gadolinium) can be incorporated into the particle (Tanke, 2011; Bünzli and Piguet, 2005). As an example, gadolinium-doped UCPs have been used *in vivo* combining luminescence imaging with MRI (Zhou *et al.*, 2011).

The instrumentation for TRFM requires some adaptations to enable signal detection after a certain delay. The implementation is dependent on the imaging mode (wide-field microscopy or confocal-type, object plane scanning microscopy). There are also some specialized techniques for TRFM, for example, fluorescence lifetime imaging microscopy and time-correlated single photon counting. They are powerful techniques, but not often used with lanthanides (Tanke, 2011). Anti-Stokes luminescence can be exploited to reduce background signal without the need for time-gating equipment, and one possibility to achieve this is to use multiphoton excitation. This can be obtained by using a femtosecond Ti: sapphire laser, and luminescence microscopes with such multiphoton excitation capability are commercially available (Bünzli, 2010). Another possibility is to use UCP-based systems requiring considerably lower excitation power densities. Because of the unavailability of dedicated commercial instruments for UCP imaging, some research groups have constructed different setups, such as a laser scanning upconversion luminescence microscopy device based on confocal pinhole technique developed by Yu *et al.* (2009). Since an instrument based on a confocal microscope scanner is rather expensive, Ylihärsilä and coworkers have developed a simple and robust anti-Stokes photoluminescence imager that has no moving optical parts, and is equipped with a low-cost infrared laser diode for exciting the UCPs. This instrument has been used for the detection and genotyping of human adenoviruses in a microarray format (Ylihärsilä *et al.*, 2011; Ylihärsilä *et al.*, 2012). These and many other reports show that the applicability and versatility of lanthanide-based reporters in microscopy and imaging is excellent. Applications may also be found outside the traditional immunohistochemistry and immunocytochemistry studies. Applications of TRFM will most likely increase in fields such as forensics, plant research, and microbiology of water and soil samples, where high

autofluorescence traditionally interferes with the imaging (Bünzli *et al.*, 2008; Montgomery *et al.*, 2009; Song *et al.*, 2009; Tanke, 2011).

#### **2.4.4 Future trends**

Although the lanthanide-based reporters for bioanalytical applications were introduced already over three decades ago (Soini and Hemmilä, 1979), they are still relative newcomers compared to many of the well-established reporters. The unique properties of lanthanide-based reporters have, however, stimulated an abundance of research aiming at finding ways to utilize them to replace some reporters working inadequately, and also to discover completely new applications. Although these efforts have been very successful, a lot still remains to be done. The field of bioanalytical applications is constantly evolving to meet the needs of the industry and the society at large.

In recent years, there has been an evident trend in bioanalytics towards, for example, multiplexing, miniaturization, HTS, and affordable diagnostics. Lateral flow (LF) tests and other formats applicable to POC testing are also emerging to bring the analytics and diagnostics closer to the end user. In addition, new reporter classes are being vigorously explored, and the use of NIR luminescence, multifunctional particles, and upconversion is being increasingly adopted. All these progressions go largely hand in hand as, for example, multiplexing and miniaturization are important prerequisites for HTS. TRF, particularly in a homogeneous format, is a fluorescence technique very well suited for HTS because of its sensitivity (reduction of background autofluorescence), robustness, and multiplexing capability. These properties enable the use of sub-nanomolar concentrations of the lanthanide-labeled biomolecules, the concentrations being considerably smaller than those used, for example, in the fluorescence polarization-based techniques (Hemmilä and Hurskainen, 2002; Mathis and Bazin, 2011).

Multiplexing in bioanalysis refers to the simultaneous detection of multiple parameters to gather more data from a single sample, or to the use of multiple different reporters to monitor distinct analytes. Both of these approaches are possible by utilizing the unique spectral and temporal properties of lanthanides (Hemmilä and Laitala, 2005). Multiplexing allows the study of complex biomolecular interactions, and it also saves both time and reagents. Terbium is an excellent lanthanide in view of multiplexing as it has evenly spread emission bands along the emission spectrum (compared to, for example, europium), enabling the use of multiple acceptors in an energy transfer application (Kokko *et al.*, 2009; Mathis and Bazin, 2011). To name just a few examples, multiplexing has been applied to the simultaneous detection of human immunodeficiency virus and hepatitis B virus infections using  $Tb^{3+}$ - and  $Eu^{3+}$ -chelates (Myyryläinen *et al.*, 2010), to the simultaneous detection of three model analytes (prostate-specific antigen, thyroid-stimulating hormone, and luteinizing hormone) using UCP reporters in a microarray format (Päkkilä *et al.*, 2012), and to an ultrasensitive lung cancer immunoassay in human serum using a commercial luminescent terbium complex (Geissler *et al.*, 2012).

Like multiplexing, miniaturization can also produce considerable time and reagent savings. In addition to the above mentioned microarray formats, for example, lab-on-a-chip microfluidic technologies offer assay miniaturization (Bünzli, 2010; Song *et al.*, 2009). The lab-on-a-chip technology has been used to develop small diagnostic devices for POC applications to be used outside the central laboratories, in hospitals, ambulances, and

doctor's offices. Another widely used test format for POC is LF, featuring simplicity, high speed, and user-friendly operation. These properties enable the LF tests to be performed by untrained personnel, making the LF format also popular in over-the-counter products. Some LF applications require higher performance quality than can be obtained using visual readout with the conventional reporters, such as gold nanoparticles or dyed latex nanoparticles. For such purposes lanthanide-based reporters, e.g., europium chelate-dyed polystyrene particles, have been utilized (Juntunen *et al.*, 2012). Lately, also UCPs have been used in a LF format for the multiplexed detection of antibodies against *Mycobacterium tuberculosis*, human immunodeficiency virus, and hepatitis C virus (Corstjens *et al.*, 2007).

As already mentioned in this review, both NIR emission and NIR excitation are phenomena that are increasingly gaining interest in different applications because of their advantages in background reduction, tissue penetration and instrument design. Because of their low excited state energies, the NIR luminescent lanthanide ions  $\text{Er}^{3+}$ ,  $\text{Nd}^{3+}$ , and  $\text{Yb}^{3+}$  can be excited with a broad range of sensitizing antenna ligands (Hemmilä and Laitala, 2005). These ions, however, have a small energy gap between the emissive energy level and the highest sublevel of the ground state multiplet, which results in low sensitization of the metal-centered luminescence and in increased non-radiative relaxation. It also leads to relatively short excited state lifetimes (Bünzli, 2006). This has stimulated the development of NIR emitting reporters with higher quantum yields and increased emission intensities. This can be achieved, for example, by confining the lanthanide complexes within nanoparticles (Bünzli, 2010). Multiphoton excitation, which can be used to sensitize  $\text{Eu}^{3+}$  and  $\text{Tb}^{3+}$  complexes, is also gaining attention because of the drawbacks of the NIR emitting lanthanide ions (Allen and Imperiali, 2010). From the instrument point of view, NIR excitation around 980 nm used, for example, with UCPs is ideal because of the availability of small low-cost laser diodes at that wavelength (Bünzli and Piguet, 2005). All these advances imply that development in systems capable of working in the NIR region, both in bioaffinity assays and in imaging, will certainly continue in the future.

In addition to the general trends in instrumentation and assay design, there are also clear developmental tracks seen within the different lanthanide reporter classes. In the field of molecular lanthanide chelates, there is a constant strive in the synthesis procedures to further improve the absorption properties, quantum yield, and stability of the complexes. Even though lanthanide chelates have already found their way into a variety of highly different applications, they will most likely keep finding more areas to expand into because of their versatility. In the field of particulate lanthanide-based reporters there has historically been an endeavor towards increasingly small particle sizes. This has been especially tricky to carry out in the production of inorganic nanoparticles, as the synthesis procedures are exceedingly sensitive to small changes in reagent ratios and environmental conditions. Currently, the extensive amount of research carried out in this field has resulted in the establishment of synthesis procedures producing sufficiently small particles with even size distribution. However, a lot still remains to be done, also in the view of surface modifications to produce colloidally stable and biologically active particles. There is also a trend towards particulate reporters providing high sensitivity and versatility. The study of UCPs has quickly expanded since their introduction in the '90s, and for a good reason. They provide autofluorescence free detection without the need of time-resolution instrumentation (Haase and Schäfer, 2011). Their exceptional photoluminescent properties combined with relatively inexpensive production and extreme photostability are inspiring

researchers in various fields, but the lack of commercial upconversion readers and imagers is still hindering their widespread use. This is expected to be alleviated in the future. The particulate reporters are excellent also in the sense that it is rather easy to construct multifunctional hybrid nanoparticles combining the useful properties of different reporters. This is yet another field under extensive research at the moment, and it bears considerable promise for the development of novel applications.

Among the different approaches in bioaffinity assays, FRET-based applications have gained a lot of popularity, not least because of the homogeneous assay format that is well suited for fast, automated systems. FRET assays also enable the study of intricate biomolecular interactions. To further improve the currently used FRET assays, there is a constant search for suitable energy transfer pairs. This may be facilitated by the recently discovered nFRET phenomenon, as it enables the use of spectrally non-overlapping acceptors. The use of nFRET also increases assay sensitivity because of the anti-Stokes energy transfer that eliminates the background originating both from the reabsorption of donor emission by the acceptors and from the direct donor emission at the wavelength used to measure the acceptor emission (Laitala and Hemmilä, 2005a). Despite the vast knowledge on fluorescent reporters, a lot remains to be learned about the very intricate energy transfer processes occurring inside the lanthanide complexes as well as between the lanthanide-based donors and fluorescent acceptors. Another aspect in the development of FRET-based assays is the labeling of biomolecules. For optimal assay performance, the biomolecules should be labeled site-specifically. A way to do this without the sometimes rather cumbersome chemical labeling is to use genetically encodable labels, such as GFP. Two fluorescent proteins can be linked to form a FRET pair using genetic encoding. However, the performance of assays based on fluorescent proteins is limited because of autofluorescence. This can be circumvented by using the LBPs and time-resolved detection. With these types of novel approaches, the versatility and sensitivity of FRET-based assays will hopefully continue to improve in the future.

All in all, there are some clear aims for development in the lanthanide-based bioanalytical applications, such as instrument development and the establishment of standardized synthesis and surface modification procedures for the particulate reporters. One clear aim is the expansion of the lanthanide reporters from *in vitro* application to *in vivo* applications. In this sense, a large amount of research still has to be conducted on, for example, the internalization and biocompatibility of these reporters (Montgomery *et al.*, 2009). However, since the early days of the lanthanide-based reporters, there have been considerable advances in their use in bioaffinity assays, biosensors, and bioimaging, which at the same time heralds that much is yet to come. In conclusion, the sophisticated, versatile, and sensitive lanthanide-based reporters show immense potential in fields as far apart as coordination chemistry, nanotechnology and medical diagnostics. It thus seems that there is still a lot to be drawn from this treasure trove of lanthanide luminescence.

### **3 AIMS OF THE STUDY**

The overall aim of the study was to evaluate the potential of different lanthanide-based donor fluorophores in energy transfer applications for the development of sensitive separation-free bioaffinity assays. A major theme was to study the excitation, energy transfer, and emission pathways of these systems. The purpose was to demonstrate the advantages that the lanthanides with their exceptional photoluminescent properties bring to the field of bioanalysis.

More specifically, the aims were:

- I** To design a homogeneous model assay utilizing energy transfer from lanthanide chelate donors to fluorescent protein acceptors demonstrating both the conventional Förster-type energy transfer phenomenon and a novel nFRET phenomenon.
- II** To study the distance and temperature dependence of conventional FRET and nFRET using a homogeneous DNA-hybridization assay, and based on the results to propose a possible excitation mechanism operating in nFRET.
- III** To verify the applicability of lanthanide-doped upconverting nanoparticles as donors in a separation-free enzyme activity assay that enables simple, rather inexpensive, and easily automated assay format with high throughput rate.
- IV** To develop a sensitive protease assay that does not require laborious, often poorly repeatable, and randomly positioned chemical labeling, but instead relies on genetically encoded components enabling a versatile approach for the monitoring of various enzyme activities.

## 4 SUMMARY OF MATERIALS AND METHODS

A detailed description of the materials and methods employed in this study can be found in the original publications (**I–IV**). A brief summary is presented here with some additional information on the materials and methods.

### 4.1 Lanthanide-based donors

All the original publications in this study feature homogeneous bioaffinity assays using a lanthanide-based FRET donor (or donors) and FRET acceptor (or acceptors). A summary of the lanthanide-based donors used in the original publications (**I–IV**) is given in Table 4.

**Table 4.** Summary of the properties of the donor fluorophores used in the original publications (**I–IV**).

Donor	Excitation $\lambda_{\text{max}}$ nm	Emission $\lambda_{\text{max}}$ nm	Conjugated to	Publication
<b>Eu<sup>3+</sup>-chelate</b>	~340	615	GTP-analog (I), oligonucleotide (II)	<b>I, II</b>
<b>Tb<sup>3+</sup>-chelate</b>	~340	545	GTP-analog	<b>I</b>
<b>UCP (Yb<sup>3+</sup>,Er<sup>3+</sup>)</b>	980	~550 (~665) <sup>a)</sup>	Streptavidin	<b>III</b>
<b>Tb<sup>3+</sup>-LBP</b>	~280	545	(recombinant protein with GFP)	<b>IV</b>

Abbreviations: GTP, guanosine triphosphate; UCP, upconverting phosphor; LBP, lanthanide-binding peptide; GFP, green fluorescent protein

<sup>a)</sup> The second major emission band in parenthesis; this band was utilized in the energy transfer

#### 4.1.1 Lanthanide chelates

The lanthanide chelates used in this study were {2,2',2'',2'''-{[2-(4-isothiocyanatophenyl)-ethylimino]-bis(methylene)bis{4- {[4-( $\alpha$ -D-glucopyranoxy)phenyl]-ethynyl}}-pyridine-6,2-diyl} bis(methylenenitrilo)}tetrakis(acetato)}-europium(III) (**I**), {2,2',2'',2'''-{{6,6'-{4''-[2-(4-isothiocyanatophenyl)ethyl]pyrazole-1'',3''-diyl}bis(pyridine)-2,2'-diyl} bis(methylenenitrilo)}tetrakis(acetato)}-terbium(III) (**I**), {2,2',2'',2'''-{{4'-{4''-[{(4,6-dichloro-1,3,5-triazin-2-yl)amino]phenyl}-2,2':6',2''-terpyridine-6,6''-diyl}bis(methylenenitrilo)}}tetrakis(acetato)} europium(III) (**II**), {2,2',2'',2'''-{[2-(4-isothiocyanatophenyl)-ethylimino]-bis(methylene)bis{4- {[4-( $\alpha$ -D-galactopyranoxy)phenyl]-ethynyl}}-pyridine-6,2-diyl} bis(methylenenitrilo)}tetrakis(acetato)}-europium(III) (**II**), and {2,2',2'',2'''-{{4-[{(4-isothiocyanatophenyl)ethynyl]pyridine-2,6-diyl}-bis(methylenenitrilo)}}-tetrakis(acetato)} europium(III) (**II**).

The lanthanide chelates were synthesized following the protocols described earlier (von Lode *et al.*, 2003; Rodriguez-Ubis *et al.*, 1997; Mukkala *et al.*, 1993; Takalo *et al.*, 1994). The structures of the chelates are presented in Figure 9.

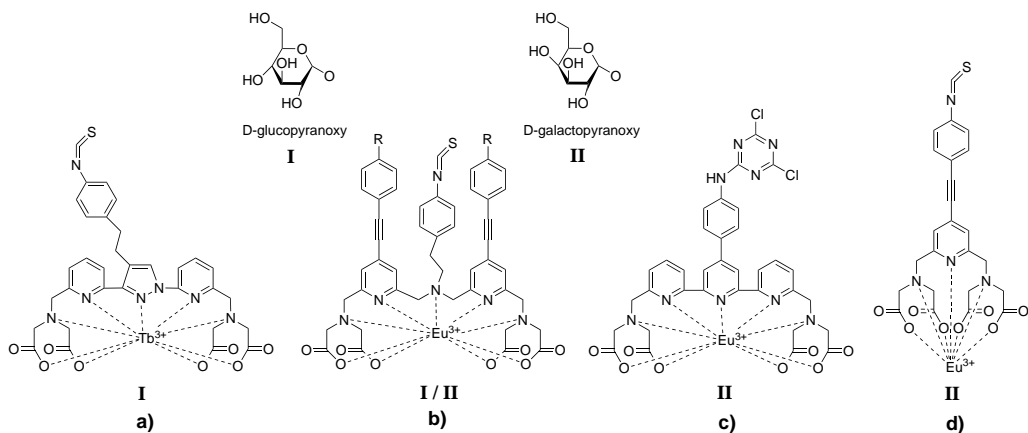


**Figure 9.** Structure of the lanthanide chelates used in the original publications (**I–II**). The structures have been published by Rodriguez-Ubis *et al.* (1997) (a), von Lode *et al.* (2003) (b), Mukkala *et al.* (1993) (c), and Takalo *et al.* (1994) (d).

#### 4.1.2 Lanthanide-doped upconverting nanoparticles

The lanthanide-doped upconverting nanoparticles used in the original publication **III** were composed of  $\text{NaYF}_4:\text{Yb}^{3+},\text{Er}^{3+}$ . They were prepared with a co-precipitation method at the Laboratory of Materials Chemistry and Chemical Analysis, University of Turku, using a previously reported method (Hypänen *et al.*, 2009). The surface modification and streptavidin functionalization of the UCP particles are described in section 4.4.2.

#### 4.1.3 Lanthanide-binding peptides

A gene encoding the LBP and GFP sequences used in the original publication **IV** was ordered from Mr. Gene DNA synthesis service (Life Technologies Corporation, Carlsbad, CA). The LBP sequence was obtained from a previously published article (Sculimbrene and Imperiali, 2006). A linker with a caspase-3 recognition site (DEVD) was inserted between the C-terminal LBP and N-terminal GFP sequences to enable the cleavage and separation of the sequences. The resulting construct was cloned into a pAK400 expression vector (Krebber *et al.*, 1997) resulting in cytoplasmic expression. The pAK400 plasmid containing the recombinant protein construct was introduced into Escherichia coli XL1-Blue cells by electroporation. Expression and purification of the recombinant protein was performed as described in section 4.4.1.

## 4.2 Acceptor fluorophores

A summary of the acceptor fluorophores used in the original publications (**I–IV**) is given in Table 5.

## Summary of Materials and Methods

**Table 5.** Summary of the properties of the acceptor fluorophores used in the original publications (**I–IV**).

Acceptor	Molecular weight g/mol	Excitation $\lambda_{\max}$ nm	Emission $\lambda_{\max}$ nm	Extinction coefficient $\epsilon$ $\text{cm}^{-1} \text{M}^{-1}$	Publication
eGFP <sup>a)</sup>	~27 000	490	509	56 000	<b>I, IV</b>
eYFP <sup>a)</sup>	~27 000	514	527	83 400	<b>I</b>
AF532 <sup>b)</sup>	721	532	554	81 000	<b>II</b>
AF546 <sup>b)</sup>	1 079	556	573	104 000	<b>II</b>
AF680 <sup>b)</sup>	1 150	679	702	184 000	<b>II, III</b>
BHQ-3 <sup>c)</sup>	790	~672 <sup>d)</sup>	620–730 <sup>e)</sup>	~42 700	<b>III</b>

Abbreviations: eGFP, enhanced green fluorescent protein (below the term enhanced is omitted for clarity); eYFP, enhanced yellow fluorescent protein (below the term enhanced is omitted for clarity); AF, Alexa Fluor; BHQ-3, Black Hole Quencher 3

<sup>a)</sup> Produced as a recombinant protein at the Department of Biotechnology

<sup>b)</sup> The dye contains a carboxylic acid succinimidyl ester modification for conjugation purposes. Purchased from Molecular Probes (Eugene, OR).

<sup>c)</sup> The dye contains a carboxylic acid succinimidyl ester modification for conjugation purposes. Purchased from Biosearch Technologies (Novato, CA).

<sup>d)</sup> Not fluorescent. Instead of the excitation maximum, the absorption maximum is reported.

<sup>e)</sup> Not fluorescent. Instead of the emission maximum, the quenching range is reported.

### 4.2.1 Fluorescent proteins

Mammalian expression vector templates (GFP-Rab21 and YFP-actin; YFP stands for yellow fluorescent protein) for cloning the GFP-Rab21 and YFP-Rab21 fusion constructs in the original publication **I** were kindly provided by Dr. Teijo Pellinen (VTT, Technical Research Centre of Finland). Standard molecular biology techniques were used for the preparation of the constructs enabling bacterial expression of the fusion proteins. In brief, a mammalian expression vector for GFP-Rab21 was used as a template to amplify by PCR the gene encoding the GFP-Rab21 fusion. The amplification product was digested and subcloned into a pAK400c bacterial expression vector (Santala and Lamminmäki, 2004). To produce the YFP-Rab21 fusion construct, the Rab21 gene was digested from the previously produced expression vector, and the YFP gene was digested from a YFP-actin mammalian expression vector. The Rab21 gene fragment was then ligated with the digested expression vector, and used as a template for PCR. The amplification product was further digested and subcloned into a pAK400c vector. Both fusion constructs were introduced into Escherichia coli XL1-Blue cells by electroporation. The expression and purification of the recombinant protein were made as described in section 4.4.1. In the original publication **IV**, the used GFP amino acid sequence in the LBP-GFP gene construct was based on Clontech Laboratories, Inc. (Mountain View, CA) pEGFP vector (LabLife database). The cloning is briefly described in section 4.1.3 and the expression and purification of the recombinant protein in section 4.4.1.

### 4.2.2 Alexa Fluor dyes

The Alexa Fluor (AF) dyes were chosen according to the extent of spectral overlap of their excitation band with the emission band of the used donor. In the original publication **II**, the Alexa Fluor 532, 546, and 680 succinimidyl esters (AF532, AF546, and AF680) were purchased from Molecular Probes (Eugene, OR). The acceptor fluorophores were chosen

so that in the energy transfer from the Eu<sup>3+</sup>-chelate, one acceptor (AF532) strictly followed the nFRET principle, one (AF680) strictly followed the conventional FRET principle, and one (AF546) might have been able to utilize both. In the original publication **III**, the biotinylated and AF680 labeled substrate peptide (bio-C[AF680]DEVDK) was purchased from Pepscan Therapeutics (Lelystad, The Netherlands). In this case, the energy transfer from the UCP particle to the AF680 followed the conventional FRET principle.

#### **4.2.3 Quencher molecule**

The BHQ-3 quencher molecule in the original publication **III** was chosen on the basis of its spectral properties and its good stability in the presence of the used reducing agent, dithiothreitol (a reducing agent is a prerequisite for the enzyme activity). The BHQ-3 NHS-ester was purchased from Biosearch Technologies (Novato, CA).

### **4.3 Instrumentation and instrument settings**

#### **4.3.1 Plate readers**

In the competitive bioaffinity assay (**I**), the TRF signal from the lanthanide chelates and the energy transfer signal from the fluorescent proteins were measured with a Victor 1420 multilabel counter (PerkinElmer, Wallac Oy, Turku, Finland) equipped with a red-sensitive photomultiplier tube. Default factory settings (Eu<sup>3+</sup>: excitation 340 nm, emission 615 nm, delay 400 µs, gate time 400 µs; Tb<sup>3+</sup>: excitation 340 nm, emission 545 nm, delay 500 µs, gate time 1400 µs) were used for the lanthanide chelate measurements. The sensitized acceptor emission was measured with a 520/10 nm emission filter (Chroma Technology Corp., Rockingham, VT) using a 75 µs delay and 50 µs gate time.

In the DNA-hybridization assay (**II**), the fluorescence of the Eu<sup>3+</sup>-chelates and the energy transfer enhanced emission of the AF dyes were measured with the Victor 1420 multilabel counter (Wallac Oy). In all cases, the excitation was at 340 nm. For the Eu<sup>3+</sup>-chelate measurements, the default factory settings described above were used. For the measurement of the energy transfer enhanced emission, a 560 nm filter was used with AF532 and AF546, and a 730 nm filter with AF680. For all the energy transfer measurements, 60 µs delay and 50 µs measurement time was used.

In the fluorescence quenching-based enzyme activity assay (**III**), the UCP emission and the sensitized emission of the AF680 acceptor was detected with a modified microtiter plate reader based on a PlateChameleon instrument (Hidex Oy, Turku, Finland). The modified reader used a 980 nm laser diode excitation light source and a 740/40 nm band-pass filter (Chroma Technology Corp., Rockingham, VT). The modified instrument is depicted in more detail in a previous publication (Soukka *et al.*, 2005).

In the enzyme activity assay (**IV**), the emission of the Tb<sup>3+</sup> and the sensitized emission of the GFP acceptor were measured with a Victor x4 plate reader (PerkinElmer Inc., Waltham, MA). To measure the Tb<sup>3+</sup> emission, an excitation wavelength of 280 nm and an emission wavelength of 545 nm were used (500 µs delay and 700 µs gate time). To measure the sensitized emission, an emission wavelength of 520 nm was used (75 µs delay and 100 µs gate time). Also, measurements without time resolution were made to correct

for the small variations in recombinant protein concentrations with 485 nm excitation and 535 nm emission.

#### **4.3.2 Fluorescence spectrophotometer**

In all the original publications (**I–IV**), the spectral measurements were performed with a Varian Cary Eclipse fluorescence spectrophotometer (Varian Scientific Instruments, Agilent Technologies, Santa Clara, CA) with a red-sensitive photomultiplier tube.

In the original publication **I**, the fluorescent protein emission spectra were measured with 10 nm excitation slit and a 5 nm emission slit with excitation at 465 nm for GFP and at 500 nm for YFP. The respective excitation spectra were measured using an emission wavelength of 520 nm for GFP and 540 nm for YFP with a 5 nm excitation slit and a 10 nm emission slit. The emission spectra from the lanthanide chelates were measured using an excitation wavelength of 340 nm for both chelates with a 10 nm excitation slit and a 5 nm emission slit. The respective excitation spectra were measured using an emission wavelength of 615 nm for Eu<sup>3+</sup> and 545 nm for Tb<sup>3+</sup> with a 5 nm excitation slit and a 10 nm emission slit (100 µs delay and 700 µs gate time). The decay spectra of the lanthanide chelate emissions and those of the sensitized acceptor emission from the fluorescent proteins were recorded using the lifetime mode of the spectrophotometer. For the lanthanide chelates, the decays were recorded using excitation at 340 nm (20 nm slit) and emission at 615 nm or 545 nm for Eu<sup>3+</sup> and Tb<sup>3+</sup>, respectively (10 nm slit). For the sensitized acceptor emission from the fluorescent proteins, the decays were recorded using excitation at 340 nm (20 nm slit) and emission at 520 nm (10 nm slit).

In the original publication **II**, the acceptor excitation spectra were measured using an emission wavelength of 559 nm for AF532, 579 nm for AF546, and 713 nm for AF680 with 20 nm emission slit and 2.5 nm excitation slit. The Eu<sup>3+</sup>-emission spectrum was measured as described above with the exception that a 20 nm excitation slit was used.

In the original publication **III**, the AF680 excitation spectrum was measured as described above. For the AF680 emission spectrum, the excitation wavelength was 671 nm (2.5 nm emission slit and 20 nm excitation slit). Emission spectrum of the UCPs was measured with the same spectrofluorometer (2.5 nm emission slit), but this time the instrument was modified with a 980 nm laser diode excitation light source (Soukka *et al.*, 2005).

In the original publication **IV**, the Tb<sup>3+</sup> and GFP excitation spectra were measured using an emission wavelength of 520 nm prior to trypsin treatment and 545 nm after trypsin treatment (20 nm emission slit and 2.5 nm excitation slit). For the emission spectra, an excitation wavelength of 280 nm was used (2.5 nm emission slit and 20 nm excitation slit). For both measurements, 0.1 ms delay and 3 ms gate time were used. The decay spectra of the GFP and terbium emissions prior to and after trypsin cleavage were recorded using the lifetime mode of the spectrophotometer. The decay spectra of the Tb<sup>3+</sup> emission and the sensitized GFP emission were recorded using excitation at 280 nm (20 nm slit) and emission at 545 nm or 520 nm (20 nm slit), respectively.

### 4.3.3 Frequency-domain luminometer

Frequency-domain (FD) fluorometry is a method which can be used to accurately determine the lifetimes and intensities of fluorescent compounds. The main advantage of the FD methods compared to time-domain (TD) methods is generally considered to be the more accurate determination of multiple lifetimes. The technique is also well suited for the determination of lanthanide luminescence (Lakowicz, 2006; Kankare and Hyppänen, 2011). The distance dependencies of the FRET and nFRET processes were studied using a modular FD luminometer (Hyppänen *et al.*, 2010). The instrument setup used is depicted in greater detail in the original publication **II**. In brief, the fluorescence lifetime of the Eu<sup>3+</sup> emission and the sensitized emission of the acceptor dyes were measured at different temperatures (5–55 °C). The detected emission wavelength was selected with an interference filter (615 nm for Eu<sup>3+</sup>, 560 nm for AF532/AF546, and 730 nm for AF680). Luminescence was measured at 200 frequencies divided equidistantly in the logarithmic scale between 10 Hz and 100 kHz. The fitting was made with out-of-phase signal only because of the in-phase interference caused by direct excitation of the acceptor dyes. The theory of the FD measurement and fitting is discussed in previous publications (Hyppänen *et al.*, 2010; Kankare and Hyppänen, 2011).

## 4.4 Reagent preparation

### 4.4.1 Expression and purification of recombinant proteins

The expression and purification of the recombinant proteins are depicted in more detail in the original publications **I** and **IV**. The expression of all the fusion proteins was made similarly, but the purification step was different for the fusion proteins containing the Rab21-joined fluorescent proteins compared to the fusion protein containing the LBP-GFP construct. For overexpression of the fusion proteins, the cells were first plated on LA plates and grown overnight. Colonies from the plates were transferred to precultures, which were again grown overnight. The precultures were then used to inoculate the main cultures, and the protein expression was induced with isopropyl β-D-thiogalactopyranoside. The cells were collected by centrifugation, and the pelleted cells were lysed by sonication to release the cytoplasmic fusion protein. The lysates were centrifuged, and the supernatants were collected.

In the original publication **I**, the supernatants were subsequently filtered. The fusion proteins were then purified using the Profinia protein purification system (Bio-Rad Laboratories Inc., Hercules, CA) according to the manufacturer's instructions. Finally, to remove nucleotides potentially bound to the fusion proteins, the purified proteins were dialyzed overnight. In the original publication **IV**, the supernatant was collected, and ammonium sulfate precipitation and heat treatment were made to collect the recombinant protein. The ammonium sulfate precipitation and heat treatment protocols were adapted from the article by McRae *et al.* (2005). The resulting recombinant protein pellet was solubilized and filtered. Finally, the product was further purified by gel-filtration using a self-packed Superdex 200 preparative grade column (GE Healthcare, Buckinghamshire, UK).

#### **4.4.2 Preparation of donor and acceptor conjugates**

In the original publication **I**, the lanthanide chelates were conjugated to one of two guanosine triphosphate (GTP) derivatives (Jena Bioscience GmbH, Jena, Germany), Eu<sup>3+</sup>-chelate to  $\gamma$ -GTP and Tb<sup>3+</sup>-chelate to EDA-GTP. In both cases, the chelate isothiocyanate group reacted with the amino group of the GTP derivative. The conjugates were isolated with reverse-phase high-performance liquid chromatography (HPLC) (SpectraSYSTEM, Thermo Fisher Scientific, Waltham, MA) using 20 mM triethylammonium acetate buffer and an acetonitrile gradient.

In the original publication **II**, the capture oligonucleotide containing a 5'-terminal amino-modification (Biomers.net GmbH, Ulm, Germany) was labeled at the 5'-end with three different Eu<sup>3+</sup>-chelates that were named 9d-ITC-, 9d-DTA-, or 7d-ITC-chelate based on the number of coordination bonds and structure of the reactive group used for conjugation (ITC: isothiocyanate; DTA: 4,6-dichloro-1,3,5-triazin-2-yl). The tracer oligonucleotides (Biomers.net GmbH) were labeled with Alexa Fluor succinimidyl ester dyes (AF532, AF546, and AF680) using the internal amino-modification on a thymine base incorporated into the sequence at various distances from the 3'-end. The labeled oligonucleotides were isolated with reverse-phase HPLC (Thermo Fisher Scientific).

In the original publication **III**, the UCPs were conjugated to streptavidin to enable the binding of the biotinylated substrate peptide. The surface modification and streptavidin functionalization of the UCPs are depicted in more detail in the supplementary data of the original publication **III**. Briefly, the synthesized UCP particles were first modified by depositing a silica layer on the particle surface to introduce functional groups. Streptavidin (BioSpa Division, Milan, Italy) was then conjugated to the silica layer using carbodiimide chemistry. The biotinylated and AF680 labeled substrate peptide (Pepscan Therapeutics, Lelystad, The Netherlands) was labeled at its C-terminal lysine with NHS-BHQ-3 quencher (Biosearch Technologies, Novato, CA). The labeled peptide was isolated with reverse-phase HPLC (Thermo Fisher Scientific).

#### **4.5 Assay principles**

In this section, the assay principles of the developed four homogeneous bioaffinity assays are described. The assay methods are also briefly introduced. The specifications of the assays (**I–IV**) are summarized in Table 6.

## Summary of Materials and Methods

**Table 6.** Summary of the assay specifications used in the homogeneous assays in publications **I–IV**.

Original Publication	I	II	III	IV
Analyte	GTP	-	Caspase-3	Caspase-3
Assay type	Competitive bioaffinity assay	DNA-hybridization assay	Fluorescence-quenching-based enzyme activity assay	Enzyme activity assay
Donor	Eu <sup>3+</sup> - or Tb <sup>3+</sup> -chelate	Eu <sup>3+</sup> -chelate	UCP (Yb <sup>3+</sup> ,Er <sup>3+</sup> )	Tb <sup>3+</sup> -LBP
Acceptor	GFP or YFP	AF532, AF546, or AF680	AF680 and BHQ-3 <sup>a)</sup>	GFP
Reaction volume ( $\mu L$ )	100	50	150, 50, or 20 <sup>b)</sup>	200
Excitation (nm)	340	340	980	280
Emission (nm)	615, 545, or 520 <sup>c)</sup>	615, 560, or 730 <sup>d)</sup>	740	545 or 520 <sup>e)</sup>

Abbreviations: GTP, guanosine triphosphate; GFP, green fluorescent protein; YFP, yellow fluorescent protein; AF, Alexa Fluor; UCP, upconverting phosphor; BHQ-3, Black Hole Quencher 3; LBP, lanthanide-binding peptide

<sup>a)</sup> AF680 acted as an intermediate acceptor and BHQ-3 as a quencher

<sup>b)</sup> Three different reaction volumes were used to study the effect of miniaturization

<sup>c)</sup> 615 nm for Eu<sup>3+</sup>-chelate, 545 nm for Tb<sup>3+</sup>-chelate, and 520 nm for sensitized acceptor emission

<sup>d)</sup> 615 nm for Eu<sup>3+</sup>-chelate, 560 nm for sensitized acceptor emission from AF532 or AF546, and 730 nm for sensitized acceptor emission from AF680

<sup>e)</sup> 545 nm for Tb<sup>3+</sup>, 520 nm for sensitized acceptor emission from GFP

### 4.5.1 Homogeneous competitive FRET assay for GTP

In the original publication **I**, a homogeneous competitive FRET assay for GTP was constructed by utilizing energy transfer from lanthanide chelate donors to spectrally overlapping and non-overlapping fluorescent protein acceptors. The assay principle is presented in Figure 10. The spectral characteristics and the fluorescence emission lifetimes of the fluorophores were also studied.

The homogeneous assays were performed at room temperature in TSA buffer, pH 7.75, with 5 mM EDTA and 1 g L<sup>-1</sup> bovine serum albumin (BSA). The assays were performed in yellow 96-well plates (Nunc MaxiSorp, Roskilde, Denmark) coated with BSA to prevent unspecific binding of the analytes. The Rab21-joined fluorescent proteins (100 nM fluorescent protein), the GTP-conjugated lanthanide chelates (10 nM chelate), and the free GTP (0–10  $\mu$ M) were incubated with slow shaking for 30 min. The fluorescence signal from the GTP-conjugated lanthanide chelates and the energy transfer signal from the Rab21-joined fluorescent proteins were measured with a Victor 1420 multilabel counter (Wallac Oy). See section 4.3.1 for instrument settings. After the measurements, 20 mM MgCl<sub>2</sub> was added to induce the binding of free GTP or GTP-conjugated lanthanide chelate to Rab21. The mixtures were subsequently incubated for 20 min, and the measurements were repeated.

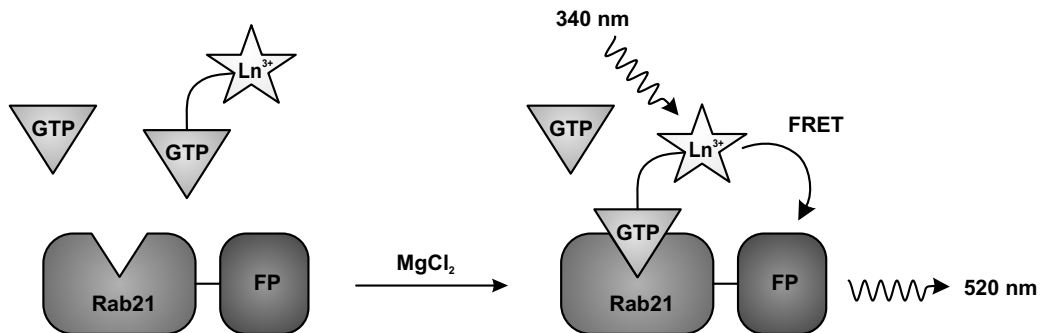


**Figure 10.** Principle of the homogeneous competitive energy transfer assay for GTP. Free GTP, the GTP-conjugated lanthanide chelate, and the Rab21-joined fluorescent protein are mixed together. After  $MgCl_2$  is added, free and conjugated GTP are able to compete for binding to the catalytic site of the Rab21 moiety of the fusion protein. When conjugated GTP is in the catalytic site, the close proximity between the GTP-conjugated lanthanide chelate donor ( $Ln^{3+}$ ) and the Rab21-joined fluorescent protein acceptor (FP) enables energy transfer from the donor excited with UV light at 340 nm. The sensitized acceptor emission is detected at 520 nm.

#### 4.5.2 Homogeneous DNA-hybridization assay

In the original publication **II**, a homogeneous DNA-hybridization assay was constructed to study the distance and temperature dependence of both nFRET and conventional FRET. Capture oligonucleotides were labeled at the 5'-end with a  $Eu^{3+}$ -chelate, and these conjugates were then hybridized to complementary tracer oligonucleotides labeled with an organic fluorophore at various distances from the 3'-end. The assay principle is presented in Figure 11. The distance dependence was studied with a fluorometer utilizing time-resolution, and the temperature dependence was studied using a FD luminometer.

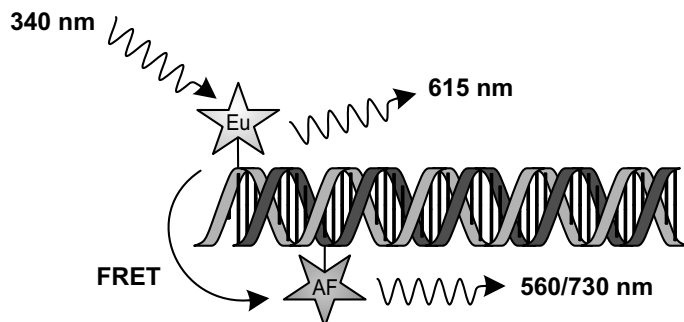


**Figure 11.** Principle of the homogeneous DNA-hybridization assay. A europium chelate (Eu) labeled capture oligonucleotide and an Alexa Fluor dye (AF) labeled tracer oligonucleotide hybridize together to form an energy transfer pair. The chelate is excited at 340 nm, the europium signal is measured at 615 nm, and the energy transfer enhanced emission of the acceptor is measured either at 560 nm (AF532 and AF546) or at 730 nm (AF680).

The difference in the donor–acceptor distance dependence between conventional FRET and nFRET was studied by comparing the energy transfer efficiency in samples containing hybridized oligonucleotides with a varying donor–acceptor distance. Measurements were made in triplicate in yellow LowFluor MaxiSorp microtiter wells (Nunc, Roskilde, Denmark). The optimized hybridization mixtures contained 12 nM capture oligonucleotide and 18 nM tracer oligonucleotide in 50 mM Tris-HCl pH 8.0, 600 mM NaCl, 0.01% (v/v)

Tween 20. The mixtures were incubated for 30 min at +37 °C protected from light. Fluorescence of the Eu<sup>3+</sup>-chelates and the energy transfer enhanced emission of the Alexa Fluor dyes were measured at room temperature with a Victor 1420 Multilabel Counter (Wallac Oy). See section 4.3.1 for instrument settings.

For the temperature dependence studies, samples containing 100 nM capture oligonucleotide (labeled with 9d-DTA Eu<sup>3+</sup>-chelate) and 150 nM tracer oligonucleotide (labeled with AF532, AF546 or AF680) in 50 mM Tris-HCl pH 8.0, 600 mM NaCl, 0.01% (v/v) Tween 20 were incubated at 37 °C for 1 h. The fluorescence lifetimes at different temperatures (5–55 °C) were measured with a modular FD luminometer. See section 4.3.3 for instrument settings.

#### 4.5.3 Homogeneous enzyme activity assays for caspase-3

In both original publications **III** and **IV**, a homogeneous enzyme activity assay was developed for caspase-3. In publication **III**, the assay was based on fluorescence quenching, and UCP particles were used as donors. On the other hand, in publication **IV**, the assay was based on FRET between a LBP and a GFP, therefore two highly different approaches were set up. The assay principles are presented in Figure 12 and Figure 13, respectively.

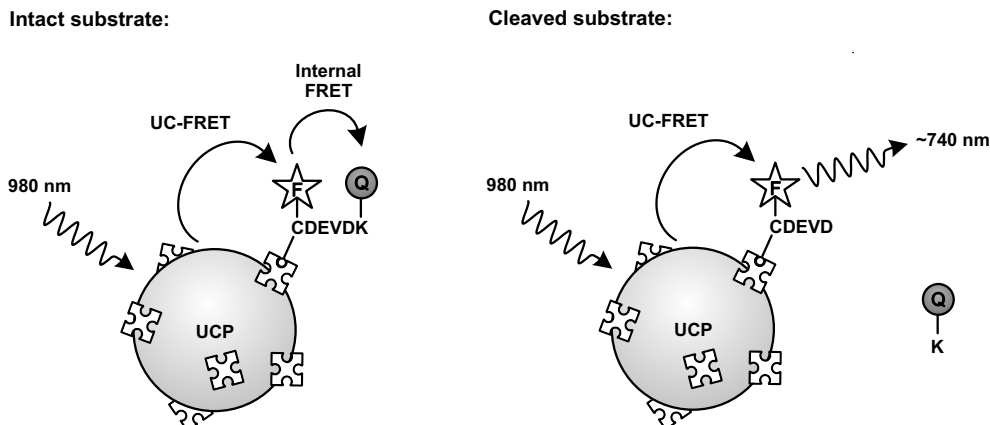


**Figure 12.** Principle of the fluorescence quenching-based caspase-3 activity assay. The streptavidin-coated UCP donor is excited with NIR light at 980 nm, and the energy is transferred through upconversion Förster resonance energy transfer (UC-FRET) to the AF680 acceptor fluorophore (F). If the biotinylated substrate peptide is intact, the energy from the excited acceptor is transferred internally to the Black Hole Quencher 3 dye (Q). If the substrate peptide is cleaved, the quencher is released into the solution. This leads to sensitized acceptor emission measured at approximately 740 nm.

In the original publication **III**, the assay was performed in three steps. In the first step, the caspase-3 enzyme (0.72 mg L<sup>-1</sup>) was allowed to react with the inhibitor Z-DEVD-FMK (0–810 nM) in a microcentrifuge tube for 2.5 h at +37 °C. In the second step, the biotinylated substrates were added into the reaction (100 nM substrate, 6 ng enzyme per pmol of substrate), and the incubation was continued for another 3 h. In the third step, the biotinylated substrates (5 nM in reaction) were collected on streptavidin coated UCP donors (15 mg L<sup>-1</sup> in reaction) in a microtiter well. The assays were performed using both black and white microtiter plates with different degrees of miniaturization (150, 50, and

20  $\mu\text{L}$ ). Finally, the sensitized acceptor emission was measured with a modified PlateChameleon reader (Hidex Oy). See section 4.3.1 for instrument settings.

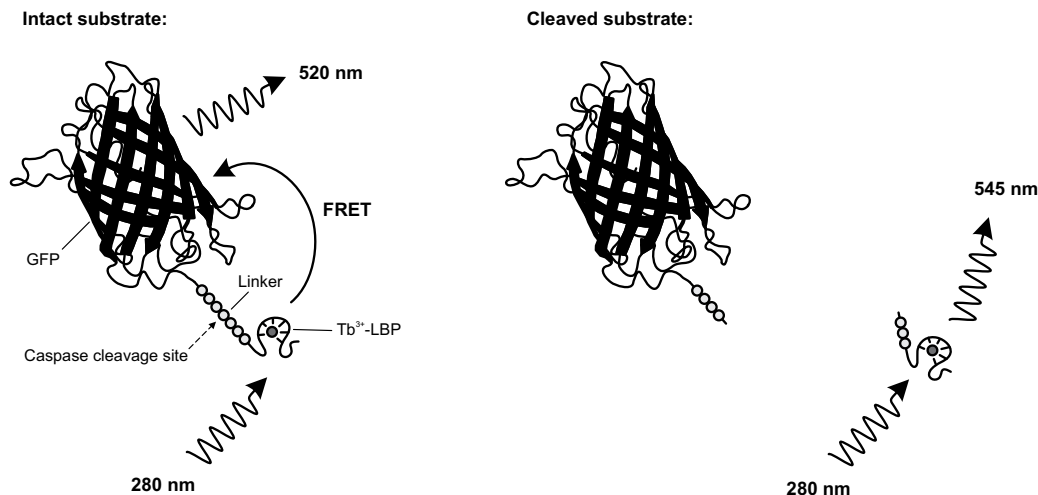


**Figure 13.** Principle of the homogeneous caspase-3 activity assay. Terbium ion adheres to the lanthanide-binding peptide (LBP) forming a luminescent donor complex  $\text{Tb}^{3+}\text{-LBP}$ , which is excited with UV light at 280 nm. In the intact substrate, the energy is transferred through Förster resonance energy transfer (FRET) to the green fluorescent protein (GFP) acceptor, and the sensitized emission can be measured at 520 nm. When the caspase cleaves the substrate, the donor is separated, making the donor–acceptor distance too long for efficient non-radiative energy transfer. This leads to a decrease in the sensitized acceptor emission and increase in the donor emission measured at 545 nm.

In the original publication IV, the assay was also performed in three steps. In the first step, the caspase-3 enzyme (5 nM) was allowed to react with the inhibitor Z-DEVD-FMK (0–1000 nM) in a microcentrifuge tube for 30 min at room temperature. In the second step, 2.5  $\mu\text{M}$  recombinant protein incorporating the substrate peptide was added to the reaction, and the incubation was continued for 4 h at 37 °C. Thereafter,  $\text{TbCl}_3$  (1  $\mu\text{M}$ ) was added, and after a 5-minute incubation at room temperature the samples were measured on MaxiSorp 96-well microtiter plates (Thermo Fisher Scientific) using a Victor x4 plate reader (PerkinElmer). See section 4.3.1 for instrument settings.

## 5 SUMMARY OF RESULTS AND DISCUSSION

### 5.1 Energy transfer mechanisms

All assays in this work relied on some form of resonance energy transfer to monitor the specific signal. A very widely applied assay technology in biomedical research is the Förster resonance energy transfer, or FRET (Förster, 1948). In FRET, as described in section 2.2.5, an excited fluorescent donor transfers energy via a non-radiative dipole-dipole mechanism to a fluorescent acceptor in close proximity. The theoretical basis of the phenomenon was first introduced in 1948. For energy transfer to take place, according to the traditional definition of FRET, a substantial spectral overlap between the donor emission and acceptor excitation spectra is required (Förster, 1948; Clegg, 1992; Stryer, 1978).

As briefly discussed in section 2.2.5, a phenomenon termed nFRET has recently been reported with europium and samarium lanthanides (Laitala and Hemmilä, 2005a; Laitala and Hemmilä, 2005b; Vuojola *et al.*, 2009). The nFRET phenomenon is based on non-radiative energy transfer between a lanthanide chelate donor and a spectrally non-overlapping acceptor, meaning that the acceptor is excited at a higher energy level than where the donor has its main emissive transitions. In the case of Eu<sup>3+</sup>, the term non-overlapping thus indicates absence of spectral overlap between the europium  $^5D_0 \rightarrow ^7F_J$  transitions and the acceptor excitation spectrum. In the original publication **II**, for example, there was an overlap with the very weak  $^5D_1 \rightarrow ^7F_J$  transitions, and thus the term non-overlapping is somewhat misleading. The term anti-Stokes shift FRET has also been used to describe the phenomenon, but the term nFRET was chosen to be used based on its previous usage in the publications describing the phenomenon (Laitala and Hemmilä, 2005a; Laitala and Hemmilä, 2005b). Also contradictory to traditional FRET, in nFRET the lifetime of the sensitized emission from the acceptor is not directly dependent on the energy transfer rate.

A simplified energy level diagram of the different donors and acceptors used in original publications **I** and **II** is shown in Figure 14. The energy levels of the fluorescent acceptors are less well-defined than the energy levels of the lanthanide ions. For this reason, instead of showing discrete energy bands, the energy levels of the acceptors are depicted as excitation maxima together with the half-widths of the excitation spectra.

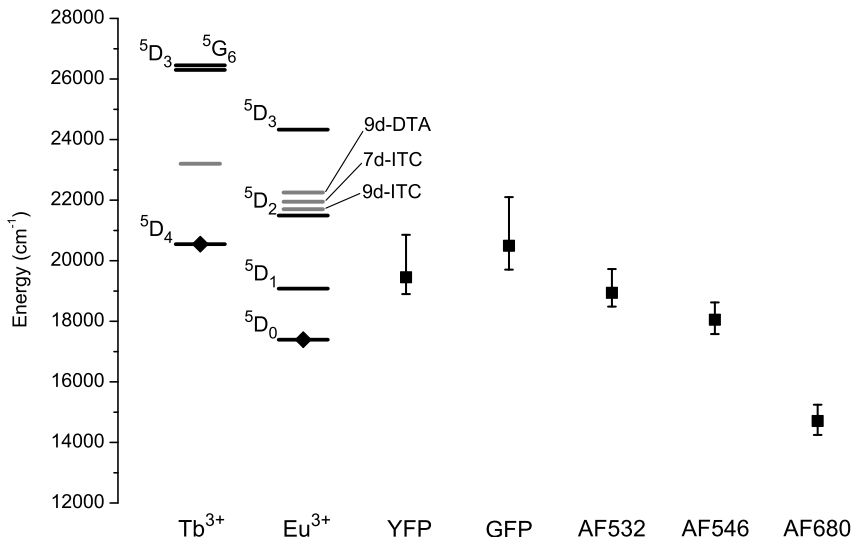


**Figure 14.** Simplified energy level diagram of the fluorophores used in original publications **I** and **II**. The black diamonds represent the emissive energy level of the Eu<sup>3+</sup> and Tb<sup>3+</sup> ions (Carnall *et al.*, 1968c; Carnall *et al.*, 1968d). The lowest triplet states of the used light-harvesting ligands are illustrated as shorter gray-colored lines (Latva *et al.*, 1997) (the exact values may differ slightly from the values indicated in the references because of conjugation and small differences in the chelate structure). The black squares mark the excitation maxima of the acceptors, and the error bars mark the half-width of the excitation spectrum.

As described in sections 2.2.2 and 2.2.3, energy transfer from a ligand to a lanthanide ion mainly occurs from the lowest triplet state of the ligand via a suitable accepting energy level of the ion (typically  ${}^5D_1$  or  ${}^5D_2$  for europium) to the lowest emissive energy level of the ion ( ${}^5D_0$  for europium) (Soini and Lövgren, 1987). This is due to the rapid vibration-mediated non-radiative relaxation that deactivates more highly excited states to the lowest emissive energy level (Werts, 2005). If a suitable acceptor is nearby, the energy can be further transferred to the acceptor. In conventional FRET, the excitation band of the acceptor is at lower energy levels than the lowest emissive energy level of the lanthanide ion. This was the case with the Tb<sup>3+</sup>-GFP pair (in original publication **I**) and the Eu<sup>3+</sup>-AF680 pair (in original publication **II**). On the other hand, the Eu<sup>3+</sup>-YFP (**I**) and the Eu<sup>3+</sup>-AF532 pairs (**II**) followed the nFRET principle. In addition, the Eu<sup>3+</sup>-AF546 pair (**II**) had a very minor spectral overlap with the  ${}^5D_0 \rightarrow {}^7F_J$  transitions, and might, therefore, be able to utilize both conventional FRET and nFRET. The  ${}^5D_3$  and higher energy levels were not considered as possible energy-donating states because they lie above the lowest triplet state of the ligands.

Laitala and Hemmilä were the first to report the nFRET mechanism. They studied the nFRET process using Eu<sup>3+</sup> as a donor together with different Alexa Fluor acceptor fluorophores. They proposed that in nFRET, the energy transfer arises from the upper excited energy levels of europium ( ${}^5D_1$  and  ${}^5D_2$ ) (Laitala and Hemmilä, 2005a). In their studies, they also demonstrated the nFRET mechanism using Sm<sup>3+</sup> as a donor (Laitala and Hemmilä, 2005b). In original publication **I**, the nFRET mechanism was demonstrated for the first time for fluorescent proteins, and in the original publication **II**, the nFRET mechanism was studied in more detail, constructing an assay for the evaluation of distance and temperature dependence of both nFRET and conventional FRET.

Based on the results of the distance and temperature dependencies, two alternative explanations for the nFRET effect were suggested. One hypothesis is that nFRET is essentially a property of the lanthanide ion, not the ligand or the acceptor. Thus the observation that the nFRET phenomenon has been reported with europium and samarium, but not with terbium, could be explained by the ionic energy levels of terbium being unsuitable for this energy transfer mechanism. The long lifetime of the energy transfer enhanced emission also supports the role of the lanthanide ion in the process. One possible mechanism for the nFRET phenomenon could be the already previously studied energy transfer mechanism through thermal excitation (Hyppänen *et al.*, 2010; Kropp and Dawson, 1966; Haas and Stein, 1971) that leads to the population of the higher ionic energy levels above the emissive energy level. The  $^5D_0$  and  $^5D_1$  levels of europium are energetically very close to each other, the difference being approximately  $1700\text{ cm}^{-1}$ , which facilitates thermal excitation. However, the activation energies observed in the work for the AF532 and AF546 were above  $1700\text{ cm}^{-1}$  ( $4045 \pm 35\text{ cm}^{-1}$  for AF532 and  $2861 \pm 77\text{ cm}^{-1}$  or  $2228 \pm 20\text{ cm}^{-1}$  for AF546 calculated based on the longest or second longest lifetime estimates, respectively), and thus it is possible that the energy is transferred from  $^5D_0$  to an energy level higher than  $^5D_1$ .

An alternative explanation for the observed activation energies could be the presence of a LMCT state, proposing that nFRET would be a property of the light harvesting ligand (An *et al.*, 2002). The observation that the nFRET phenomenon has been reported with europium and samarium, but not with terbium, could thus be explained by the oxidation states of terbium being unsuitable for charge-transfer through this mechanism (terbium cannot be reduced to +2 oxidation stage, unlike europium and samarium). The open question in this hypothesis is why the hybridization reactions containing AF532 and AF546 gave different activation energies even though the same ligand was used in both experiments. These results warrant further studies of the nFRET phenomenon using other lanthanide ions, different chelating structures, and donor-acceptor distances optimized for the short distance range.

## 5.2 Donor and acceptor conjugates

The used donor and acceptor fluorophores were chosen based on their spectral properties (including suitable excitation and emission wavelengths and desired extent of overlap between the emission spectrum of the donor and the excitation spectrum of the acceptor), their fluorescence intensity, and their stability.

In the original publication I, two different energy transfer pairs were used. Conventional FRET was observed with the  $\text{Tb}^{3+}$ -GFP pair and nFRET was observed with the  $\text{Eu}^{3+}$ -YFP pair. The spectra are presented in Figure 15. The excitation spectrum of the GFP moiety has an extensive overlap with the terbium  $^5D_4 \rightarrow ^7F_6$  transition at 490 nm, thus providing for efficient FRET. In addition,  $\text{Tb}^{3+}$  cross-talk is negligible in the 520 nm channel used to monitor the acceptor emission. In contrast with regular FRET, the  $\text{Eu}^{3+}$ -YFP pair demonstrated the nFRET principle. The europium donor has no long lifetime emission lines below 580 nm, and thus, spectral overlap between YFP excitation and the europium  $^5D_0 \rightarrow ^7F_J$  transitions is minimal. Again, there is no cross-talk from the donor emission, and further, the acceptor is not excited via reabsorption of the donor emission.

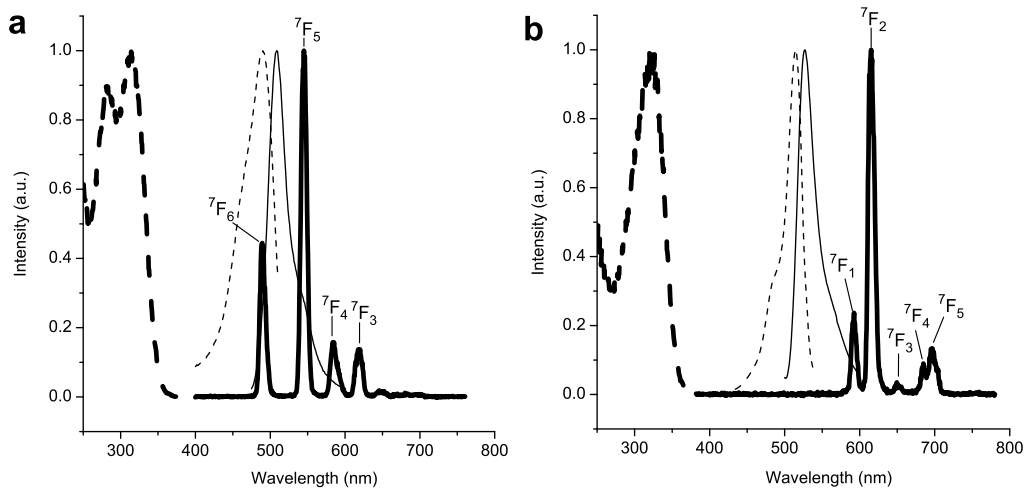


**Figure 15.** Normalized excitation and emission spectra (dashed and solid lines, respectively) of the GTP-conjugated lanthanide chelate donors (thick lines) and the Rab21-joined fluorescent protein acceptors (thin lines). Excitation and emission spectra of the Tb<sup>3+</sup>-GFP pair are illustrated in figure a. The radiative transitions of Tb<sup>3+</sup> from the <sup>5</sup>D<sub>4</sub> energy level to different ground levels (<sup>5</sup>D<sub>4</sub> → <sup>7</sup>F<sub>J</sub>) are assigned to the corresponding emission bands. Corresponding excitation and emission spectra of the Eu<sup>3+</sup>-YFP pair are illustrated in figure b. The radiative transitions of Eu<sup>3+</sup> from the <sup>5</sup>D<sub>0</sub> energy level to different ground levels (<sup>5</sup>D<sub>0</sub> → <sup>7</sup>F<sub>J</sub>) are also assigned to the corresponding emission bands. a.u., arbitrary unit.

In the original publication II, different energy transfer pairs again demonstrated the FRET and nFRET principles. The AF532 acceptor followed the nFRET principle as it had no spectral overlap with the <sup>5</sup>D<sub>0</sub> → <sup>7</sup>F<sub>J</sub> transitions of the Eu<sup>3+</sup>-chelate donor. Conventional FRET was demonstrated using AF680, which has a strong spectral overlap with the donor. In the case of AF546, both mechanisms were, in principle, possible as AF546 has a minor spectral overlap with the <sup>5</sup>D<sub>0</sub> → <sup>7</sup>F<sub>0</sub> and the <sup>5</sup>D<sub>0</sub> → <sup>7</sup>F<sub>1</sub> transition (it has to be noted that the <sup>5</sup>D<sub>0</sub> → <sup>7</sup>F<sub>1</sub> transition is defined to a MD transition and cannot participate in Förster-type energy transfer over a long distance (Dexter, 1953; Selvin *et al.*, 1994; Selvin, 1996)). The spectra of the fluorophores are presented in Figure 16. The inset in Figure 16 shows the time-resolved donor emission spectrum measured from a concentrated solution of unconjugated chelate, and it visualizes the low-intensity emission from the <sup>5</sup>D<sub>1</sub> → <sup>7</sup>F<sub>J</sub> transitions of the Eu<sup>3+</sup>-chelate resulting from thermal excitation (Hyppänen *et al.*, 2010). The intensity of these bands is over 3 orders of magnitude smaller compared to the intensity of the main band at 615 nm.

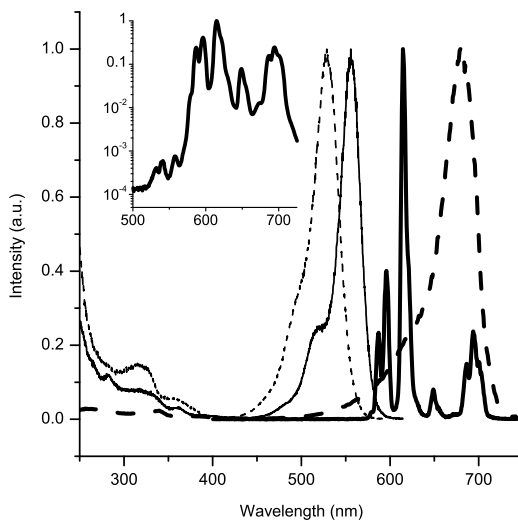


**Figure 16.** Normalized excitation spectra of the Alexa Fluor dyes AF532 (thin dashed line), AF546 (thin solid line), and AF680 (thick dashed line) conjugated to a tracer oligonucleotide, and the normalized emission spectrum of the 9d-DTA Eu<sup>3+</sup>-chelate (thick solid line) conjugated to a capture oligonucleotide. In the inset, the emission spectrum of an unconjugated 9d-DTA Eu<sup>3+</sup>-chelate is depicted on a logarithmic scale (same axes as in the main picture). a.u., arbitrary unit.

In the original publication **III**, the assay utilized dual-step energy transfer. In the first step, the excited UCP particle transferred energy via UC-FRET to the AF680 fluorophore, and in the second step, the energy was further transferred via FRET to the BHQ-3 quencher. The fluorescence and absorption spectra of the fluorophores used are illustrated in Figure 17.

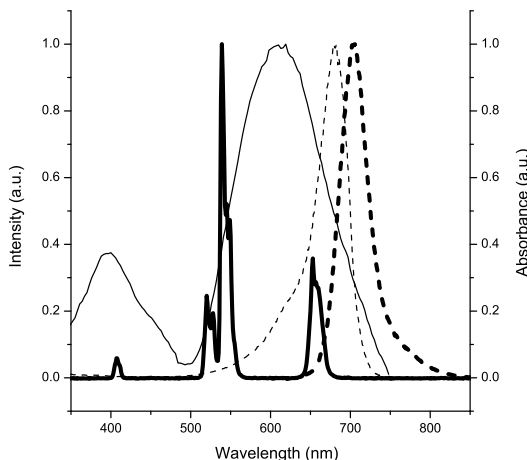


**Figure 17.** The normalized fluorescence emission spectra of the UCP donor (thick solid line) and the AF680 acceptor (thick dashed line) are presented together with the normalized fluorescence excitation spectrum of the AF680 acceptor (thin dashed line) and the absorption spectrum of the BHQ-3 quencher (thin solid line; axis on the right). a.u., arbitrary unit.

Under infrared excitation, the UCPs generated intense and sharp emission bands around 540 nm and 650 nm. The AF680 fluorophore had an overlapping excitation spectrum with the latter band, and thus was a suitable acceptor molecule for energy transfer. To avoid any

donor cross-talk from the 650 nm band, a wavelength of 740 nm was selected to measure the sensitized acceptor emission. The BHQ-3 quencher had a broad absorption spectrum reaching to the emission wavelengths of AF680. Although the absorption of BHQ-3 is also efficient at the emission wavelengths of UCP, direct quenching of the large UCPs is not efficient.

In the original publication IV, the assay utilized FRET between a  $\text{Tb}^{3+}$ -LBP and GFP. The excitation and fluorescence emission spectra prior to and after trypsin cleavage are shown in Figure 18. Since GFP emits at a wavelength where terbium emission is negligible, the sensitized acceptor emission could be measured without spectral cross-talk from the donor emission. In addition to the GFP emission, the 280 nm excitation prior to trypsin cleavage also resulted in some terbium emission. This is mainly due to the inability of the energy transfer to completely quench the donor emission because of the relatively long linker sequence.

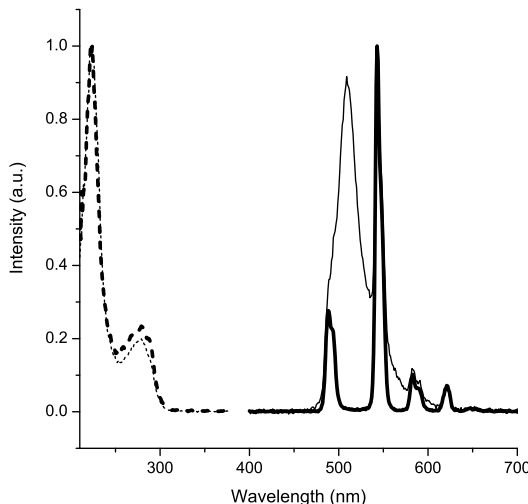


**Figure 18.** Normalized excitation and emission spectra (dashed and solid lines, respectively) of the terbium donor and the GFP acceptor prior to (thin lines) and after (thick lines) trypsin cleavage. For the emission spectra, an excitation wavelength of 280 nm was used. For the excitation spectra, the emission was recorded at 520 nm prior to the trypsin treatment and at 545 nm after the trypsin treatment. a.u., arbitrary unit.

## 5.3 Homogeneous assays

### 5.3.1 Homogeneous competitive FRET assay for GTP (I)

Lanthanide chelates are increasingly used as FRET donors because of their long emission lifetime that enables the use of time resolution to improve assay sensitivity. Fluorescent proteins, on the other hand, owe their popularity to the intrinsic luminescent properties that facilitate their use as fusion proteins in recombinant hosts (Morise *et al.*, 1974). Regardless of the popularity of both lanthanide chelates and fluorescent proteins, fairly few reports utilizing resonance energy transfer between these components have been published to date.

A homogeneous competitive FRET assay for GTP was constructed with two energy transfer pairs,  $\text{Tb}^{3+}$ -chelate with GFP and  $\text{Eu}^{3+}$ -chelate with YFP. The former was used to study conventional FRET, and the latter to study nFRET. In the studies, the fluorescent

protein acceptor was expressed as a fusion protein together with a Rab21 GTPase. GTPases are involved in various processes during the cell cycle, and thus there is a need for monitoring the GTPase activity. To achieve the close proximity between the lanthanide chelate donor and the fluorescent protein acceptor required by the energy transfer, the lanthanide chelate was chemically coupled to amino-modified GTP.

The assay gave descending sigmoidal curves typical of competitive assays. The standard curves are illustrated in Figure 19. The dynamic range of the assay was extensive for a competitive assay format, ranging over 2 orders of magnitude for both energy transfer pairs. The IC<sub>50</sub> value (analyte concentration giving 50% of the maximum signal) for both pairs was approximately 100 nM. The maximum signal-to-background ratio was 15 for the Tb<sup>3+</sup>-GFP pair and 75 for the Eu<sup>3+</sup>-YFP pair. Thus, regardless of the lower signal levels measured with the Eu<sup>3+</sup>-YFP nFRET pair, a 5-fold improvement in the signal-to-background ratio was attainable compared to the Tb<sup>3+</sup>-GFP pair excited via conventional FRET. The reason for the increased assay sensitivity in nFRET was the lack of spectral overlap (there was no cross-talk from the donor emission, and the acceptor was not excited via reabsorption of the donor emission).

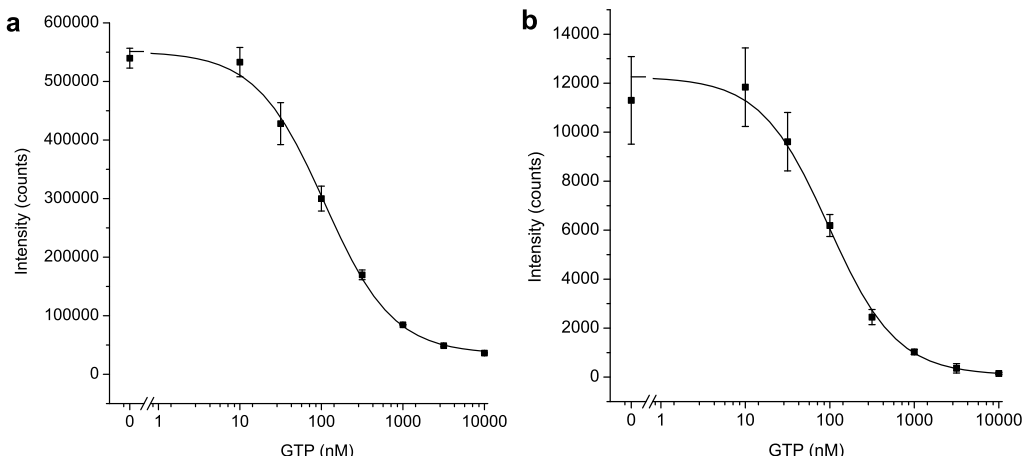


**Figure 19.** Standard curves for the homogeneous competitive GTP assay. The assay used either the GTP-conjugated Tb<sup>3+</sup>-chelate donor and the Rab21-joined GFP acceptor (a) or the GTP-conjugated Eu<sup>3+</sup>-chelate donor and the Rab21-joined YFP acceptor (b). The assay utilized conventional FRET in the case of the Tb<sup>3+</sup>-GFP pair and nFRET in the case of the Eu<sup>3+</sup>-YFP pair. The error bars represent the standard deviation between replicate reactions.

The decay spectra of the lanthanide chelate donors and the apparent lifetimes of the sensitized fluorescent protein acceptors are shown in Figure 20. The fluorescence lifetime data of the GTP-conjugated lanthanide chelates gave traditional millisecond-scale lifetime components of  $1.04 \pm 0.01$  ms for Eu<sup>3+</sup> and  $0.95 \pm 0.02$  ms for Tb<sup>3+</sup>. The data from FRET between the Tb<sup>3+</sup>-GFP pair were fitted one-exponentially, giving an apparent lifetime component of  $60 \pm 2$   $\mu$ s. The data from nFRET between the Eu<sup>3+</sup>-YFP pair diverged notably from the data of the conventional FRET reaction, giving two apparent lifetimes of  $1.08 \pm 0.02$  ms and  $8 \pm 0.1$   $\mu$ s (fractional contributions of 9.6% and 90.4%, respectively, with an average lifetime of 111  $\mu$ s). The decay data explain the lower signal levels observed with the Eu<sup>3+</sup>-YFP pair (see Figure 19) compared to the Tb<sup>3+</sup>-GFP pair, as the sensitized YFP emission had longer decay, and the signal was consequently divided over a longer time frame.

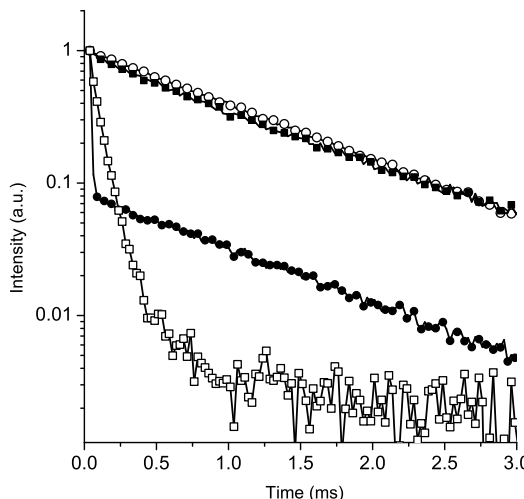


**Figure 20.** Normalized decay spectra of the lanthanide chelate donors and apparent lifetimes of the sensitized fluorescent protein acceptors from energy transfer reactions containing both the GTP-conjugated lanthanide chelate and the Rab21-joined fluorescent protein. Curves from top to bottom: decay spectrum of the GTP-conjugated Eu<sup>3+</sup>-chelate (open circles) measured at 615 nm, decay spectrum of the GTP-conjugated Tb<sup>3+</sup>-chelate (closed squares) measured at 545 nm, and decay spectra of the YFP acceptor (closed circles) and the GFP acceptor (open squares) showing sensitized emission at 520 nm. a.u., arbitrary unit.

### 5.3.2 Homogeneous DNA-hybridization assay (II)

In the original publication **I**, the subject of nFRET was touched upon. It seemed to open possibilities for sensitive bioassays with an unorthodox choice of fluorophores. With only a few previous publications on the subject, the mechanism of nFRET and resulting implications to assay design had not been thoroughly examined. In the original publication **II**, the subject was studied in more detail using both TD and FD measurements.

A homogeneous DNA-hybridization assay was constructed to study the distance and temperature dependence of both nFRET and conventional FRET. Capture oligonucleotides were labeled at the 5'-end with a Eu<sup>3+</sup>-chelate, and these conjugates hybridized to complementary tracer oligonucleotides labeled with an organic fluorophore at various distances from the 3'-end.

The distance dependence was studied with a fluorometer utilizing time-resolution. In the absence of any mathematical model for the calculation of energy transfer efficiency for the nFRET, the Förster model was applied to both nFRET and FRET reactions. This way it could also be seen whether there is a discrepancy between nFRET and the model. Energy transfer efficiency depends on the Förster radius,  $R_0$ . At  $R_0$  the rate of the energy transfer is equal to the fluorescence decay rate. First, the theoretical Förster radii were calculated, and based on those values, the theoretical energy transfer efficiencies could be calculated. The experimental energy transfer efficiencies were calculated based on the observed assay signals, and, finally, also the experimental Förster radii were calculated. Comparison of the theoretical and experimental energy transfer efficiencies is depicted in Figure 21.

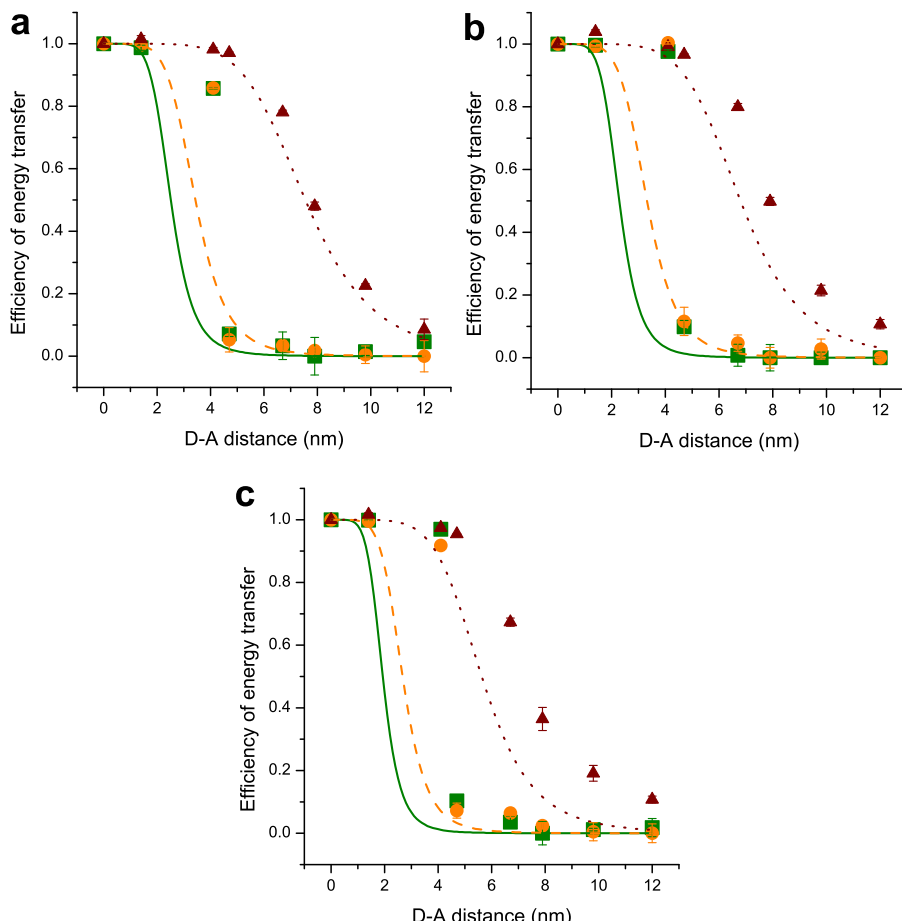


**Figure 21.** Comparison of the theoretical energy transfer efficiencies (lines; calculated based on spectral overlap) and actual experimental energy transfer efficiencies (symbols) with different donor–acceptor distances (0, 1.4, 4.1, 4.7, 6.7, 7.9, 9.8, and 12.0 nm). The Eu<sup>3+</sup>-chelate donors used were (a) 9d-DTA-, (b) 9d-ITC-, and (c) 7d-ITC-chelate. The acceptors used were AF532 (green solid line, square), AF546 (orange dashed line, circle), and AF680 (red dotted line, triangle). The error bars represent the standard deviation between three replicate reactions. With AF532 and AF546, especially at the distance of 4.1 nm, the experimental energy transfer efficiency is substantially greater than the theoretical value.

As can be seen in the figure, the energy transfer efficiency with the FRET acceptor AF680 remains high when the donor-acceptor distance extends from 4.1 to 4.7 nm, whereas with the other two acceptors, the energy transfer efficiency declines very rapidly. With AF680, the experimental results follow the theoretical energy transfer efficiency, but with AF532 and AF546, especially at the distance of 4.1 nm, the experimental energy transfer efficiency clearly deviates from the theoretical value being considerably more effective than could be expected on the basis of the Förster theory. This indicates a distance dependence greater than R<sup>-6</sup>.

The temperature dependence was studied using a FD luminometer. As mentioned in section 4.3.3, FD fluorometry can be used to accurately determine the lifetimes and intensities of fluorescent compounds, and it is well suited to be used with lanthanides. The low-frequency domain below 100 kHz used with lanthanides also makes it possible to employ

highly accurate and inexpensive digital lock-in amplifiers, and, all in all, a complete FD luminometer can be relatively easily constructed (Kankare and Hyppänen, 2011). In Figure 22, the graphs of the out-of-phase signal of the lock-in amplifier are shown as a function of modulation frequency in different temperatures. When the temperature increased, a clear shift towards a shorter lifetime (higher frequency) was observed with the acceptors AF532 and AF546, while with the conventional FRET acceptor AF680 and with the Eu<sup>3+</sup>-chelate alone, the lifetime remained nearly constant. It was proposed that this shift is due to a thermal excitation process from the <sup>5</sup>D<sub>0</sub> level to higher excited states, which increases the likelihood of the nFRET process with increasing temperature.

The results demonstrated a difference in both the distance and temperature dependence between conventional FRET and nFRET. On the basis of the measurements, it was proposed that in nFRET, thermal excitation occurs from the lowest emissive state of the ion to a higher excited state that is either ionic or associated with a ligand-to-metal charge-transfer state.

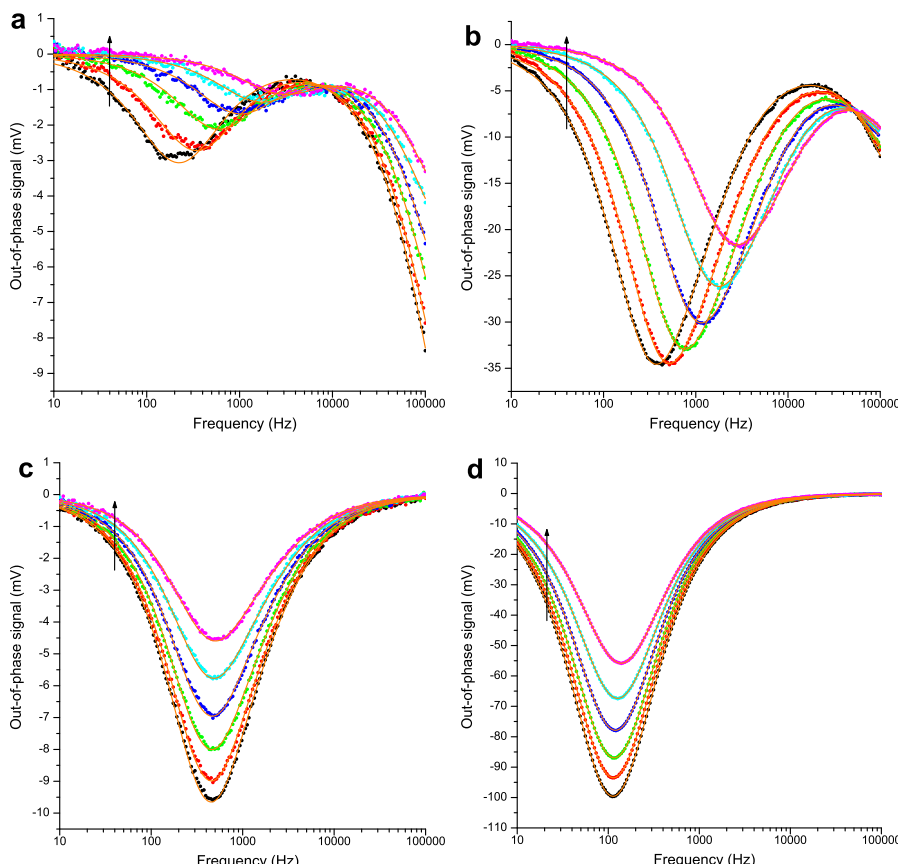


**Figure 22.** Out-of-phase signals of the emission from hybridization reactions containing 9d-DTA Eu<sup>3+</sup>-chelate donor oligonucleotide together with a tracer oligonucleotide labeled with (a) AF532, (b) AF546, and (c) AF680 acceptor, or (d) no acceptor at 560, 560, 730, and 615 nm, respectively, are shown as a function of modulation frequency in different temperatures. In order to obtain sufficient signal intensity, donor–acceptor distance of 4.1 nm was used with AF532 and AF546, and a distance of 6.7 nm was used with AF680. The experimental points are marked by circles, and the solid lines are the fitted signals with two (a, c, and d) or three (b) lifetimes. The temperatures ranged from 5 to 55 °C with 10 °C intervals. The arrow indicates increasing temperature.

### 5.3.3 Homogeneous enzyme activity assays (III, IV)

Apoptosis is the regulated disposal of cells that occurs either during the course of development, during the normal maintenance of homeostasis, or in pathological circumstances (Kerr *et al.*, 1972). Excessive cell death may play a role in several disease states, such as in sepsis, ischemia–reperfusion injury, and in neurodegenerative diseases such as Parkinson's disease, Huntington's disease, and Alzheimer's disease (Philchenkov, 2004; Robertson *et al.*, 2000). On the other hand, insufficient apoptotic activity may facilitate the development of cancer and autoimmune diseases. During the last decade, immense interest and effort have been directed towards the study of apoptosis-based therapeutics (Nicholson, 2000; Fischer and Schulze-Osthoff, 2005). Essential for the control of the apoptosis self-destruction machinery is a large family of cysteine proteases called caspases (Alnemri *et al.*, 1996). An important member of the so called effector caspase subfamily is caspase-3, which is a key mediator in the proteolytic cleavage cascade activated during apoptosis (Sakahira *et al.*, 1998). Several caspase-3 related therapeutics are already being tested in human clinical trials, but tools still need to be further developed to efficiently obtain potent drug candidates for the treatment of apoptosis-associated diseases.

In the original publication III, a homogeneous enzyme activity assay using UCPs as donors was constructed. Conventional homogeneous fluorescence-based assays are susceptible to autofluorescence originating from biological material. This background autofluorescence could be eliminated by using the upconversion phenomenon. In the assay, energy was transferred from a UCP-donor to a conventional acceptor fluorophore that resided at one end of a caspase-3-specific substrate peptide. Attached to the other end was a quencher molecule that was used to attenuate the acceptor emission through intramolecular energy transfer in an intact peptide. In non-inhibitory conditions, the enzyme reaction separated the fluorophore from the quencher, and the emission of the fluorophore was recovered. The method was applied to the detection of a known caspase-3 inhibitor Z-DEVD-FMK. The assay was performed in three degrees of miniaturization. The sigmoidal inhibition curves are shown in Figure 23.

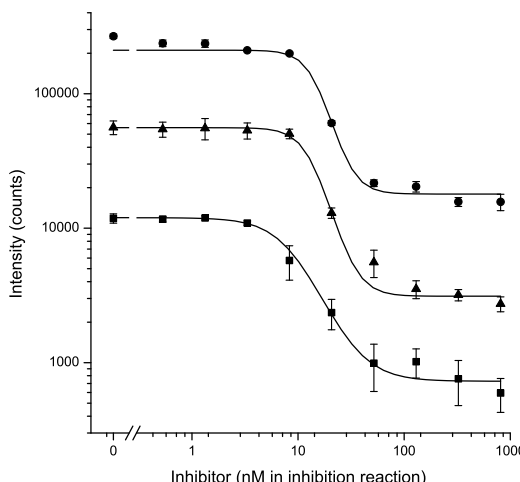


**Figure 23.** Inhibitor dose-response curves comparing different degrees of miniaturization using black polystyrene standard 96-well- (circle), half-area 96-well- (triangle), or 384-well plates (square). The error bars represent the standard deviation measured from four (or eight with 384-plate) replicate microtiter wells.

## *Summary of Results and Discussion*

---

The IC<sub>50</sub> value of the dose-response curve depicts the affinity of the inhibitor towards the enzyme. All the assays gave similar IC<sub>50</sub> values, with an average of 13 nM. This is in good agreement with the previous reports on the Z-DEVD-FMK inhibitor, where Valanne *et al.* (2008) and Gopalakrishnan *et al.* (2002) obtained IC<sub>50</sub> values of 12 nM and 4 nM, respectively. The highest signal-to-background ratios (compared to reactions with no enzyme) were approximately 45, obtained with the standard 96-well plate. There was no considerable difference between the assays performed in different degrees of miniaturization (the half-area 96-well plates and 384-well plates giving an average signal-to-background ratio of 25). The separation-free *in vitro* assay used enabled simple, rather inexpensive, and easily automated format with a high throughput rate. The results also demonstrated the applicability of the UCPs in a fluorescence quenching-based homogeneous enzyme activity assay. Additionally, the use of an internally quenched substrate molecule diminished the background caused by radiatively excited acceptor molecules. Together with the autofluorescence-free upconversion phenomenon this enabled the development of a sensitive homogeneous assay concept.

In the original publication **IV**, a different approach was used for the detection of caspase-3 activity. In this work, the favorable characteristics of a Tb<sup>3+</sup>-LBP and GFP were combined. The popularity of fluorescent proteins arises principally from their intrinsic luminescence, which allows the fluorescent proteins to be expressed as fusion proteins in recombinant hosts (Tsien, 1998). However, the performance of bioanalytical assays based on fluorescent proteins is limited because of autofluorescence originating from biological materials. A common solution has been to use lanthanide-based reporters, e.g., lanthanide chelates, to enable time-resolved detection (Karvinen *et al.*, 2004; Preaudat *et al.*, 2002). However, these labels require chemical labeling to be attached to biomolecules. LBPs offer a means to circumvent this. To construct a protease activity substrate that was entirely genetically encodable, a recombinant protein was designed, in which the LBP and GFP sequences were separated by a peptide linker incorporating a recognition sequence for caspase-3. The aim of the study was to develop a sensitive protease assay that does not require the laborious, often poorly repeatable, and randomly positioned chemical labeling, but instead relies on genetically encoded components enabling a versatile approach to the monitoring of various enzyme activities.

In the assay, both the terbium signal at 545 nm and the sensitized acceptor emission at 520 nm were monitored. The inhibitor dose-response curves are presented in Figure 24. The observed IC<sub>50</sub> values (61.2 nM and 60.7 nM for terbium and energy transfer data, respectively) were somewhat larger compared to the previously reported values for the ZDEVD-FMK inhibitor, where Valanne *et al.* (2008) and Gopalakrishnan *et al.* (2002) obtained IC<sub>50</sub> values of 12 nM and 4 nM, respectively. It has to be noted, however, that the selection of reagents and their concentrations have an impact on the observed values. Maximum signal-to-background ratios of 7 and 33 were achieved when monitoring the terbium and energy transfer signals, respectively. The coefficients of variation between replicate reactions were small, with the maximum of 4.2%.

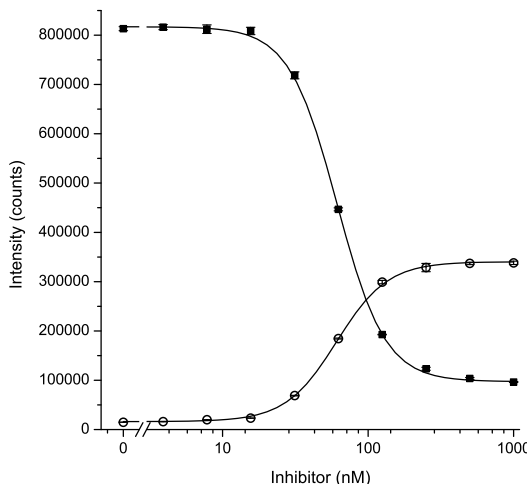


**Figure 24.** Inhibitor dose-response curves. The terbium emission was measured at 545 nm (closed square) and the sensitized acceptor emission was measured at 520 nm (open circle). To correct for the small variations in recombinant protein concentrations, the data were normalized relative to the directly measured GFP signal at 535 nm. The error bars represent the standard deviation measured from three replicate microtiter wells.

The normalized time-resolved decay spectra of the terbium emission and the sensitized acceptor emission from the energy transfer reaction are shown in Figure 25. The fluorescence lifetime data of the terbium component prior to trypsin cleavage gave a main lifetime component of  $0.95 \pm 0.01$  ms, which, after trypsin cleavage increased to  $2.47 \pm 0.01$  ms. The considerably shorter terbium lifetime in the intact peptide is evidence of efficient resonance energy transfer.

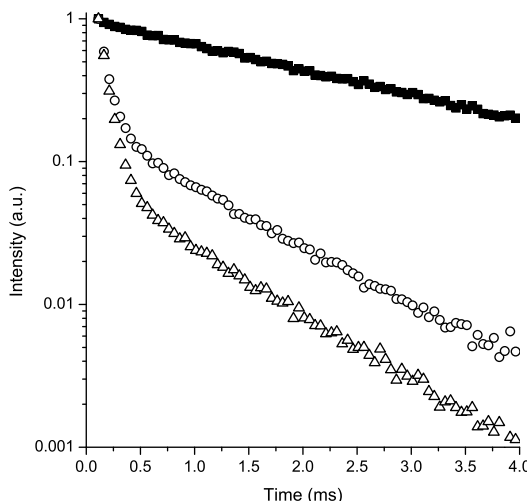


**Figure 25.** Normalized time-resolved decay spectra of the terbium emission and the sensitized GFP acceptor emission. Curves from top to bottom: decay spectrum of terbium in a cleaved substrate (closed squares) measured at 545 nm, decay spectrum of terbium in an intact substrate (open circles) measured at 545 nm, and decay spectrum of GFP in an intact peptide (open triangles) measured at 520 nm. a.u., arbitrary unit.

---

*Summary of Results and Discussion*

---

This was the first report of a protease assay using a LBP and a fluorescent protein enabling TRF detection. In addition to the site-specific genetical encoding, the useful features of LBPs include good photostability and biocompatibility. The genetically encoded FRET-pair designed in this work could potentially be used in *in vivo* experiments, as the construct is expressed in living cells. However, in this case, issues of cell permeability of the lanthanide ion should be considered.

## 6 CONCLUSIONS

Lanthanide-based reporters are increasingly popular labels in bioanalytical applications. This is due to the advantages they bring compared to conventional fluorescent reporters. These advantages are related to the very unique photophysical properties of the lanthanide-based reporters, such as the narrow emission bands, the large Stokes shifts, and the long luminescence lifetimes.

In this study, different homogeneous energy transfer assays were constructed, all utilizing the useful features of lanthanide-based donor fluorophores. In most of the constructed assays, time-resolved detection was used to eliminate the autofluorescence originating from biological materials. This resulted in high signal-to-background ratios, which are often compromised in homogeneous assay formats. The study covered a broad range of lanthanide-based reporter classes from traditionally used lanthanide chelates to emerging reporter classes, e.g., UCPs and LBPs. Additionally, different energy transfer mechanisms were studied shedding light on a novel spectrally non-overlapping energy transfer mechanism.

The main conclusions based on the original publications are presented below.

- I     Although both lanthanide chelates and fluorescent proteins are widely used in bioanalytical applications, rather few reports have been published on energy transfer between these components. A straightforward and sensitive homogeneous competitive bioaffinity assay was constructed where, in addition to the conventional Förster-type energy transfer, a spectrally non-overlapping energy transfer mechanism was demonstrated for the first time for fluorescent proteins. Lack of spectral overlap minimizes the assay background caused by donor cross-talk and radiative energy transfer from the donor to unbound acceptors, thus making the assay more sensitive. The nFRET mechanism also creates new opportunities for donor-acceptor pairs in energy transfer-based assays by enabling the use of different lanthanide chelate donors in combination with fluorescent proteins or various other acceptor fluorophores.
  
- II    Very little is known about the actual mechanism behind the nFRET phenomenon and, therefore, there was a need for a more detailed study on the subject. In the developed homogeneous DNA-hybridization assay both the distance and the temperature dependence of conventional and non-overlapping FRET were investigated. The energy transfer efficiency measurements showed that the nFRET mechanism resulted in highly efficient energy transfer despite the lack of spectral overlap, but only at short distances. Unlike conventional FRET, nFRET also showed clear temperature dependence. Based on the measurements, it was proposed that in nFRET, a thermal excitation occurs from the lowest emissive  $^5D_0$  level of Eu $^{3+}$  ion to higher excited states, these states being either ionic or associated with a ligand-to-metal charge-transfer state. The nFRET widens the range of applicable fluorophores with favorable characteristics and paves the way for new and increasingly sensitive assay applications.

## *Conclusions*

---

- III** Particulate reporters have some distinct advantages over small molecular weight labels featuring, for example, improved binding capacity and high specific activity. An added benefit of lanthanide containing UCP particles is the total elimination of autofluorescence at the wavelength used to monitor the acceptor emission. A sensitive fluorescence quenching-based homogeneous model assay was developed for monitoring caspase-3 activity. The lack of autofluorescence combined with the careful selection of stable label components resulted in very high signal-to-background ratios. The effect of assay miniaturization was also studied, and it revealed that considerable decrease of reagent consumption may be achieved without compromising the assay performance. This is due to the assay design using an internally quenched double-labeled substrate diminishing the background caused by radiatively excited acceptor molecules. The designed separation-free assay was suitable for miniaturization and automation, and could be applied to high-throughput screening.
- IV** LBPs are an interesting class of lanthanide-based reporters. Even though LBPs have been studied for several decades, few reports exist on their use in energy transfer applications. A protease activity assay was designed where the energy transfer from a LBP to a GFP was demonstrated by a reduction in the fluorescence intensity and emission lifetime of the donor fluorophore, and by fluorescence emission at a wavelength specific for the acceptor. The assay demonstrated, for the first time, the applicability of a LBP-GFP energy transfer pair in a protease activity assay. The intrinsically fluorescent and genetically encodable components enable easy expression of the construct without the need of cumbersome chemical labeling. By varying the fluorescent protein and the protease specificity of the internal linker sequence, the method can be applied to the detection of a wide variety of proteases.

In conclusion, the lanthanide-based reporter technologies have quickly gained interest in bioanalysis. They can be utilized in a multitude of fields, from bioaffinity assays to microscopy and imaging. In some applications, either the fluorescence intensity or the sensitivity achievable with the lanthanide chelates is not sufficient. In these cases, particulate labels, such as lanthanide chelate-dyed nanoparticles or UCPs, can be used. UCPs offer the additional benefit of reduced background without the need of time-resolution, thus simplifying the detection instrumentation. Because of the NIR excitation, UCPs can also be used as reporters in whole blood. Instead of chemically synthesizing the reporter complex and attaching it to the biomolecule *in vitro*, lanthanide-binding peptides offer a means to develop entirely genetically encodable reporter systems, which open new possibilities, e.g., in bioaffinity assays and imaging. The advances in the current lanthanide reporter technologies and the development of novel lanthanide-based reporters with exciting properties hold great promise for the field of bioanalytics.

## ACKNOWLEDGEMENTS

This study was carried out at the Department of Biotechnology, University of Turku, in the years 2008–2012. Financial support from the Finnish Funding Agency for Technology and Innovation (Tekes), the Academy of Finland, and the National Doctoral Programme of Advanced Diagnostic Technologies and Applications (DIA-NET) is gratefully acknowledged.

I wish to express my sincere gratitude to the professors of the Department of Biotechnology, Professor Emeritus Timo Lövgren, Professor Kim Pettersson, Professor Tero Soukka, and Professor Urpo Lamminmäki for giving me the opportunity to work and carry out my PhD studies at the department, a truly unique place in so many ways. I wish to thank the professors for also trusting me with administrative responsibilities in the DIA-NET Doctoral Programme and in the UPCORE research project. These tasks have taught me a lot, allowed me to get acquainted with wonderful people, and made me realize I really enjoy coordinating.

My deepest gratitude goes to my supervisor Tero Soukka. He has been the pillar of strength and the driving force behind my PhD studies. His practically inhumane intelligence and his complete dedication to his PhD students make him the best supervisor one could possibly hope for. Tero's uncompromising passion and devotion to his work has created flourishing research projects, and I am forever grateful for having had the chance to be a part of them.

I wish to thank my esteemed pre-examiners Adjunct Professor Timo Piironen (SYRINX Bioanalytics Oy) and PD Dr. habil. Axel Dürkop (University of Regensburg) for reviewing this thesis. I am very grateful for their valuable comments. I am also grateful to Anu Toivonen for reviewing the language of the thesis.

I wish to thank all my co-authors for their vital role in this thesis. Markku Syrjänpää, Marika Nummela, Essi Kulta, and Riikka Arppe have conducted valuable experiments in the lab and shown real expertise in their work. Dr. Terhi Riuttamäki has given important guidance and set an example by her diligent and professional practices. I am extremely grateful to Dr. Ilko Hyppänen and Professor Emeritus Jouko Kankare (Laboratory of Materials Chemistry and Chemical Analysis) for their kind guidance and invaluable contribution especially regarding the original publication **II**. Furthermore, this thesis would certainly not have been accomplished without the essential aid, encouragement and skill of Professor Urpo Lamminmäki and Professor Tero Soukka. They are true specialists in their fields. In addition, I wish to acknowledge Professor Jorma Hölsä, Dr. Mika Lastusaari, Emilia Palo, and coworkers at the Laboratory of Materials Chemistry and Chemical Analysis for providing material and knowledge regarding the upconverting nanoparticles used in the original publication **III**.

International collaboration has provided some of the definite highlights in my PhD studies. I wish to thank the entire Institute of Analytical Chemistry, Chemo- and Biosensors at the University of Regensburg, Germany, for welcoming me so warmly to their community, and for kindly inviting me to wonderful events and get-togethers (the trip to Steiermark was just one of the so many unforgettable experiences). I especially want to thank Professor Emeritus Otto S. Wolfbeis for making it all possible, Dr. Heike Mader for her enormous

### *Acknowledgements*

---

help and her friendship, and Dr. Daniela Achatz, Raphaela Liebherr, and Dr. Michael Schäferling for the mutual joy and benefit of the continuing international exchange between our Universities. I also wish to warmly thank the Rölz family for giving me so much more than just accommodation during my stay in Germany. It is amazing that now I have a home to come to every time I visit Regensburg.

An integral part of my PhD studies has been the exceedingly wonderful research team working mainly on upconverting nanoparticles. I joined this group already while working on my Master's thesis. Back then it was a small core group of Dr. Katri Kuningas, Dr. Terhi Riuttamäki, Telle Ukonaho, and Henna Päkkilä, collectively known as "Tero's angels" or "Tero's sewing club". Since then, the team has expanded enormously alternating in composition and name (LEAP, INFRA, UPCORE), but never losing the hard-working mentality, great skill, and relaxed atmosphere. Special thanks to Marja-Leena Järvenpää, Riikka Arppe, Minna Ylihärsilä, Marika Nummela, Timo Valta, Sami Blom, Satu Lahtinen, Kari Kopra, Leena Mattsson, Oskari Salovaara, and Juho Terrijärvi for making research so much fun. Besides these people, there have been many brilliant students and great new additions to this group that I shall simply call the "Team UCP" – Team of Unbelievably Clever People.

I want to express my warmest thanks to all the previous and present staff members at the Department of Biotechnology. This outstanding group has also grown and changed during the years, but retained the warm and welcoming atmosphere that has made me, and so many others, feel privileged to work there. I want to thank the technical staff, including Mirja Jaala, Marja Maula, and Martti Sointusalo for keeping everything running smoothly in the lab. As in the notions of Mr. Wilde, the bureaucracy is expanding to meet the needs of the expanding bureaucracy also in the academic world. A great big thanks, therefore, to all the previous and current members of the administrative staff, including Marja-Liisa Knuuti, Kaisa Linderborg, Görel Salomaa, Marika Silvennoinen, Maria Saalpo, and Sanna Koivuniemi for all their efforts. Thanks to Pirjo Laaksonen and others for the refreshing recess exercise moments that have ensured proper blood flow to my brain also in the afternoons. Special thanks to Dr. Mari Peltola for her considerable help and valuable advice on preparing the thesis, and to Ulla Karhunen for sharing the challenges and joys of PhD studies and for finding time to review this thesis.

I boldly emigrated from Kangasala to Turku in 2002 without having any friends or relatives here. That situation has luckily changed over the years as well, and I wish to warmly thank all my friends here in Turku, Aki, Juho, Jenni, Liisa, Kim, and all the others, and those who have already moved away, including Maria, Petri, and Minna. Thank you for all the hilarious get-togethers and events that have brightened up my life so much, and made Turku very quickly feel like home. A warm thanks also to all the friends in and around Kangasala. Esa, Suvi, Valtteri, Veeti, Heli, Pasi, Satu, and Joonas: it is always a great pleasure to spend time with you. Big thanks to Kari, Juha, and Pekka for the countless movie and board game nights at the great Sipilä-ranch. These evenings have been the joy and highlight of so many weekends. Special thanks to Kati and Jore for being there and for being you.

I wish to thank the Pyylampi family for all their friendship and support over the years. Irma, Inkeri, Riikka, Elias, Veera and Tapio, thank you for so warmly welcoming me into

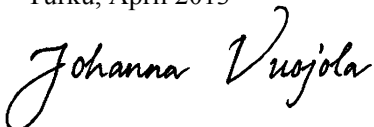
---

*Acknowledgements*

your wonderful family. Thank you also Elsa and other members of the large family. You bring such richness to life.

Without a doubt the biggest reason for me to be at this point has been the love and never-ending support of my family. Suunnaton kiitos äidille ja isälle, jotka ovat aina jaksaneet uskoa ja tukea. Kiitos siitä valtavasta määristä rakkautta ja huolenpitoa, joka on kantanut minua tähän asti, ja kantaa edelleen tulevaisuuteen. My most sincere gratitude goes also to my brother Timo, and to my sister Elina and her husband Janne. It is impossible to describe how very important and dear you are to me. Finally, my deepest gratitude goes to my beloved Kari-Pekka for all the years, and all the care and support. The world is wide open, let's go!

Turku, April 2013



Johanna Vuojola

## REFERENCES

- Abdul Jalil, R. and Zhang, Y. (2008) Biocompatibility of silica coated NaYF<sub>4</sub> upconversion fluorescent nanocrystals. *Biomaterials* **29**:4122-4128.
- Achatz, D.E., Meier, R.J., Fischer, L.H. and Wolfbeis, O.S. (2011) Luminescent sensing of oxygen using a quenchable probe and upconverting nanoparticles. *Angew Chem Int Ed Engl* **50**:260-263.
- Allen, K.N. and Imperiali, B. (2010) Lanthanide-tagged proteins - an illuminating partnership. *Curr Opin Chem Biol* **14**:247-254.
- Alnemri, E.S., Livingston, D.J., Nicholson, D.W., Salvesen, G., Thornberry, N.A., Wong, W.W. and Yuan, J. (1996) Human ICE/CED-3 protease nomenclature. *Cell* **87**:171.
- Alpha, B., Ballardini, R., Balzani, V., Lehn, J.M., Perathoner, S. and Sabbatini, N. (1990) Antenna effect in luminescent lanthanide cryptates: a photophysical study. *Photochem Photobiol* **52**:299-306.
- Alpha, B., Balzani, V., Lehn, J.M., Perathoner, S. and Sabbatini, N. (1987) Luminescence probes: The Eu<sup>3+</sup>- and Tb<sup>3+</sup>-cryptates of polypyridine macrobicyclic ligands. *Angew Chem Int Ed Engl* **26**:1266-1267.
- An, Y., Schramm, G.E. and Berry, M.T. (2002) Ligand-to-metal charge-transfer quenching of the Eu<sup>3+</sup>(<sup>5</sup>D<sub>1</sub>) state in europium-doped tris(2,2,6,6-tetramethyl-3,5-heptanedionato)gadolinium (III). *J Lumin* **97**:7-12.
- André, A. and Henry, F. (1998) "Emulsifier-free" emulsion copolymerization of styrene and butylacrylate: particle size control with synthesis parameters. *Colloid Polym Sci* **276**:1061-1067.
- Arslanbaeva, L.P., Zherdeva, V.V., Ivashina, T.V., Vinokurov, L.M., Morozov, B.V., Olenin, A.N. and Savitskii, A.P. (2011) Induction-resonance energy transfer between the terbium-binding peptide and the red fluorescent proteins Dsred2 and TagRFP. *Biofizika* **56**:389-395.
- Arslanbaeva, L.R., Zherdeva, V.V., Ivashina, T.V., Vinokurov, L.M., Rusanov, A.L. and Savitskii, A.P. (2010) Genetically encoded FRET-pair on the basis of terbium-binding peptide and red fluorescent protein. *Prikl Biokhim Mikrobiol* **46**:166-171.
- Aspinall, H.C. (2002) Chiral lanthanide complexes: coordination chemistry and applications. *Chem Rev* **102**:1807-1850.
- Auzel, F. (2004) Upconversion and anti-stokes processes with f and d ions in solids. *Chem Rev* **104**:139-173.
- Barbieri, R., Bertini, I., Cavallaro, G., Lee, Y.M., Luchinat, C. and Rosato, A. (2002) Paramagnetically induced residual dipolar couplings for solution structure determination of lanthanide binding proteins. *J Am Chem Soc* **124**:5581-5587.
- Barthelmes, K., Reynolds, A.M., Peisach, E., Jonker, H.R., DeNunzio, N.J., Allen, K.N., Imperiali, B. and Schwalbe, H. (2011) Engineering encodable lanthanide-binding tags into loop regions of proteins. *J Am Chem Soc* **133**:808-819.
- Bazin, H., Trinquet, E. and Mathis, G. (2002) Time resolved amplification of cryptate emission: a versatile technology to trace biomolecular interactions. *Rev Mol Biotechnol* **82**:233-250.
- Beeby, A., Clarkson, I.M., Dickins, R.S., Faulkner, S., Parker, D., Royle, L., de Sousa, A.S., Williams, J.A.G. and Woods, M. (1999) Non-radiative deactivation of the excited states of europium, terbium and ytterbium complexes by proximate energy-matched OH, NH and CH oscillators: an improved luminescence method for establishing solution hydration states. *J Chem Soc, Perkin Trans 2*:493-504.
- Beverloo, H.B., van Schadewijk, A., van Gelderen-Boele, S. and Tanke, H.J. (1990) Inorganic phosphors as new luminescent labels for immunocytochemistry and time-resolved microscopy. *Cytometry* **11**:784-792.
- Beverloo, H.B., van Schadewijk, A., Zijlmans, H.J. and Tanke, H.J. (1992) Immunochemical detection of proteins and nucleic acids on filters using small luminescent inorganic crystals as markers. *Anal Biochem* **203**:326-334.
- Bielefeld-Sevigny, M. (2009) AlphaLISA immunoassay platform – the “no-wash” high-throughput alternative to ELISA. *Assay Drug Dev Technol* **7**:90-92.
- Binnemanns, K. (2009) Lanthanide-based luminescent hybrid materials. *Chem Rev* **109**:4283-4374.
- Blasse, G. (1976) The influence of charge-transfer and Rydberg states on the luminescence properties of lanthanides and actinides. Vol. 26. Springer-Verlag, Berlin. p.p. 43-79.
- Blasse, G. and Grabmaier, B.C. (1994) Luminescent materials. Springer-Verlag, Berlin.

## References

---

- Buissette, V., Moreau, M., Gacoin, T., Boilot, J.P., Chane-Ching, J.Y. and Le Mercier, T. (2004) Colloidal synthesis of luminescent rhabdophane  $\text{LaPO}_4\text{:Ln}^{3+}\cdot\text{xH}_2\text{O}$  ( $\text{Ln} = \text{Ce}, \text{Tb}, \text{Eu}; \text{x} \approx 0.7$ ) nanocrystals. *Chem Mater* **16**:3767-3773.
- Bünzli, J.C. (2006) Benefiting from the unique properties of lanthanide ions. *Acc Chem Res* **39**:53-61.
- Bünzli, J.C. (2010) Lanthanide luminescence for biomedical analyses and imaging. *Chem Rev* **110**:2729-2755.
- Bünzli, J.C., Chauvin, A.S., Vandevyver, C.D., Bo, S. and Comby, S. (2008) Lanthanide bimetallic helicates for in vitro imaging and sensing. *Ann N Y Acad Sci* **1130**:97-105.
- Bünzli, J.C. and Choppin, G.R. (1989) Lanthanide probes in life, chemical and earth sciences: theory and practice. Elsevier Science Ltd, Amsterdam. p.p. 219-293.
- Bünzli, J.C., Comby, S., Chauvin, A.S. and Vandevyver. (2007) New opportunities for lanthanide luminescence. *J Rare Earth* **25**:257-274.
- Bünzli, J.C. and Eliseeva, S.V. (2011) Basics of lanthanide photophysics. Springer series on fluorescence; lanthanide luminescence: photophysical, analytical and biological aspects. Vol. 7. Springer-Verlag, Berlin. p.p. 1-45.
- Bünzli, J.C. and Piguet, C. (2002) Lanthanide-containing molecular and supramolecular polymetallic functional assemblies. *Chem Rev* **102**:1897-1928.
- Bünzli, J.C. and Piguet, C. (2005) Taking advantage of luminescent lanthanide ions. *Chem Soc Rev* **34**:1048-1077.
- Carlos, L.D., Ferreira, R.A., de Zea Bermudez, V., Julián-López, B. and Escrivano, P. (2011) Progress on lanthanide-based organic-inorganic hybrid phosphors. *Chem Soc Rev* **40**:536-549.
- Carnall, W.T., Fields, P.R. and Rajnak, K. (1968a) Electronic energy levels of the trivalent lanthanide aquo ions. I.  $\text{Pr}^{3+}$ ,  $\text{Nd}^{3+}$ ,  $\text{Pm}^{3+}$ ,  $\text{Sm}^{3+}$ ,  $\text{Dy}^{3+}$ ,  $\text{Ho}^{3+}$ ,  $\text{Er}^{3+}$ , and  $\text{Tm}^{3+}$ . *J Chem Phys* **49**:4424-4442.
- Carnall, W.T., Fields, P.R. and Rajnak, K. (1968b) Electronic energy levels of the trivalent lanthanide aquo ions. II.  $\text{Gd}^{3+}$ . *J Chem Phys* **49**:4443-4446.
- Carnall, W.T., Fields, P.R. and Rajnak, K. (1968c) Electronic energy levels of the trivalent lanthanide aquo ions. III.  $\text{Tb}^{3+}$ . *J Chem Phys* **49**:4447-4449.
- Carnall, W.T., Fields, P.R. and Rajnak, K. (1968d) Electronic energy levels of the trivalent lanthanide aquo ions. IV.  $\text{Eu}^{3+}$ . *J Chem Phys* **49**:4450-4455.
- Charbonniere, L.J. (2011) Luminescent lanthanide labels. *Curr Inorg Chem* **1**:2-16.
- Charbonniere, L.J., Weibel, N., Retailleau, P. and Ziessel, R. (2006) Relationship between the ligand structure and the luminescent properties of water-soluble lanthanide complexes containing bis(bipyridine) anionic arms. *Chem Eur J* **13**:346-358.
- Chatterjee, D.K., Rufaihah, A.J. and Zhang, Y. (2008) Upconversion fluorescence imaging of cells and small animals using lanthanide doped nanocrystals. *Biomaterials* **29**:937-943.
- Chen, M.Q., Serizawa, T., Kishida, A. and Akashi, M. (1999) Graft copolymers having hydrophobic backbone and hydrophilic branches. XXIII. Particle size control of poly(ethylene glycol)-coated polystyrene nanoparticles prepared by macromonomer method. *J Polym Sci, Part A: Polym Chem* **37**:2155-2166.
- Chen, Y., Chi, Y., Wen, H. and Lu, Z. (2007) Sensitized luminescent terbium nanoparticles: preparation and time-resolved fluorescence assay for DNA. *Anal Chem* **79**:960-965.
- Clark, I.D., Hill, I., Sikorska-Walker, M., MacManus, J.P. and Szabo, A.G. (1993) A novel peptide designed for sensitization of terbium (III) luminescence. *FEBS Lett* **333**:96-98.
- Clegg, R.M. (1992) Fluorescence resonance energy transfer and nucleic acids. *Methods Enzymol* **211**:353-388.
- Clegg, R.M. (1995) Fluorescence resonance energy transfer. *Curr Opin Biotechnol* **6**:103-110.
- Connally, R.E. and Piper, J.A. (2008) Time-gated luminescence microscopy. *Ann N Y Acad Sci* **1130**:106-116.
- Corstjens, P.L., Chen, Z., Zuiderwijk, M., Bau, H.H., Abrams, W.R., Malamud, D., Sam Niedbala, R. and Tanke, H.J. (2007) Rapid assay format for multiplex detection of humoral immune responses to infectious disease pathogens (HIV, HCV, and TB). *Ann N Y Acad Sci* **1098**:437-445.
- Cotton, S. (2006) Lanthanide and actinide chemistry. John Wiley & Sons Ltd, England. p.p. 1-22.
- Crosby, G.A., Whan, R.E. and Alire, R.M. (1961) Intramolecular energy transfer in rare earth chelates. Role of the triplet state. *J Chem Phys* **34**:743-748.
- Davies, C. (2001) Introduction to immunoassay principles. The immunoassay handbook. 2nd Ed. Nature publishing group, London. p.p. 3-40.

## References

---

- De Cola, L., Smailes, D.L. and Vallarino, L.M. (1986) Hexaaza macrocyclic complexes of the lanthanides. *Inorg Chem* **25**:1729-1732.
- de Sá, G.F., Malta, O.L., de Mello Donegá, C., Simas, A.M., Longo, R.L., Santa-Cruz, P.A. and E.F. d.S.J. (2000) Spectroscopic properties and design of highly luminescent lanthanide coordination complexes. *Coord Chem Rev* **196**:165-195.
- Dexter, D.L. (1953) A theory of sensitized luminescence in solids. *J Chem Phys* **21**:836-850.
- Dickson, E.F., Pollak, A. and Diamandis, E.P. (1995) Time-resolved detection of lanthanide luminescence for ultrasensitive bioanalytical assays. *J Photochem Photobiol B* **27**:3-19.
- Dorenbos, P. (2000) Predictability of 5d level positions of the triply ionized lanthanides in halogenides and chalcogenides. *J Lumin* **87-89**:970-972.
- dos Santos, C.M.G., Harte, A.J., Quinn, S.J. and Gunnlaugsson, T. (2008) Recent developments in the field of supramolecular lanthanide luminescent sensors and self-assemblies. *Coord Chem Rev* **252**:2512-2527.
- Dosev, D., Nichkova, M. and Kennedy, I.M. (2008) Inorganic lanthanide nanophosphors in biotechnology. *J Nanosci Nanotechnol* **8**:1052-1067.
- Dürkop, A. and Wolfbeis, O.S. (2005) Nonenzymatic direct assay of hydrogen peroxide at neutral pH using the Eu<sub>3</sub>Tc fluorescent probe. *J Fluoresc* **15**:755-761.
- Eglen, R.M., Reisine, T., Roby, P., Rouleau, N., Illy, C., Bossé, R. and Bielefeld, M. (2008) The use of AlphaScreen technology in HTS: current status. *Curr Chem Genomics* **1**:2-10.
- Ekins, R.P. (1960) The estimation of thyroxine in human plasma by an electrophoretic technique. *Clin Chim Acta* **5**:453-459.
- Ekins, R.P. (1998) Ligand assays: from electrophoresis to miniaturized microarrays. *Clin Chem* **44**:2015-2030.
- Ekins, R.P. and Chu, F.W. (1991) Multianalyte microspot immunoassay-microanalytical "compact disk" of the future. *Clin Chem* **37**:1955-1967.
- Ekins, R.P. and Dakubu, S. (1985) The development of high sensitivity pulsed light, time-resolved fluoroimmunoassays. *Pure Appl Chem* **57**:473-482.
- Eliseeva, S.V. and Bünzli, J.C. (2010) Lanthanide luminescence for functional materials and bio-sciences. *Chem Soc Rev* **39**:189-227.
- Engvall, E. and Perlmann, P. (1971) Enzyme-linked immunosorbent assay (ELISA). Quantitative assay of immunoglobulin G. *Immunochemistry* **8**:871-874.
- Fairclough, R.H. and Cantor, C.R. (1978) The use of singlet-singlet energy transfer to study macromolecular assemblies. *Methods Enzymol* **48**:347-379.
- Fang, Y.P., Xu, A.W. and Dong, W.F. (2005) Highly improved green photoluminescence from CePO<sub>4</sub>:Tb/LaPO<sub>4</sub> core/shell nanowires. *Small* **1**:967-971.
- Faulkner, S., Natrajan, L.S., Perry, W.S. and Sykes, D. (2009) Sensitised luminescence in lanthanide containing arrays and d-f hybrids. *Dalton Trans*:3890-3899.
- Faulkner, S., Pope, S.A. and Burton-Pye, B.P. (2005) Lanthanide complexes for luminescence imaging applications. *Appl Spectrosc Rev* **40**:1-31.
- Fischer, U. and Schulze-Osthoff, K. (2005) Apoptosis-based therapies and drug targets. *Cell Death Differ* **12**:942-961.
- Frank, D.S. and Sundberg, M.W. (1978) Fluorescent labels comprising rare earth chelates. US Patent 4,283,382.
- Frey, S.T. and Horrocks, W.D.J. (1995) On correlating the frequency of the <sup>7</sup>F<sub>0</sub> - <sup>5</sup>D<sub>0</sub> transition in Eu<sup>3+</sup> complexes with the sum of 'nephelauxetic parameters' for all of the coordinating atoms. *Small* **229**:383-390.
- Förster, T. (1948) Zwischenmolekulare Energiewanderung und Fluoreszenz. *Ann Phys* **437**:55-75.
- Gamelin, D.R. and Güdel, H.U. (2000) Design of luminescent inorganic materials: new photophysical processes studied by optical spectroscopy. *Acc Chem Res* **33**:235-242.
- Geissler, D., Stufler, S., Löhmannsröben, H.G. and Hildebrandt, N. (2012) Six-color time-resolved Förster resonance energy transfer for ultrasensitive multiplexed biosensing. *J Am Chem Soc* DOI: 10.1021/ja310317n.
- Giroud-Godquin, A.M. and Maitilis, P.M. (1991) Metallomesogens: metal complexes in organized fluid phases. *Angew Chem, Int Ed Engl* **30**:375-402.
- Gopalakrishnan, S.M., Karvinen, J., Kofron, J.L., Burns, D.J. and Warrior, U. (2002) Application of micro arrayed compound screening (microARCS) to identify inhibitors of caspase-3. *J Biomol Screen* **7**:317-323.

## References

---

- Gosling, J.P. (1990) A decade of development in immunoassay methodology. *Clin Chem* **36**:1408-1427.
- Guo, C.Y., Shankar, R.R., Abe, S., Ye, Z., Thomas, R.N. and Kuo, J.E. (1992) Functionalized, probe-containing, latex nanospheres. *Anal Biochem* **207**:241-248.
- Gutierrez, F., Tedeschi, C., Maron, L., Daudey, J.P., Poteau, R., Azema, J., Tisnes, P. and Picard, C. (2004) Quantum chemistry-based interpretations on the lowest triplet state of luminescent lanthanides complexes. Part 1. Relation between the triplet state energy of hydroxamate complexes and their luminescence properties. *Dalton Trans*:1334-1347.
- Güdel, H.U. and Pollnau, M. (2000) Near-infrared to visible photon upconversion processes in lanthanide doped chloride, bromide and iodide lattices. *J Alloys Compd* **303-304**:307-315.
- Haas, Y. and Stein, G. (1971) Pathways of radiative and radiationless transitions in Eu<sup>3+</sup> solutions: Anti-Stokes emission. *Chem Phys Lett* **8**:366-368.
- Haase, M. and Schäfer, H. (2011) Upconverting nanoparticles. *Angew Chem Int Ed Engl* **50**:5808-5829.
- Hagan, A.K. and Zuchner, T. (2011) Lanthanide-based time-resolved luminescence immunoassays. *Anal Bioanal Chem* **400**:2847-2864.
- Hagren, V., von Lode, P., Syrjälä, A., Soukka, T., Lövgren, T., Kojola, H. and Nurmi, J. (2008) An automated PCR platform with homogeneous time-resolved fluorescence detection and dry chemistry assay kits. *Anal Biochem* **374**:411-416.
- Hai, X., Tan, M., Wang, G., Ye, Z., Yuan, J. and Matsumoto, K. (2004) Preparation and a time-resolved fluoroimmunoassay application of new europium fluorescent nanoparticles. *Anal Sci* **20**:245-246.
- Handl, H.L. and Gillies, R.J. (2005) Lanthanide-based luminescent assays for ligand-receptor interactions. *Life Sci* **77**:361-371.
- Harris, E.A. and Furniss, D. (1991) Electron paramagnetic resonance of non-Kramers ion in a fluorozirconate glass. *J Phys: Condens Matter* **3**:1889-1900.
- Hebbink, G.A., Stouwdam, J.W., Reinhoudt, D.N. and van Veggel, F.C.J.M. (2002) Lanthanide(III)-doped nanoparticles that emit in the near-Infrared. *Adv Mater* **14**:1147-1150.
- Hemmilä, I. (1985) Fluoroimmunoassays and immunofluorometric assays. *Clin Chem* **31**:359-370.
- Hemmilä, I. (1999) LANCEtrade mark: homogeneous assay platform for HTS. *J Biomol Screen* **4**:303-308.
- Hemmilä, I., Dakubu, S., Mukkala, V.M., Siitari, H. and Lövgren, T. (1984) Europium as a label in time-resolved immunofluorometric assays. *Anal Biochem* **137**:335-343.
- Hemmilä, I. and Hurskainen, P. (2002) Novel detection strategies for drug discovery. *Drug Discov Today* **7**:S150-S156.
- Hemmilä, I. and Laitala, V. (2005) Progress in lanthanides as luminescent probes. *J Fluoresc* **15**:529-542.
- Hemmilä, I. and Mukkala, V.M. (2001) Time-resolution in fluorometry technologies, labels, and applications in bioanalytical assays. *Crit Rev Clin Lab Sci* **38**:441-519.
- Hemmilä, I., Mukkala, V.M. and Takalo, H. (1997) Development of luminescent lanthanide chelate labels for diagnostic assays. *J Alloys Compd* **249**:158-162.
- Hilderbrand, S.A., Shao, F., Salthouse, C., Mahmood, U. and Weissleder, R. (2009) Upconverting luminescent nanomaterials: application to in vivo bioimaging. *Chem Commun*:4188-4190.
- Horrocks, W.D.J. and Sudnick, D.R. (1979) Lanthanide ion probes of structure in biology. Laser-induced luminescence decay constants provide a direct measure of the number of metal-coordinated water molecules. *J Am Chem Soc* **101**:334-340.
- Horrocks, W.D.J. and Sudnick, D.R. (1981) Lanthanide ion luminescence probes of the structure of biological macromolecules. *Acc Chem Res* **14**:384-392.
- Huang, C. and Bian, Z. (2010) Rare earth coordination chemistry: fundamentals and applications, Chapter 1. John Wiley & Sons (Asia) Pte Ltd., Singapore.
- Huang, Y.G., Jiang, F.L. and Hong, M.C. (2009) Magnetic lanthanide-transition-metal organic-inorganic hybrid materials: From discrete clusters to extended frameworks. *Coord Chem Rev* **253**:2814-2834.
- Huhtinen, P., Kivelä, M., Kuronen, O., Hagren, V., Takalo, H., Tenhu, H., Lövgren, T. and Härmä, H. (2005) Synthesis, characterization, and application of Eu(III), Tb(III), Sm(III), and Dy(III) lanthanide chelate nanoparticle labels. *Anal Chem* **77**:2643-2648.
- Huignard, A., Gacoin, T. and Boilot, J.P. (2000) Synthesis and luminescence properties of colloidal YVO<sub>4</sub>:Eu phosphors. *Chem Mater* **12**:1090-1094.
- Hyppänen, I., Soukka, T. and Kankare, J. (2010) Frequency-domain measurement of luminescent lanthanide chelates. *J Phys Chem A* **114**:7856-7867.
- Härmä, H., Soukka, T. and Lövgren, T. (2001) Europium nanoparticles and time-resolved fluorescence for ultrasensitive detection of prostate-specific antigen. *Clin Chem* **47**:561-568.

## References

---

- Izatt, R.M., Bradshaw, J.S., Nielsen, S.A., Lamb, J.D., Christensen, J.J. and Sen, D. (1985) Thermodynamic and kinetic data for cation-macrocycle interaction. *Chem Rev* **85**:271-339.
- Jaakohuhta, S., Härmä, H., Tuomola, M. and Lövgren, T. (2007) Sensitive Listeria spp. immunoassay based on europium(III) nanoparticulate labels using time-resolved fluorescence. *Int J Food Microbiol* **114**:288-294.
- James, C. and Willand, P.S. (1916) The rare earth cobaltcyanide. *J Am Chem Soc* **38**:1497-1500.
- Junker, R., Schlebusch, H. and Luppia, P.B. (2010) Point-of-care testing in hospitals and primary care. *Dtsch Arztebl Int* **107**:561-567.
- Juntunen, E., Myyryläinen, T., Salminen, T., Soukka, T. and Pettersson, K. (2012) Performance of fluorescent europium(III) nanoparticles and colloidal gold reporters in lateral flow bioaffinity assay. *Anal Biochem* **428**:31-38.
- Järvenpää, M.L., Kuningas, K., Niemi, I., Hedberg, P., Ristiniemi, N., Pettersson, K. and Lövgren, T. (2012) Rapid and sensitive cardiac troponin I immunoassay based on fluorescent europium(III)-chelate-dyed nanoparticles. *Clin Chim Acta* **414**:70-75.
- Jääskeläinen, A., Harinen, R.R., Lamminmäki, U., Korpimaki, T., Pelliniemi, L.J., Soukka, T. and Virta, M. (2007) Production of apoferitin-based bioinorganic hybrid nanoparticles by bacterial fermentation followed by self-assembly. *Small* **3**:1362-1367.
- Kankare, J. and Hyppänen, I. (2011) Frequency-domain measurements. Springer series on fluorescence; lanthanide luminescence: photophysical, analytical and biological aspects. Vol. 7. Springer-Verlag, Berlin. p.p. 279-312.
- Karhunen, U., Rosenberg, J., Lamminmaki, U. and Soukka, T. (2011) Homogeneous detection of avidin based on switchable lanthanide luminescence. *Anal Chem* **83**:9011-9016.
- Karvinen, J., Hurskainen, P., Gopalakrishnan, S., Burns, D., Warrior, U. and Hemmilä, I. (2002) Homogeneous time-resolved fluorescence quenching assay (LANCE) for caspase-3. *J Biomol Screen* **7**:223-231.
- Karvinen, J., Laitala, V., Mäkinen, M.L., Mulari, O., Tamminen, J., Hermonen, J., Hurskainen, P. and Hemmilä, I. (2004) Fluorescence quenching-based assays for hydrolyzing enzymes. Application of time-resolved fluorometry in assays for caspase, helicase, and phosphatase. *Anal Chem* **76**:1429-1436.
- Kerr, J.F., Wyllie, A.H. and Currie, A.R. (1972) Apoptosis: a basic biological phenomenon with wide-ranging implications in tissue kinetics. *Br J Cancer* **26**:239-257.
- Khalil, G.E., Lau, K., Phelan, G.D., Carlson, B.G., M., Callis, J.B. and R., D.L. (2004) Europium beta-diketonate temperature sensors: Effects of ligands, matrix, and concentration. *Rev Sci Instrum* **75**:192-206.
- Kido, J. and Okamoto, Y. (2002) Organo lanthanide metal complexes for electroluminescent materials. *Chem Rev* **102**:2357-2368.
- Kokko, L., Jaakohuhta, S., Lindroos, P. and Soukka, T. (2006) Improved homogeneous proximity-based screening assay of potential inhibitors of 17beta-hydroxysteroid dehydrogenases. *Assay Drug Dev Technol* **4**:671-678.
- Kokko, L., Johansson, N., Lövgren, T. and Soukka, T. (2005) Enzyme inhibitor screening using a homogeneous proximity-based immunoassay for estradiol. *J Biomol Screen* **10**:348-354.
- Kokko, L., Lövgren, T. and Soukka, T. (2007) Europium(III)-chelates embedded in nanoparticles are protected from interfering compounds present in assay media. *Anal Chim Acta* **585**:17-23.
- Kokko, L., Sandberg, K., Lövgren, T. and Soukka, T. (2004) Europium(III) chelate-dyed nanoparticles as donors in a homogeneous proximity-based immunoassay for estradiol. *Anal Chim Acta* **503**:155-162.
- Kokko, T., Kokko, L. and Soukka, T. (2009) Terbium(III) chelate as an efficient donor for multiple-wavelength fluorescent acceptors. *J Fluoresc* **19**:159-164.
- Krebber, A., Bornhauser, S., Burmester, J., Honegger, A., Willuda, J., Bosshard, H.R. and Pluckthun, A. (1997) Reliable cloning of functional antibody variable domains from hybridomas and spleen cell repertoires employing a reengineered phage display system. *J Immunol Methods* **201**:35-55.
- Kricka, L.J. (1994) Selected strategies for improving sensitivity and reliability of immunoassays. *Clin Chem* **40**:347-357.
- Kropp, J.L. and Dawson, W.R.J. (1966) Temperature dependent quenching of fluorescence of europic-ion solutions. *J Chem Phys* **45**:2419-2420.
- Kuningas, K., Päkkilä, H., Ukonaho, T., Rantanen, T., Lövgren, T. and Soukka, T. (2007) Upconversion fluorescence enables homogeneous immunoassay in whole blood. *Clin Chem* **53**:145-146.

## References

---

- Kömpe, K., Borchert, H., Storz, J., Lobo, A., Adam, S., Möller, T. and Haase, M. (2003) Green-emitting CePO<sub>4</sub>:Tb/LaPO<sub>4</sub> core-shell nanoparticles with 70% photoluminescence quantum yield. *Angew Chem Int Ed* **42**:5513-5516.
- Laitala, V. and Hemmilä, I. (2005a) Homogeneous assay based on anti-Stokes' shift time-resolved fluorescence resonance energy-transfer measurement. *Anal Chem* **77**:1483-1487.
- Laitala, V. and Hemmilä, I. (2005b) Homogeneous assay based on low quantum yield Sm(III)-donor and anti-Stokes' shift time-resolved fluorescence resonance energy-transfer measurement. *Anal Chim Acta* **551**:73-78.
- Laitala, V., Ylikoski, A., Raussi, H.M., Ollikka, P. and Hemmilä, I. (2007) Time-resolved detection probe for homogeneous nucleic acid analyses in one-step format. *Anal Biochem* **361**:126-131.
- Lakowicz, J. (1997) Nonlinear and two-photon-induced fluorescence. Topics in fluorescence spectroscopy. Vol. 5. Plenum Press, New York.
- Lakowicz, J. (2006) Principles of fluorescence spectroscopy. 3rd Ed. Springer, New York. p.p. 158-204.
- Latva, M., Takalo, H., Mukkala, V.M., Matachescu, C., Rodriguez-Ubis, J.C. and Kankare, J. (1997) Correlation between the lowest triplet state energy level of the ligand and lanthanide(III) luminescence quantum yield. *J Lumin* **75**:149-169.
- Laukkonen, M.L., Orellana, A. and Keinänen, K. (1995) Use of genetically engineered lipid-tagged antibody to generate functional europium chelate-loaded liposomes. Application in fluoroimmunoassay. *J Immunol Methods* **185**:95-102.
- Lehmusvuori, A., Karhunen, U., Tapiola, A.H., Lamminmäki, U. and Soukka, T. (2012) High-performance closed-tube PCR based on switchable luminescence probes. *Anal Chim Acta* **731**:88-92.
- Leonard, J.P. and Gunnlaugsson, T. (2005) Luminescent Eu(III) and Tb(III) complexes: developing lanthanide luminescent-based devices. *J Fluoresc* **15**:585-595.
- Leonard, J.P., Nolan, C.B., Stomeo, F. and Gunnlaugsson, T. (2007) Photochemistry and photophysics of coordination compounds: lanthanides. Topics in Current Chemistry; Photochemistry and Photophysics of Coordination Compounds II. Vol. 281. Springer-Verlag, Berlin. p.p. 1-43.
- Lim, S. and Franklin, S.J. (2004) Lanthanide-binding peptides and the enzymes that might have been. *Cell Mol Life Sci* **61**:2184-2188.
- Lim, S.F., Riehn, R., Ryu, W.S., Khanarian, N., Tung, C.K., Tank, D. and Austin, R.H. (2006) In vivo and scanning electron microscopy imaging of up-converting nanophosphors in *Caenorhabditis elegans*. *Nano Lett* **6**:169-174.
- Lis, S. (2002) Luminescence spectroscopy of lanthanide(III) ions in solution. *J Alloys Compd* **341**:45-50.
- Lobnik, A., Majcen, N., Niederreiter, K. and Uray, G. (2001) Optical pH sensor based on the absorption of antenna generated europium luminescence by bromothymolblue in a sol-gel membrane. *Sens Actuators, B* **74**:200-206.
- Luo, F., Batten, S.R., Che, Y. and Zheng, J.M. (2007) Synthesis, structure, and characterization of three series of 3d-4f metal-organic frameworks based on rod-shaped and (6,3)-sheet metal carboxylate substructures. *Chemistry* **13**:4948-4955.
- Lück, M., Paulke, B.R., Schröder, W., Blunk, T. and Müller, R.H. (1998) Analysis of plasma protein adsorption on polymeric nanoparticles with different surface characteristics. *J Biomed Mater Res* **39**:478-485.
- MacManus, J.P., Hogue, C.W., Marsden, B.J., Sikorska, M. and Szabo, A.G. (1990) Terbium luminescence in synthetic peptide loops from calcium-binding proteins with different energy donors. *J Biol Chem* **265**:10358-10366.
- Mader, H.S., Kele, P., Saleh, S.M. and Wolfbeis, O.S. (2010) Upconverting luminescent nanoparticles for use in bioconjugation and bioimaging. *Curr Opin Chem Biol* **14**:582-596.
- Mader, H.S. and Wolfbeis, O.S. (2010) Optical ammonia sensor based on upconverting luminescent nanoparticles. *Anal Chem* **82**:5002-5004.
- Mahon, E., Hristov, D.R. and Dawson, K.A. (2012) Stabilising fluorescent silica nanoparticles against dissolution effects for biological studies. *Chem Commun (Camb)* **48**:7970-7972.
- Mansfield, J.R., Hoyt, C. and Levenson, R.M. (2008) Visualization of microscopy-based spectral imaging data from multi-label tissue sections. *Curr Protoc Mol Biol* **12**:14-19.
- Marinsky, J.A., Glendenin, L.E. and Coryell, C.D. (1947) The chemical identification of radioisotopes of neodymium and of element 61. *J Am Chem Soc* **69**:2781-2785.
- Martin, L.J., Hahnke, M.J., Nitz, M., Wohner, J., Silvaggi, N.R., Allen, K.N., Schwalbe, H. and Imperiali, B. (2007) Double-lanthanide-binding tags: design, photophysical properties, and NMR applications. *J Am Chem Soc* **129**:7106-7113.

## References

---

- Massue, J., Quinn, S.J. and Gunnlaugsson, T. (2008) Lanthanide luminescent displacement assays: the sensing of phosphate anions using Eu(III)-cyclen-conjugated gold nanoparticles in aqueous solution. *J Am Chem Soc* **130**:6900-6901.
- Mathis, G. (1993) Rare earth cryptates and homogeneous fluoroimmunoassays with human sera. *Clin Chem* **39**:1953-1959.
- Mathis, G. (1999) HTRF(R) Technology. *J Biomol Screen* **4**:309-314.
- Mathis, G. and Bazin, H. (2011) Stable luminescent chelates and macrocyclic compounds. Springer series on fluorescence; lanthanide luminescence: photophysical, analytical and biological aspects. Vol. 7. Springer-Verlag, Berlin. p.p. 47-88.
- Matko, J., Jenei, A., Wei, T. and Edidin, M. (1995) Luminescence quenching by long range electron transfer: a probe of protein clustering and conformation at the cell surface. *Cytometry* **19**:191-200.
- McRae, S.R., Brown, C.L. and Bushell, G.R. (2005) Rapid purification of EGFP, EYFP, and ECFP with high yield and purity. *Protein Expr Purif* **41**:121-127.
- Medintz, I.L., Uyeda, H.T., Goldman, E.R. and Mattoussi, H. (2005) Quantum dot bioconjugates for imaging, labelling and sensing. *Nat Mater* **4**:435-446.
- Melcher, C.L., Friedrich, S., Cramer, S.P., Spurrier, M.A., Szupryczynski, P. and Nutt, R. (2005) Cerium oxidation state in LSO:Ce scintillators. *IEEE Trans Nucl Sci* **52**:1809-1812.
- Melhuish, W.H. (1984) Nomenclature, symbols, units and their usage in spectrochemical analysis - Part VI: molecular luminescence spectroscopy. *Pure Appl Chem* **56**:231-245.
- Mi, C., Tian, Z., Cao, C., Wang, Z., Mao, C. and Xu, S. (2011) Novel microwave-assisted solvothermal synthesis of NaYF<sub>4</sub>:Yb,Er upconversion nanoparticles and their application in cancer cell imaging. *Langmuir* **27**:14632-14637.
- Mizukami, S., Tonai, K., Kaneko, M. and Kikuchi, K. (2008) Lanthanide-based protease activity sensors for time-resolved fluorescence measurements. *J Am Chem Soc* **130**:14376-14377.
- Montgomery, C.P., Murray, B.S., New, E.J., Pal, R. and Parker, D. (2009) Cell-penetrating metal complex optical probes: targeted and responsive systems based on lanthanide luminescence. *Acc Chem Res* **42**:925-937.
- Moore, E.G., Samuel, A.P. and Raymond, K.N. (2009) From antenna to assay: lessons learned in lanthanide luminescence. *Acc Chem Res* **42**:542-552.
- Morise, H., Shimomura, O., Johnson, F.H. and Winant, J. (1974) Intermolecular energy transfer in the bioluminescent system of Aequorea. *Biochemistry* **13**:2656-2662.
- Morrison, L.E. (1988) Time-resolved detection of energy transfer: theory and application to immunoassays. *Anal Biochem* **174**:101-120.
- Mujumdar, R.B., Ernst, L.A., Mujumdar, S.R. and Waggoner, A.S. (1989) Cyanine dye labeling reagents containing isothiocyanate groups. *Cytometry* **10**:11-19.
- Mukkala, V.M., Helenius, M., Hemmilä, I., Kankare, J. and Takalo, H. (1993) Development of luminescent europium(III) and terbium(III) chelates of 2,2':6',2"- terpyridine derivatives for protein labelling. *Helv Chim Acta* **76**:1361-1378.
- Myyryläinen, T., Talha, S.M., Swaminathan, S., Vainionpää, R., Soukka, T., Khanna, N. and Pettersson, K. (2010) Simultaneous detection of Human Immunodeficiency Virus 1 and Hepatitis B virus infections using a dual-label time-resolved fluorometric assay. *J Nanobiotechnol* **8**:27-32.
- Nicholson, D.W. (2000) From bench to clinic with apoptosis-based therapeutic agents. *Nature* **407**:810-816.
- Niedbala, R.S., Feindt, H., Kardos, K., Vail, T., Burton, J., Bielska, B., Li, S., Milunic, D., Bourdelle, P. and Vallejo, R. (2001) Detection of analytes by immunoassay using up-converting phosphor technology. *Anal Biochem* **293**:22-30.
- Nitz, M., Sherawat, M., Franz, K.J., Peisach, E., Allen, K.N. and Imperiali, B. (2004) Structural origin of the high affinity of a chemically evolved lanthanide-binding peptide. *Angew Chem Int Ed Engl* **43**:3682-3685.
- Okabayashi, Y. and Ikeuchi, I. (1998) Liposome immunoassay by long-lived fluorescence detection. *Analyst* **123**:1329-1332.
- Orellana, A., Laukkonen, M.L. and Keinänen, K. (1996) Europium chelate-loaded liposomes: a tool for the study of binding and integrity of liposomes. *Biochim Biophys Acta* **1284**:29-34.
- Pelkkikangas, A.M., Jaakohuhta, S., Lövgren, T. and Härmä, H. (2004) Simple, rapid, and sensitive thyroid-stimulating hormone immunoassay using europium(III) nanoparticle label. *Anal Chim Acta* **517**:169-176.

## References

---

- Pérez-Luna, V.H., Yang, S., Rabinovich, E.M., Buranda, T., Sklar, L.A., Hampton, P.D. and Lopez, G.P. (2002) Fluorescence biosensing strategy based on energy transfer between fluorescently labeled receptors and a metallic surface. *Biosens Bioelectron* **17**:71-78.
- Petoud, S., Bünzli, J.C., Glanzman, T., Piguet, C., Xiang, Q. and Thummel, R.P. (1999) Influence of charge-transfer states on the Eu(III) luminescence in mononuclear triple helical complexes with tridentate aromatic ligands. *J Lumin* **82**:69-79.
- Petoud, S., Cohen, S.M., Bünzli, J.C. and Raymond, K.N. (2003) Stable lanthanide luminescence agents highly emissive in aqueous solution: multidentate 2-hydroxyisophthalamide complexes of Sm<sup>3+</sup>, Eu<sup>3+</sup>, Tb<sup>3+</sup>, Dy<sup>3+</sup>. *J Am Chem Soc* **125**:13324-13325.
- Philchenkov, A. (2004) Caspases: potential targets for regulating cell death. *J Cell Mol Med* **8**:432-444.
- Piguet, C., Borkovec, M., Hamacek, J. and Zeckert, K. (2005) Strict self-assembly of polymetallic helicates: the concepts behind the semantics. *Coord Chem Rev* **249**:705-726.
- Pihlasalo, S., Hara, M., Hänninen, P., Slotte, J.P., Peltonen, J. and Härmä, H. (2009) Liposome-based homogeneous luminescence resonance energy transfer. *Anal Biochem* **384**:231-237.
- Preaudat, M., Ouled-Diaf, J., Alpha-Bazin, B., Mathis, G., Mitsugi, T., Aono, Y., Takahashi, K. and Takemoto, H. (2002) A homogeneous caspase-3 activity assay using HTRF technology. *J Biomol Screen* **7**:267-274.
- Päkkilä, H., Ylihärsilä, M., Lahtinen, S., Hattara, L., Salminen, N., Arppe, R., Lastusaari, M., Saviranta, P. and Soukka, T. (2012) Quantitative multianalyte microarray immunoassay utilizing upconverting phosphor technology. *Anal Chem* **84**:8628-8634.
- Rantanen, T., Järvenpää, M.L., Vuojola, J., Arppe, R., Kuningas, K. and Soukka, T. (2009) Upconverting phosphors in a dual-parameter LRET-based hybridization assay. *Analyst* **134**:1713-1716.
- Rantanen, T., Järvenpää, M.L., Vuojola, J., Kuningas, K. and Soukka, T. (2008) Fluorescence-quenching-based enzyme-activity assay by using photon upconversion. *Angew Chem Int Ed Engl* **47**:3811-3813.
- Richardson, F. S. (1982) Terbium (III) and europium (III) ions as luminescent probes and stains for biomolecular systems. *Chem Rev* **82**:541-552.
- Riwotzki, K., Meyssamy, H., Kornowski, A. and Haase, M. (2000) Liquid-phase synthesis of doped nanoparticles: colloids of luminescing LaPO<sub>4</sub>:Eu and CePO<sub>4</sub>:Tb particles with a narrow particle size distribution. *J Phys Chem B* **104**:2824-2828.
- Robers, M.B., Machleidt, T., Carlson, C.B. and Bi, K. (2008) Cellular LanthaScreen and beta-lactamase reporter assays for high-throughput screening of JAK2 inhibitors. *Assay Drug Dev Technol* **6**:519-529.
- Robertson, G.S., Crocker, S.J., Nicholson, D.W. and Schulz, J.B. (2000) Neuroprotection by the inhibition of apoptosis. *Brain Pathol* **10**:283-292.
- Rodriguez-Ubis, J.C., Takalo, H. and Mukkala, V.M. (1997) Biospecific binding reactants labelled with luminescent lanthanide chelates and their use. EP0770610.
- Roy, B.C., Santos, M., Mallik, S. and Campiglia, A.D. (2003) Synthesis of metal-chelating lipids to sensitize lanthanide ions. *J Org Chem* **68**:3999-4007.
- Sabbatini, N. (1987) Radiative and nonradiative transitions in the Eu(III) hexaaza macrocyclic complex [Eu(C<sub>22</sub>H<sub>26</sub>N<sub>6</sub>)(CH<sub>3</sub>COO)](CH<sub>3</sub>COO)Cl·2H<sub>2</sub>O. *J Chem Phys* **91**:4681-4685.
- Sabbatini, N. and Guardigli, M. (1993) Luminescent lanthanide complexes as photochemical supramolecular devices. *Coord Chem Rev* **123**:201-228.
- Sabbatini, N., Perathoner, S., Lattanzi, G., Dellonte, S. and Balzani, V. (1988) Electron- and energy-transfer processes involving excited states of lanthanide complexes: evidence for inner-sphere and outer-sphere mechanisms. *Inorg Chem* **27**:1628-1633.
- Sakahira, H., Enari, M. and Nagata, S. (1998) Cleavage of CAD inhibitor in CAD activation and DNA degradation during apoptosis. *Nature* **391**:96-99.
- Samuel, A.P.S., Moore, E.G., Melchior, M., Xu, J. and Raymond, K.N. (2008) Water-soluble 2-hydroxyisophthalamides for sensitization of lanthanide luminescence. *Inorg Chem* **47**:7535-7544.
- Santala, V. and Lamminmäki, U. (2004) Production of a biotinylated single-chain antibody fragment in the cytoplasm of *Escherichia coli*. *J Immunol Methods* **284**:165-175.
- Santra, S., Zhang, P., Wang, K., Tapec, R. and Tan, W. (2001) Conjugation of biomolecules with luminophore-doped silica nanoparticles for photostable biomarkers. *Anal Chem* **73**:4988-4993.
- Schäfer, H., Ptacek, P., Kömppe, K. and Haase, M. (2007) Lanthanide-doped NaYF<sub>4</sub> nanocrystals in aqueous solution displaying strong up-conversion emission. *Chem Mater* **19**:1396-1400.

## References

---

- Schäferling, M., Wu, M. and Wolfbeis, O.S. (2004) Time-resolved fluorescent imaging of glucose. *J Fluoresc* **14**:561-568.
- Sculimbrene, B.R. and Imperiali, B. (2006) Lanthanide-binding tags as luminescent probes for studying protein interactions. *J Am Chem Soc* **128**:7346-7352.
- Sedlmeier, A., Achatz, D.E., Fischer, L.H., Gorris, H.H. and Wolfbeis, O.S. (2012) Photon upconverting nanoparticles for luminescent sensing of temperature. *Nanoscale* **4**:7090-7096.
- Self, C.H. and Cook, D.B. (1996) Advances in immunoassay technology. *Curr Opin Biotechnol* **7**:60-65.
- Selvin, P.R. (1995) Fluorescence resonance energy transfer. *Methods Enzymol* **246**:300-334.
- Selvin, P.R. (1996) Lanthanide-based resonance energy transfer. *IEEE J Sel Top Quantum Electron* **2**:1077-1087.
- Selvin, P.R. (2000) The renaissance of fluorescence resonance energy transfer. *Nat Struct Biol* **7**:730-734.
- Selvin, P.R. (2002) Principles and biophysical applications of lanthanide-based probes. *Annu Rev Biophys Biomol Struct* **31**:275-302.
- Selvin, P.R. and Hearst, J.E. (1994) Luminescence energy transfer using a terbium chelate: Improvements on fluorescence energy transfer. *Proc Natl Acad Sci U S A* **91**:10024-10028.
- Selvin, P.R., Rana, T.M. and Hearst, J.E. (1994) Luminescence resonance energy transfer. *J Am Chem Soc* **116**:6029-6030.
- Shavaleev, N.M., Accorsi, G., Virgili, D., Bell, Z.R., Lazarides, T., Calogero, G., Armaroli, N. and Ward, M.D. (2005) Syntheses and crystal structures of dinuclear complexes containing d-block and f-block luminophores. Sensitization of NIR luminescence from Yb(III), Nd(III), and Er(III) centers by energy transfer from Re(I)- and Pt(II)-bipyrimidine metal centers. *Inorg Chem* **44**:61-72.
- Shim, S.E., Cha, Y.J., Byun, J.M. and Choe, S. (1999) Size control of polystyrene beads by multistage seeded emulsion polymerization. *J Appl Polym Sci* **71**:2259-2269.
- Siitari, H., Hemmilä, I., Soini, E., Lövgren, T. and Koistinen, V. (1983) Detection of hepatitis B surface antigen using time-resolved fluoroimmunoassay. *Nature* **301**:258-260.
- Siivola, P., Pettersson, K., Piironen, T., Lövgren, T., Lilja, H. and Bjartell, A. (2000) Time-resolved fluorescence imaging for specific and quantitative immunodetection of human kallikrein 2 and prostate-specific antigen in prostatic tissue sections. *Urology* **56**:682-688.
- Silvaggi, N.R., Martin, L.J., Schwalbe, H., Imperiali, B. and Allen, K.N. (2007) Double-lanthanide-binding tags for macromolecular crystallographic structure determination. *J Am Chem Soc* **129**:7114-7120.
- Smith, D.R., Rossi, C.A., Kijek, T.M., Henchal, E.A. and Ludwig, G.V. (2001) Comparison of dissociation-enhanced lanthanide fluorescent immunoassays to enzyme-linked immunosorbent assays for detection of staphylococcal enterotoxin B, Yersinia pestis-specific F1 antigen, and Venezuelan equine encephalitis virus. *Clin Diagn Lab Immunol* **8**:1070-1075.
- Snyder, E.E., Buoscio, B.W. and Falke, J.J. (1990) Calcium(II) site specificity: effect of size and charge on metal ion binding to an EF-hand-like site. *Biochemistry* **29**:3937-3943.
- Soini, E. and Hemmilä, I. (1979) Fluoroimmunoassay: present status and key problems. *Clin Chem* **25**:353-361.
- Soini, E. and Lövgren, T. (1987) Time-resolved fluorescence of lanthanide probes and applications in biotechnology. *Crit Rev Anal Chem* **18**:105-154.
- Soini, E., Pelliniemi, L., Hemmilä, I., Mukkala, V.M., Kankare, J. and Fröjdman, K. (1988) Lanthanide chelates as new fluorochrome labels for cytochemistry. *J Histochem Cytochem* **36**:1449-1451.
- Son, A., Dhirapong, A., Dosev, D.K., Kennedy, I.M., Weiss, R.H. and Hristova, K.R. (2008) Rapid and quantitative DNA analysis of genetic mutations for polycystic kidney disease (PKD) using magnetic/luminescent nanoparticles. *Anal Bioanal Chem* **390**:1829-1835.
- Son, A., Dosev, D., Nichkova, M., Ma, Z., Kennedy, I.M., Scow, K.M. and Hristova, K.R. (2007) Quantitative DNA hybridization in solution using magnetic/luminescent core-shell nanoparticles. *Anal Biochem* **370**:186-194.
- Song, B., Sivagnanam, V., Vandevyver, C.D., Hemmilä, I., Lehr, H.A., Gijs, M.A. and Bünzli, J.C. (2009) Time-resolved lanthanide luminescence for lab-on-a-chip detection of biomarkers on cancerous tissues. *Analyst* **134**:1991-1993.
- Soukka, T., Anttonen, K., Härmä, H., Pelkkikangas, A.M., Huhtinen, P. and Lövgren, T. (2003) Highly sensitive immunoassay of free prostate-specific antigen in serum using europium(III) nanoparticle label technology. *Clin Chim Acta* **328**:45-58.

## References

---

- Soukka, T. and Härmä, H. (2011) Lanthanide nanoparticles as photoluminescent reporters. Springer series on fluorescence; lanthanide luminescence: photophysical, analytical and biological aspects. Vol. 7. Springer-Verlag, Berlin. p.p. 89-113.
- Soukka, T., Kuningas, K., Rantanen, T., Haaslahti, V. and Lövgren, T. (2005) Photochemical characterization of up-converting inorganic lanthanide phosphors as potential labels. *J Fluoresc* **15**:513-528.
- Soukka, T., Paukkunen, J., Härmä, H., Lönnberg, S., Lindroos, H. and Lövgren, T. (2001) Supersensitive time-resolved immunofluorometric assay of free prostate-specific antigen with nanoparticle label technology. *Clin Chem* **47**:1269-1278.
- Spangler, C. and Schäferling, M. (2011) Luminescent chemical and physical sensors based on lanthanide complexes. Springer series on fluorescence; lanthanide luminescence: photophysical, analytical and biological aspects. Vol. 7. Springer-Verlag, Berlin. p.p. 235-262.
- Stang, P.J. and Olenyuk, B. (1997) Self-assembly, symmetry, and molecular architecture: coordination as the motif in the rational design of supramolecular metallacyclic polygons and polyhedra. *Acc Chem Res* **30**:502-518.
- Stenman, U.H. (2011) Clinical application of time-resolved fluorometric assays. Springer series on fluorescence; lanthanide luminescence: photophysical, analytical and biological aspects. Vol. 7. Springer-Verlag, Berlin. p.p. 329-341.
- Stouwdam, J.W. and van Veggel, F.C. (2004) Improvement in the luminescence properties and processability of LaF<sub>3</sub>/Ln and LaPO<sub>4</sub>/Ln nanoparticles by surface modification. *Langmuir* **20**:11763-11771.
- Stryer, L. (1978) Fluorescence energy transfer as a spectroscopic ruler. *Annu Rev Biochem* **47**:819-846.
- Stryer, L. and Haugland, R.P. (1967) Energy transfer: a spectroscopic ruler. *Proc Natl Acad Sci U S A* **58**:719-726.
- Stöber, W., Fink, A. and Bohn, E. (1968) Controlled growth of monodisperse silica spheres in the micron size range. *J Colloid Interface Sci* **26**:62-69.
- Sun, L.N., Peng, H., Stich, M.I., Achatz, D. and Wolfbeis, O.S. (2009) pH sensor based on upconverting luminescent lanthanide nanorods. *Chem Commun (Camb)*:5000-5002.
- Sun, Y., Jiu, H., Zhang, D., Gao, J., Guo, B. and Zhang, Q. (2005) Preparation and optical properties of Eu(III) complexes J-aggregate formed on the surface of silver nanoparticles. *Chem Phys Lett* **410**:204-208.
- Sun, Y., Zheng, Z., Yan, Q., Gao, J., Jiu, H. and Zhang, Q. (2006) Effects of Ag colloidal nanoparticles on luminescent properties of Eu(III) β-diketone. *Mater Lett* **60**:2756-2758.
- Suyver, J.F., Aebsicher, A., Biner, D., Gerner, P., Grimm, J., Heer, S., Krämer, K.W., Reinhard, C. and Güdel, H.U. (2005) Novel materials doped with trivalent lanthanides and transition metal ions showing near-infrared to visible photon upconversion. *Opt Mater* **27**:1111-1130.
- Takalo, H., Mukkala, V.M., Meriö, L., Rodríguez-Ubis, J.C., Sedano, R., Juanes, O. and Brunet, E. (1997) Development of luminescent terbium(III) chelates for protein labelling: effect of triplet-state energy level. *Helv Chim Acta* **80**:372-387.
- Takalo, H., Mukkala, V.M., Mikola, H., Liitti, P. and Hemmilä, I. (1994) Synthesis of europium(III) chelates suitable for labeling of bioactive molecules. *Bioconjug Chem* **5**:278-282.
- Tamaki, K. and Shimomura, M. (2002) Fabrications of luminescent polymeric nanoparticles containing lanthanide (III) ion complexes. *Int J Nanosci* **1**:533-537.
- Tanke, H.J. (2011) Imaging of lanthanide luminescence by time-resolved microscopy. Springer series on fluorescence; lanthanide luminescence: photophysical, analytical and biological aspects. Vol. 7. Springer-Verlag, Berlin. p.p. 313-328.
- Tanner, P.A. (2011) Lanthanide luminescence in solids. Springer series on fluorescence; lanthanide luminescence: photophysical, analytical and biological aspects. Vol. 7. Springer-Verlag, Berlin. p.p. 183-233.
- Torelli, S., Imbert, D., Cantuel, M., Bernardinelli, G., Delahaye, S., Hauser, A., Bünzli, J.C. and Piguet, C. (2005) Tuning the decay time of lanthanide-based near infrared luminescence from micro- to milliseconds through d-→f energy transfer in discrete heterobimetallic complexes. *Chemistry* **11**:3228-3242.
- Tsien, R.Y. (1998) The green fluorescent protein. *Annu Rev Biochem* **67**:509-544.
- Tsukube, H. and Shinoda, S. (2002) Lanthanide complexes in molecular recognition and chirality sensing of biological substrates. *Chem Rev* **102**:2389-2403.

## References

---

- Tsukube, H., Shinoda, S. and Tamiaki, H. (2002) Recognition and sensing of chiral biological substrates via lanthanide coordination chemistry. *Coord Chem Rev* **226**:227-234.
- Tyler, G. (2004) Rare earth elements in soil and plant systems - A review. *Plant Soil* **267**:191-206.
- Ullman, E.F., Kirakossian, H., Switchenko, A.C., Ishkanian, J., Ericson, M., Wartchow, C.A., Piro, M., Pease, J., Irvin, B.R., Singh, S., Singh, R., Patel, R., Dafforn, A., Davalian, D., Skold, C., Kurn, N. and Wagner, D.B. (1996) Luminescent oxygen channeling assay (LOCITM): sensitive, broadly applicable homogeneous immunoassay method. *Clin Chem* **42**:1518-1526.
- Ullman, E.F. (2001) Homogeneous immunoassays. The Immunoassay Handbook. Nature publishing group, London. p.p. 177-197.
- Valanne, A., Huopalahti, S., Soukka, T., Vainionpää, R., Lövgren, T. and Härmä, H. (2005a) A sensitive adenovirus immunoassay as a model for using nanoparticle label technology in virus diagnostics. *J Clin Virol* **33**:217-223.
- Valanne, A., Huopalahti, S., Vainionpää, R., Lövgren, T. and Härmä, H. (2005b) Rapid and sensitive HBsAg immunoassay based on fluorescent nanoparticle labels and time-resolved detection. *J Virol Methods* **129**:83-90.
- Valanne, A., Malmi, P., Appelblom, H., Niemelä, P. and Soukka, T. (2008) A dual-step fluorescence resonance energy transfer-based quenching assay for screening of caspase-3 inhibitors. *Anal Biochem* **375**:71-81.
- Valta, T., Puputti, E.M., Hyppänen, I., Kankare, J., Takalo, H. and Soukka, T. (2012) Ligand enabling visible wavelength excitation of europium(III) for fluoroimmunoassays in aqueous micellar solutions. *Anal Chem* **84**:7708-7712.
- van Peterson, L., Heeroma, M., de Heer, E. and Meijerink, A. (2000) Charge transfer luminescence of  $\text{Yb}^{3+}$ . *J Lumin* **91**:177-193.
- van Weemen, B.K. and Schuurs, A.H. (1971) Immunoassay using antigen-enzyme conjugates. *FEBS Lett* **15**:232-236.
- Wang, F., Han, Y., Lim, C.S., Lu, Y., Wang, J., Xu, J., Chen, H., Zhang, C., Hong, M. and Liu, X. (2010) Simultaneous phase and size control of upconversion nanocrystals through lanthanide doping. *Nature* **463**:1061-1065.
- Wang, M., Mi, C., Zhang, Y., Liu, J., Li, F., Mao, C. and Xu, S. (2009) NIR-responsive silica-coated  $\text{NaYbF}_4:\text{Er/Tm/Ho}$  upconversion fluorescent nanoparticles with tunable emission colors and their applications in immunolabeling and fluorescent imaging of cancer cells. *J Phys Chem C* **113**:19021-19027.
- Wang, Y., Zhou, X., Wang, T. and Zhou, J. (2008) Enhanced luminescence from lanthanide complex by silver nanoparticles. *Mater Lett* **62**:3582-3584.
- Vazquez-Ibar, J.L., Weinglass, A.B. and Kaback, H.R. (2002) Engineering a terbium-binding site into an integral membrane protein for luminescence energy transfer. *Proc Natl Acad Sci U S A* **99**:3487-3492.
- Weber, M.J. (1973) Multiphonon relaxation of rare-earth ions in yttrium orthoaluminate. *Phys Rev B* **8**:54-64.
- Weibel, N., Charbonniere, L.J., Guardigli, M., Roda, A. and Ziessel, R. (2004) Engineering of highly luminescent lanthanide tags suitable for protein labeling and time-resolved luminescence imaging. *J Am Chem Soc* **126**:4888-4896.
- Weissman, S.I. (1942) Intramolecular energy transfer, the fluorescence of complexes of europium. *J Chem Phys* **10**:214-217.
- Wen, X., Li, M., Wang, Y., Zhang, J., Fu, L., Hao, R., Ma, Y. and Ai, X. (2008) Colloidal nanoparticles of a europium complex with enhanced luminescent properties. *Langmuir* **2008**:6932-6936.
- Werts, M.H. (2005) Making sense of lanthanide luminescence. *Sci Prog* **88**:101-131.
- Werts, M.H., Duin, M.A., Hofstraat, J.W. and Verhoeven, J.W. (1999) Bathochromicity of Michler's ketone upon coordination with lanthanide(III) beta-diketonates enable efficient sensitisation of  $\text{Eu}^{3+}$  for luminescence under visible light excitation. *Chem Commun* **1999**:799-800.
- Vetrone, F., Boyer, J.C., Capobianco, J.A., Speghini, A. and Bettinelli, M. (2004) Significance of  $\text{Yb}^{3+}$  concentration on the upconversion mechanisms in codoped  $\text{Y}_2\text{O}_3:\text{Er}^{3+}$ ,  $\text{Yb}^{3+}$  nanocrystals. *J Appl Phys* **96**:661-667.
- Wide, L., Bennich, H. and Johansson, S.G. (1967) Diagnosis of allergy by an in-vitro test for allergen antibodies. *Lancet* **2**:1105-1107.
- von Lode, P., Rosenberg, J., Pettersson, K. and Takalo, H. (2003) A europium chelate for quantitative point-of-care immunoassays using direct surface measurement. *Anal Chem* **75**:3193-3201.

## References

---

- Wright, W.H., Mufti, N.A., Tagg, N.T., Webb, R.R. and Schneider, L.V. (1997) High-sensitivity immunoassay using a novel upconverting phosphor reporter. *Proc SPIE - Int Soc Opt Eng* **2985**:248-255.
- Wu, M., Lin, Z. and Wolfbeis, O.S. (2003) Determination of the activity of catalase using a europium(III)-tetracycline-derived fluorescent substrate. *Anal Biochem* **320**:129-135.
- Vuojola, J., Lamminmäki, U. and Soukka, T. (2009) Resonance energy transfer from lanthanide chelates to overlapping and nonoverlapping fluorescent protein acceptors. *Anal Chem* **81**:5033-5038.
- Vuojola, J., Hyppänen, I., Nummela, M., Kankare, J. and Soukka, T. (2011). Distance and temperature dependency in nonoverlapping and conventional Förster resonance energy-transfer. *J Phys Chem B* **115**:13685-13694.
- Xu, Y. and Li, Q. (2007) Multiple fluorescent labeling of silica nanoparticles with lanthanide chelates for highly sensitive time-resolved immunofluorometric assays. *Clin Chem* **53**:1503-1510.
- Xu, Y.Y., Hemmilä, I. and Lövgren, T. (1992a) Co-fluorescence effect in time-resolved fluoroimmunoassays - a review. *Analyst* **117**:1061-1069.
- Xu, Y.Y., Pettersson, K., Blomberg, K., Hemmilä, I., Mikola, H. and Lövgren, T. (1992b) Simultaneous quadruple-label fluorometric immunoassay of thyroid-stimulating hormone, 17-alpha-hydroxyprogesterone, immunoreactive trypsin, and creatine-kinase MM isoenzyme in dried blood spots. *Clin Chem* **38**:2038-2043.
- Yallow, R.S. and Berson, S.A. (1960) Immunoassay of endogenous plasma insulin in man. *J Clin Invest* **39**:1157-1175.
- Yang, C., Fu, L.M., Wang, Y., Zhang, J.P., Wong, W.T., Ai, X.C., Qiao, Y.F., Zou, B.S. and Gui, L.L. (2004) A highly luminescent europium complex showing visible-light-sensitized red emission: direct observation of the singlet pathway. *Angew Chem Int Ed Engl* **43**:5010-5013.
- Yao, G., Wang, L., Wu, Y., Smith, J., Xu, J., Zhao, W., Lee, E. and Tan, W. (2006) FloDots: luminescent nanoparticles. *Anal Bioanal Chem* **385**:518-524.
- Ylihärsilä, M., Harju, E., Arppe, R., Hattara, L., Hölsä, J., Saviranta, P., Soukka, T. and Waris, M. (2012) Genotyping of clinically relevant human adenoviruses by array-in-well hybridization assay. *Clin Microbiol Infect* DOI: 10.1111/j.1469-0691.2012.03926.x.
- Ylihärsilä, M., Valta, T., Karp, M., Hattara, L., Harju, E., Hölsä, J., Saviranta, P., Waris, M. and Soukka, T. (2011) Oligonucleotide array-in-well platform for detection and genotyping human adenoviruses by utilizing upconverting phosphor label technology. *Anal Chem* **83**:1456-1461.
- Ylikoski, A., Elomaa, A., Ollikka, P., Hakala, H., Mukkala, V.M., Hovinen, J. and Hemmilä, I. (2004) Homogeneous time-resolved fluorescence quenching assay (TruPoint) for nucleic acid detection. *Clin Chem* **50**:1943-1947.
- Yu, M., Li, F., Chen, Z., Hu, H., Zhan, C., Yang, H. and Huang, C. (2009) Laser scanning up-conversion luminescence microscopy for imaging cells labeled with rare-earth nanophosphors. *Anal Chem* **81**:930-935.
- Yuan, J. and Wang, G. (2006) Lanthanide-based luminescence probes and time-resolved luminescence bioassays. *Trends Anal Chem* **25**:490-500.
- Yuan, J., Wang, G., Kimura, H. and Matsumoto, K. (1997) Highly sensitive time-resolved fluoroimmunoassay of human immunoglobulin E by using a new europium fluorescent chelate as a label. *Anal Biochem* **254**:283-287.
- Zhang, H., Xu, Y., Yang, W. and Li, Q. (2007) Dual-lanthanide-chelated silica nanoparticles as labels for highly sensitive time-resolved fluorometry. *Chem Mater* **19**:5875-5881.
- Zhao, B., Gao, H.L., Chen, X.Y., Cheng, P., Shi, W., Liao, D.Z., Yan, S.P. and Jiang, Z.H. (2006) A promising Mg(II)-ion-selective luminescent probe: structures and properties of Dy-Mn polymers with high symmetry. *Chem Eur J* **12**:149-158.
- Zhou, J., Yu, M., Sun, Y., Zhang, X., Zhu, X., Wu, Z., Wu, D. and Li, F. (2011) Fluorine-18-labeled Gd<sup>3+</sup>/Yb<sup>3+</sup>/Er<sup>3+</sup> co-doped NaYF<sub>4</sub> nanophosphors for multimodality PET/MR/UCL imaging. *Biomaterials* **32**:1148-1156.
- Zhou, Y., Xia, X., Xu, Y., Ke, W., Yang, W. and Li, Q. (2012) Application of europium(III) chelates-bonded silica nanoparticle in time-resolved immunofluorometric detection assay for human thyroid stimulating hormone. *Anal Chim Acta* **722**:95-99.
- Zijlmans, H.J., Bonnet, J., Burton, J., Kardos, K., Vail, T., Niedbala, R.S. and Tanke, H.J. (1999) Detection of cell and tissue surface antigens using up-converting phosphors: a new reporter technology. *Anal Biochem* **267**:30-36.

---

*References*

- Zolin, V.F., Puntus, L.N., Tsaryuk, V.I., Kudryashova, V.A., Legendziewicz, J., Gawryszecka, P. and Szostak, R. (2004) Spectroscopy of europium and terbium pyridine-carboxylates. *J Alloys Compd* **380**:279-284.
- Zou, W., Visser, C., Maduro, J.A., Pshenichnikov, M.S. and Hummelen, J.C. (2012) Broadband dye-sensitized upconversion of near-infrared light. *Nat Photonics* **6**:560-564.